

Copyright

by

Michael Patterson

2014

Additional Copyrights shared by

© American Society for Microbiology: Patterson M, Seregin A, Huang C, Kolokoltsova O, Smith J, Miller M, Smith J, Yun N, Poussard A, Grant A, Tigabu B, Walker A, Paessler S. 2013. Rescue of a Recombinant Machupo Virus from Cloned cDNAs and In Vivo Characterization in Interferon ($\alpha\beta/\gamma$) Receptor Double Knockout Mice. Journal of Virology

And

© Current Opinions in Virology: Patterson, M., Grant, A., Paessler, S.

**The Dissertation Committee for Michael Patterson Certifies that this is the
approved version of the following dissertation:**

**THE DEVELOPMENT OF A REVERSE GENETICS
SYSTEM FOR MACHUPO VIRUS**

Committee:

Slobodan Paessler, PhD, DVM, Mentor
Chair

Scott Weaver, PhD, Co-Mentor

Judith Aronson, MD

Roberto Garofalo, MD

Barry Rockx, PhD

Martin Pfeffer, PhD

Dean, Graduate School

**THE DEVELOPMENT OF A REVERSE GENETICS
SYSTEM FOR MACHUPO VIRUS**

by

Michael Patterson, MPH BA

Dissertation

Presented to the Faculty of the Graduate School of

The University of Texas Medical Branch

in Partial Fulfillment

of the Requirements

for the Degree of

Doctor of Philosophy

The University of Texas Medical Branch

March, 2014

Acknowledgements

There are a large number of people I would like to acknowledge but I also want to keep this short so I will consolidate. First, I would like to thank my fiancée, Julie, for putting up with me throughout the years and understanding my drive and love for science. This last year apart has been annoying in that we have been apart, but now we have decades to look forward to my craziness together. To my parents and siblings (including Tamara here, ha you are related now) for always being there and never wondering too obviously why I switched from math/computer science to biology (it's cooler of course). To friends who are family; the Hasletts and Greenes, you have always been family to me and I appreciate all of your support. No matter where life takes me I know we will always be there for each other. Additionally, special thanks to Jim for taking so much time reading both this dissertation and my capstone and providing valuable insight.

To my mentor, Dr. Paessler, I have grown and matured as a scientist under your tutelage. You have been critical when I needed it and always ensured I have learned from my mistakes. You gave me the freedom to handle and advance my projects independently but you were also available to help me handle the hurdles the projects threw my way. To all other members of the laboratory, there is no way all of my projects could have been planned, implemented, or analyzed without your assistance. I have learned from all of you and greatly appreciate your time and knowledge. To my graduate committee, during the last few years you have been making sure to ask the right questions, pushing me

always to think past the 'correct' answer; to try and get me to understand why the question is being asked and where the answer can lead me in the future projects.

To Heidi Lutz, thank you for volunteering to edit my dissertation. I am sure it never got more interesting after the first read but you kept at it and I appreciate it greatly. Hope trivia continues to go well for everyone once I am gone.

THE DEVELOPMENT OF A REVERSE GENETICS SYSTEM FOR MACHUPO VIRUS

Publication No. _____

Michael Patterson, PhD

The University of Texas Medical Branch, 2014

Supervisor: Slobodan Paessler

The etiologic agent of Bolivian hemorrhagic fever (BHF), Machupo virus (MACV), is a highly lethal viral pathogen with no approved vaccine or therapeutic to limit infection or outbreaks. Following implementation of rodent population controls after the initial outbreak, no cases of BHF were reported from 1976 to 1993. Reports in the last five years from the endemic region have identified a surge in reported cases and deaths from the disease. Since then, very little characterization or research of MACV has been accomplished. In this research, I describe the development of two major tools for studying MACV: The development of a mini-genome for both the small and large

segments, and the establishment of a reverse genetics system and rescue of a recombinant MACV. Using these tools, I present the first modern *in vitro* characterization of MACV, the development of a novel and lethal murine animal model, and the generation of a rationally attenuated MACV.

Table of Contents

THE DEVELOPMENT OF A REVERSE GENETICS SYSTEM FOR MACHUPO VIRUS	I
Table of Contents	iii
List of Tables	vii
List of Figures	viii
List of Abbreviations	xi
CHAPTER 1: INTRODUCTION.....	1
Virus Genome	1
Geographic Distribution and Epidemiology of Machupo Virus.....	4
Clinical Manifestations of Bolivian Hemorrhagic Fever.....	7
Diagnosis, Treatment, and Care for Bolivian Hemorrhagic Fever	9
Animal Models for Machupo Virus	11
Non-Human Primates:	11
Small Mammals:	13
The Innate Immune Response to Arenavirus Infection	15
The Interferon Response to Viral Infection	15
Modulation of the Innate Immune Response by Arenaviruses	17
Proposal Aims:.....	19
Significance:	20
CHAPTER 2: RESCUE OF RECOMBINANT MACHUPO VIRUS	22
Introduction:.....	22
Background	22
Gaps in knowledge.....	25
Hypothesis.....	26

Significance.....	26
Methods:	27
Cells, viruses, and biosafety.....	27
Sequencing of Full Length S and L Genomic RNAs from MACV Carvalho	28
Determination of 5' and 3' Termini of Both S and L Segments.....	29
MACV Minigenome Systems.....	29
Rescue of rMACV	30
Plaque Titrations	30
Animal Experiments	31
Histopathological and Immunohistochemical Analysis	32
Statistical Analysis.....	33
Results:.....	33
5' and 3' Terminal Sequences for Machupo Virus:.....	33
Construction of Plasmids for MACV Reverse Genetic System	35
Development of the Machupo Virus Minigenome	37
Rescue of Recombinant Machupo Virus and <i>In Vitro</i> Characterization..	39
<i>In vivo</i> Characterization of Machupo Virus in IFN- $\alpha\beta/\gamma$ R -/- Mice	41
Discussion:.....	44
Chapter Summary:	49
CHAPTER 3: CHARACTERIZATION OF THE INNATE IMMUNE RESPONSE TO MACV INFECTION <i>IN VITRO</i>.....	51
Introduction:.....	51
Background	51
Gaps in knowledge.....	53
Hypothesis.....	54
Significance.....	54
Methods:	55
Cells, Viruses, and Biosafety	55

Knockdown of RIG-I in A549 Cells	56
Plaque Titrations	56
Western Blots and Antibodies:	56
Statistics:	58
Results:	58
Effect of RIG-I Knockdown on MACV Growth	58
Effect of Infection on IFN Competent Cells	59
Effect of MACV Infection on Cellular Protein Biosynthesis	61
Discussion:	61
Chapter Summary:	66
CHAPTER 4: RATIONAL ATTENUATION OF MACV*	67
Introduction:	67
Background	67
Gaps in knowledge	69
Hypothesis	70
Significance	70
Methods:	71
Cells, viruses, and biosafety	71
Construction of the F437I Mutant S Plasmid	71
Rescue of rMACV-F437I	73
Sequencing of Full Length S and L Genomic RNAs from rMACV-F437I	73
Plaque Titrations	74
Animal Experiments	75
Statistical Analysis	76
Results:	76
<i>In Vitro</i> Characterization of rMACV-F437I	76
<i>In Vivo</i> Characterization of rMACV-F437I	77

Isolation of Viral RNA from Two rMACV-F437I Infected Mice	80
Discussion:	81
Chapter Summary:	86
CHAPTER 5: DISSERTATION SUMMARY	87
Appendix:	93
I: Table of MACV Animal Experiments	93
II: Brain and Spleen Histology from Infected Mice	94
III: Immunohistochemistry from Infected Mice	95
IV: Viral Load of Different Organs from Infected Mice	96
PERMISSION TO PUBLISH	97
From the Journal of Virology:	97
From the Journal Current Opinions in Virology:	99
From the Journal of Molecular Biology	101
REFERENCES	106

List of Tables

Table 1: Table of published animal models from the 1960s to present.	93
---	----

List of Figures

Figure 1: The Genome and Replication Strategy of MACV.	2
Figure 2: Reported Cases of BHF Since 1959.	3
Figure 3: Map of Bolivia.....	4
Figure 4: Clinical Disease Progression of Bolivian Hemorrhagic Fever in Humans.	7
Figure 5: Proposed Mechanisms of Arenavirus Control of the Innate Immune Response.	16
Figure 6: Graphical representation of Six MACV Plasmids.	25
Figure 7: Sequence of the MACV 19 Nucleotide 5' and 3' Genomic Termini.	34
Figure 8: Silent Mutation in rMACV.....	35
Figure 9: Bioluminescent Signal From Reporter Plasmids.	36
Figure 10: Image of Fluorescent Cells.....	37
Figure 11: Plaque Morphology of MACV and rMACV.....	38
Figure 12: Infection of A549 Cells With MACV and rMACV.	39

Figure 13: Infection of Vero Cells.	40
Figure 14: Change in Percent Bodyweight of Infected IFN- $\alpha\beta/\gamma$ R $-/-$ mice.	41
Figure 15: Kaplan Meier Curve of MACV and rMACV Infected Animals.	42
Figure 16: Titration of Organ Samples.	45
Figure 17: MACV Segment Termini Alignment.	46
Figure 18: Effect of RIG-I Knockdown on MACV Growth in A549 Cells.	58
Figure 19: Activation of the JAK/STAT Pathway in IFN Competent A549 Cells Infected With MACV.	59
Figure 20: Recognition of MACV Infection by PKR in A549 Cells.	60
Figure 21: Passage History of Candid#1.	68
Figure 22: Transmembrane Region of MACV and JUNV.	69
Figure 23: Sequence Analysis of rMACV-F437L.	72
Figure 24: Infection of IFN Competent A549 Cells with MACV, rMACV, and rMACV-F437L.	76
Figure 25: Infection of IFN Incompetent Vero-CLL81 Cells with MACV, rMACV, and rMACV-F437L.	77

Figure 26: Kaplan Meier Curve of rMACV and rMACV-F437I Infected IFN- $\alpha\beta/\gamma$ R - /- Mice.....	78
Figure 27: Weight Change of IFN- $\alpha\beta/\gamma$ R -/- Mice infected with rMACV and rMACV-F437I.	80
Figure 28: Change in Temperature in rMACV and rMACV-F437I Infected Mice. .	81
Figure 29: Histopathology Staining of Brain and Spleen Tissues.	94
Figure 30: Immunohistochemistry of Brain and Spleen Tissue Slides from IFN $\alpha\beta/\gamma$ R -/- Mice.	95
Figure 31: Titrations From Organ Homogenates of Infected IFN $\alpha\beta/\gamma$ R -/- Mice. ..	96

List of Abbreviations

AHF	Argentine hemorrhagic fever
ANOVA	Analysis of Variance
BHF	Bolivian hemorrhagic fever
BHK-21	Baby hamster kidney cells
Bp	base pair (nucleotide)
BSL	Biosafety level
CDC	Centers for Disease Control/Prevention
DMEM	Dulbecco's Modified Eagle Medium
DNA	Deoxyribonucleic acid
DPI	Days post infection
dsRNA	Double stranded RNA
eIF2 α	Eukaryotic initiation factor 2
ELISA	Enzyme linked immunosorbent assays
ER	Endoplasmic reticulum
FBS	Fetal Bovine Serum
FDA	Food and Drug Administration
FRhL	Fetal rhesus lung
GNL	Galveston National Laboratory
GP-1	Glycoprotein 1
GP-2	Glycoprotein 2
GPC	Glycoprotein Precursor
HPI	Hours post infection
HRP	Horseradish peroxidase
IC	Intracranial
IFN	Interferon
IGR	Intergenic region
IKK ϵ /TBK-1	Serine/threonine kinases I κ B kinase ϵ /TANK-binding kinase-1
IN	Intranasal
IP	Intraperitoneal
IPS-1	IFN- β promoter stimulator-1
IRF3	IFN regulatory factor 3
ISGs	IFN stimulated genes
JAKs	Janus protein kinases

JUNV	Junin virus
L	Large segment of the arenavirus
L protein	RNA dependent RNA polymerase
LASF	Lassa hemorrhagic fever
LASV	Lassa virus
LCMV	Lymphocytic Choriomeningitis virus
LNS	Late neurological syndrome
MACV	Machupo virus
MEM	Modified eagles medium
MOI	Multiplicity of infection
MOPV	Mopeia virus
MTD	Mean time to death
NF- κ B	Nuclear factor kappa B
NHP	Non-human primates
NP	Nucleoprotein
NSAID	National Institute of Allergy and Infectious Diseases
NWAs	New World arenaviruses
ORFs	Open Reading Frames
OWAs	Old World arenaviruses
P/S	Penicillin-Streptomycin Antibiotics
PACT	PKR activating protein
PAMPs	Pathogen associated molecular patterns
PCR	Polymerase chain reaction
p-eIF2 α	Phosphorylated eukaryotic initiation factor 2
PFU	Plaque forming units
PKR	Protein kinase R
Poly I:C	Polyinosinic:polycytidylic acid
PPE	Personal protection equipment
p-PKR	Phosphorylated Protein kinase R
PRNT	Plaque reducing neutralization test
PRR	Pattern Recognition Receptor
RIG-I	Retinoic acid-inducible gene-I
rMACV	recombinant Machupo virus
RNA	Ribonucleic acid
RT-PCR	Reverse transcription polymerase chain reaction
S	Small segment of the arenavirus
SC	Sub-cutaneous
STAT	Signal transducer and activator of transcription

SSP	Stable Signal Peptide
ssRNA	Single Strand RNA
TCS	Tissue culture supernatant
TRAF-3	Tumor necrosis factor-receptor-associated factor-3
UTMB	University of Texas Medical Branch
UTR	Untranslated region
Z	RING finger protein

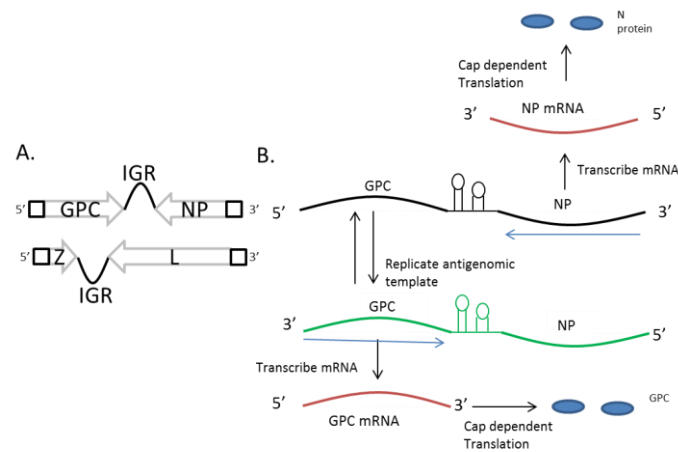
CHAPTER 1: INTRODUCTION

Machupo virus (MACV) is the etiological agent of Bolivian hemorrhagic fever (BHF) (1, 2) and a member of the family *Arenaviridae* (3-9). Bolivian hemorrhagic fever was first described in human patients in the Beni district of northeast Bolivia near the city of San Joaquin during an outbreak that lasted from 1959 to 1963. A team of doctors from the Middle American Research Unit (MARU), led by Dr. Karl Johnson, were the first investigators to identify and characterize BHF in humans (10-12).

The prototypical strain of MACV, Carvallo, was isolated from the spleen of a 2 year old lethal human case. The spleen homogenate was used to infect newborn hamsters and sick animals were euthanized and brain homogenate used for a second passage. The strain Carvallo has two passages in hamsters (1, 13, 14). Current research with MACV is limited; the virus is classified as a Center for Disease Control and Prevention (CDC) Select Agent and National Institute of Allergy and Infectious Diseases (NIAID) category A pathogen requiring a biosafety level (BSL)-4 laboratory for research within the United States (15). With the reemergence of BHF in the Beni district and the construction of the interoceanic highway along northern Bolivia, the public health threat to the region must be addressed prior to another major outbreak.

VIRUS GENOME

Members of the *Arenaviridae* family are enveloped, bi-segmented, negative-sense RNA viruses (16). The virions are pleomorphic when viewed by electron microscopy and the name *Arenaviridae* is derived from the ‘sandy’ appearance caused by cellular ribosomes found within the virion (17). The large (L) segment (~7.2kb) encodes two viral proteins:



the RNA dependent RNA polymerase (L protein) (18, 19) and a RING finger protein (Z), the arenavirus equivalent to a matrix protein (20-24). The small (S) segment (~3.3kb) encodes two viral proteins: the viral glycoprotein precursor (GPC) and the nucleoprotein (NP) (Fig. 1A). The GPC is post-translationally cleaved in two steps; 1) the cellular signal peptidase cleaves GPC to generate the stable signal peptide (SSP) and 2) the SKI-1/S1P subtilase cleaves the remainder into two glycoproteins, GP-1 and GP-2 (25-30). The SSP is myristoylated following cleavage, and is necessary for the transport of the GP-1/2 polypeptide from the endoplasmic reticulum to the golgi and for the targeted trafficking of the GP-1 and 2 proteins to the cellular membrane prior to virion budding

(29, 31). The viral spike comprises a globular head formed by the GP-1 while GP-2 is bound in the lipid bilayer of the cellular membrane anchoring GP-1 to the viral particle (16, 32). NP is the most common viral protein produced during MACV infection and is the primary structural protein in the viral nucleocapsid (16). The L protein of arenaviruses has been shown to have a conserved N-terminal domain which is proposed to have endonuclease activity allowing for ‘cap-snatching’ and ensuring cellular driven cap-dependent translation of viral mRNAs (33).

Both the S and L segments utilize an ambisense encoding strategy with two open reading frames (ORFs), one for each gene, in opposite directions (Fig. 1B). The ORFs of both segments are separated by an intergenic region (IGR). The IGRs are predicted to form secondary RNA structures, which are necessary for terminating transcription (34, 35). At each end of the L and S segments are untranslated regions (UTRs) of which the terminal 17-19 nucleotides are highly conserved within the *Arenaviridae* family (16, 36, 37). These conserved termini regions are

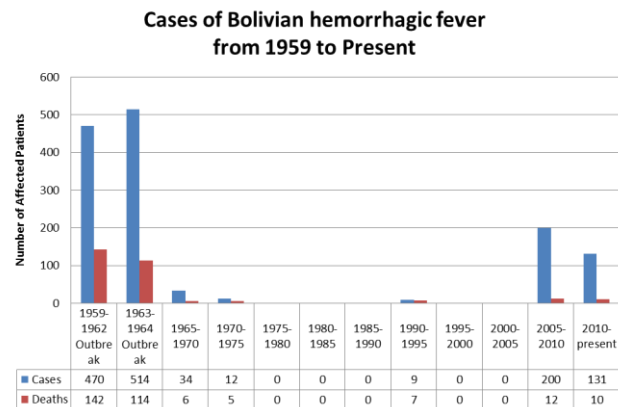


Figure 2: Reported Cases of BHF Since 1959.
A summary of the reported cases and deaths of BHF which have occurred since the original outbreak to present time (July, 2013). The reemergence of the disease is evident in the last few years with a drastic increase in reported cases since 2007. Copyright Current Opinions in Virology

59 reported to be vital in segment pan-handle formation for viral template replication and
60 transcription (16, 38, 39).

61 GEOGRAPHIC DISTRIBUTION AND EPIDEMIOLOGY OF MACHUPO VIRUS

62 The first outbreak of MACV was reported in Bolivia between 1959 and 1964.

63 Between 1976 and 1993 there were no reported cases of BHF, probably due to both the

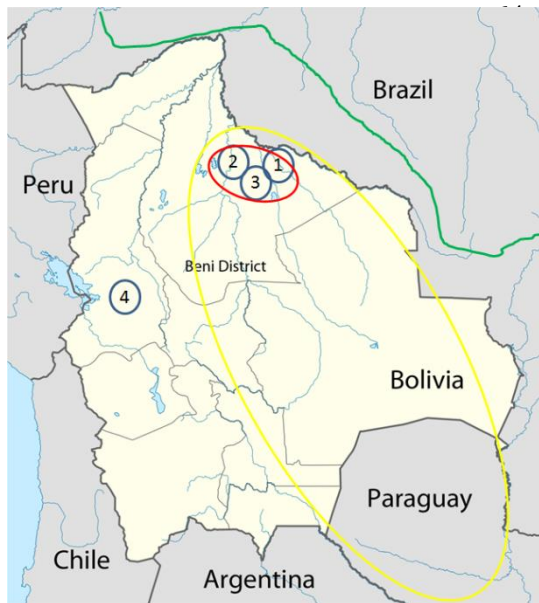


Figure 3: Map of Bolivia.

A map identifying different important locations within Bolivia. 1) The city of Magdalena which was a site of a limited number of cases in 1994. 2) City of San Joaquin and surrounding areas, the site of the original 1959-1964 outbreak. 3) The city of San Roman where 3 cases of BHF were identified in 93 and 08. 4) The capital of Bolivia and highest population city of the country, La Paz. The yellow oval identifies the predicted range of the rodent reservoir of MACV while the green line identifies the location of the pan-oceanic highway. Copyright Current Opinions in Virology

77 vector and reservoir for MACV. *C. callosus* has a wide natural geographical range
78 including portions of Bolivia, Brazil, Paraguay, and Argentina (45). While *C. callosus* are

implementation of rodent control measures in the populated urban areas and the under-reporting of disease within the region. A limited number of cases and deaths were reported in the mid-1990s including a familial outbreak resulting in 6 infections. Since 2006, there has been an increase in the cases reported compared to the previous decades, with a peak of reported cases in 2008 (1, 40-44) (Fig. 2).

During the 1959 outbreak, researchers identified *Calomys callosus* (2), the large vesper mouse, as the most likely natural

79 found throughout many countries of South America, MACV is endemic within only a
80 small geographic region of Bolivia (Fig. 3). This region of endemic MACV corresponds
81 with the same geographic region in which a specific monophyletic lineage of *C. callosus* is
82 found (46). The same phenomenon of a single rodent reservoir is reported with other
83 arenaviruses (47-50).

84 The infection rate of captured and necropsied *C. callosus* animals has ranged from
85 11% to 80% (2, 44, 51). Laboratory testing showed that nearly 100% of neonatal (≤ 3
86 days) *C. callosus* challenged IP with MACV become persistently infected with
87 detectable viremia and continued to shed from the urine and saliva. The infected animals
88 had no detectable clinical disease and never developed neutralizing antibodies against
89 MACV (52). Contrary to the young animals, older (> 2 weeks) animals challenged IP with
90 MACV developed two distinct responses to infection. One group was very similar to the
91 young animals except that they had a higher likelihood of anemia and reduced fertility
92 when compared to the infected neonate animals (14, 52, 53). The second group developed
93 neutralizing antibodies 4 weeks post infection. At the same time, the virus was cleared
94 from the blood it was no longer detectable in the urine and saliva.

95 The route of infection in humans is believed to be similar to other South
96 American hemorrhagic arenaviruses; through breathing in aerosolized excreta or secretions
97 from the rodent reservoir, consumption of contaminated food, or through direct mucus
98 membrane contact with infectious particles (12, 16). Nosocomial transmission has been

99 reported in BHF cases when family members visiting ill patients developed BHF (54,
100 55). Further evidence of human to human transmission occurred in 1971 when four
101 secondary cases of BHF were identified in hospital workers following close contact with
102 a patient suffering from BHF (56). Clinical evidence supports the nosocomial spread of
103 MACV, however, the epidemiologic evidence does not support this form of transmission
104 as a method for maintaining an epidemic (10).

105 In the first two to three years of the 1959 outbreak, most of the cases were in male
106 adults in the rural areas around San Joaquin. The high male case-rate is suspected to be
107 due to the high male-to-female ratio of individuals working in the fields. In 1962, an
108 increase in the number of urban cases was correlated to a decrease in the domestic feline
109 population (10), and to an increase in the rodent populations within the town. The drop in
110 feline population is suspected to have been caused by an over exposure to DDT and not
111 due to infection from MACV. Control of the outbreak was accomplished by 1965
112 following identification of the rodent reservoir and initiation of a systematic trapping of
113 rodents including the importation of a natural predator (12, 14). The cases reported in
114 1994 were also initially identified within a single family unit in which the primary case
115 was a rural worker (41); the most recent cases have been linked to rural/agricultural
116 activities as well (40). All of the recent reported cases of BHF have originated in the Beni
117 district of Bolivia (Fig. 3).

118

119 CLINICAL MANIFESTATIONS OF BOLIVIAN HEMORRHAGIC FEVER

120 Following aerosol exposure, arenavirus particles are likely engulfed by alveolar
 121 macrophages leading to the
 122 first cellular infection (57).
 123 The incubation period for
 124 BHF is 3 to 16 days
 125 following exposure (58).
 126 Previously, exposure was
 127 believed to consistently lead
 128 to clinical disease (10).

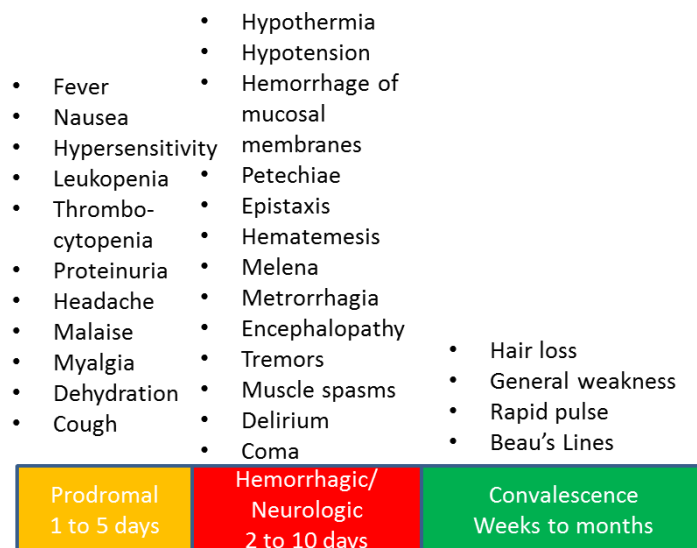


Figure 4: Clinical Disease Progression of Bolivian Hemorrhagic Fever in Humans.

A figure formed from a conglomeration of clinical reports identifying the most commonly reported clinical symptoms in humans infected with Bolivian hemorrhagic fever. Patients commonly present to local health authorities following development of severe symptoms which can develop in the late prodromal to early hemorrhagic/neurologic phases. Copyright Current Opinions in Virology

133 with no history of BHF (16). These unpublished samplings could imply a number of
 134 possibilities: MACV might be less lethal than identified in the initial outbreak; MACV
 135 might be more widespread than previously thought within the Beni district; or MACV
 136 virulence has reduced since the original outbreak in the 1960s (16).

137 The prodromal phase of BHF is similar to that of Argentine hemorrhagic fever
 138 (AHF) caused by Junin virus (JUNV), with the onset of fever, malaise, myalgia,

139 headache, and anorexia. This develops into severe symptoms including vomiting,
140 hypersensitivity to physical contact, and early signs of vascular damage. Laboratory
141 findings of clinical samples include leukopenia, thrombocytopenia, and proteinuria
142 during the prodromal phase (12, 16, 55, 58) (Fig. 4).

143 Approximately one third of patients progress into a neurologic or hemorrhagic
144 disease phase within a week of the prodromal phase. Symptoms include flushing of the
145 head and torso, petechiae, hypotension, epistaxis, hematemesis, melena, delirium,
146 convulsions, tremors, coma, and death (59). The cause of these neurological issues is
147 currently unknown. The case fatality rate varies between outbreaks of BHF but was
148 estimated to be around 25% during the initial 1959 to 1964 outbreak (16). While a late
149 neurological syndrome comparable to that reported with JUNV infected patients treated
150 with immune plasma, the neurological disease does appear to be more pronounced in
151 BHF patients (55, 60). If immune plasma treatment is initiated within the region, it is
152 possible cases of LNS will be observed at a comparable rate, 10%, to AHF (61). The
153 convalescent phase can last up to eight weeks and can include fatigue, dizziness and hair
154 loss. The effectiveness of immune serum treatment of non-human primates following
155 exposure to MACV implies clearance is mediated through a humoral immune response
156 (62). This is different from what has been identified in cases of Lassa Fever (LASF), a
157 representative of the Old World arenaviruses (OWAs), where a cellular response is
158 crucial for protection (63, 64).

159 **DIAGNOSIS, TREATMENT, AND CARE FOR BOLIVIAN HEMORRHAGIC FEVER**

160 Identification of MACV infection can be accomplished in the late stages of the
161 prodromal phase utilizing an enzyme linked immunosorbent assays (ELISAs) to identify
162 the presence of IgM and IgG antibodies to NP from collected serum or tissue (16).
163 Diagnostic reverse transcription polymerase chain reaction (RT-PCR) tests are also
164 available for quick and accurate identification of the presence of MACV RNA but the kit
165 and equipment is only available at larger hospitals and laboratories in Bolivia. Virus
166 isolated from the blood and tissue samples can be utilized to identify virus infection
167 however, there are several drawback including the length of time and required personal
168 protection equipment (PPE).

169 Currently, there are no Food and Drug Administration (FDA) approved vaccines
170 or therapeutics for BHF. During the 1959 outbreak, supportive care and proper
171 administration of fluids were the best known treatment options for patients in Bolivia
172 (55). Convalescent immune plasma from survivors was utilized in the case of four
173 infected researchers, all of whom recovered (65). Researchers have identified a dose-
174 dependent protection against MACV when rhesus monkeys were treated 4 HPI with
175 human immunoglobulin (62). However, no clinical trials have been completed in human
176 patients. In the same study 75% of infected primates treated with moderate to high (.5 to
177 1.5mL/kg of immunoglobulin) doses of immunoglobulin developed a chronic, late
178 neurological disease (62). All three treated primates that developed signs of neurological

179 impairment died weeks after clinical signs of acute BHF had abated (62). An additional
180 study in non-human primates (NHPs) identified a lethal chronic neurological disease in
181 rhesus monkeys in which six animals receiving convalescent serum succumbed to
182 neurological disease (66).

183 The efficacy of ribavirin, an antiviral therapeutic shown to be effective against
184 Lassa virus (LASV), has been used to treat two patients, both of whom recovered from
185 the disease (67, 68). While both patients recovered, it is impossible to determine if
186 ribavirin played a direct role in their recovery, expansion of clinical trials into the region
187 would be necessary. However, due to the limited number of reported cases in region, the
188 lack of infrastructure, and high costs, no clinical trials have been initiated (41, 67).
189 Preliminary reports also identified vaccination with Candid#1 (a vaccine against AHF) to
190 be protective in NHPs against MACV, but no further testing has been completed to
191 confirm these findings in humans (69). Recent studies in immunocompromised mice have
192 demonstrated a significant efficacy of ribavirin against MACV (70). The lack of clinical
193 infrastructure to support a national convalescent serum stock in Bolivia combined with no
194 proven effective therapeutics or vaccines against MACV will make controlling future
195 outbreaks of MACV difficult.

196

197

198 **ANIMAL MODELS FOR MACHUPO VIRUS**

199 Animal models have provided most of the information currently available on
200 MACV pathogenesis (Appendix I). Unlike other arenaviruses, rodent reduction programs
201 successfully controlled MACV from the 1970s to the early 1990s. The number of human
202 cases identified with LASV and JUNV has been important in developing a clearer picture
203 of disease progression and pathogenesis as well as providing key clinical isolates for
204 study within the laboratory. This has not been possible with MACV, making the early
205 NHP and other animal studies important in understanding BHF pathogenesis.

206 **Non-Human Primates:**

207 Four NHP species have been utilized in studying BHF disease pathogenesis.
208 Adult marmosets (*Saquinus geoffroyi*) have been shown to develop a lethal infection
209 following subcutaneous (SC) infection, scarified skin exposure, and corneal instillation,
210 but not through intranasal (IN) or oral administration of MACV (71). The time to death
211 in marmosets ranged from 11 to 21 days following SC infection and was dependent upon
212 infection dose. Virus was successfully isolated from the brains, spleens, kidneys, heart,
213 liver, saliva, and urine (1 sample) of animals that succumbed to disease (53). Clinical
214 signs, such as lethargy, weakness, and hypothermia appeared one to three days prior to
215 death.

216 Rhesus macaques (*Macaca mulatta*) have been shown to develop a lethal
217 infection following SC infection with MACV. Disease progression was described as bi-
218 phasic, similar to human disease. Two studies, both utilizing adult and young rhesus
219 macaques, identified clinical illness developing five to six days post infection (DPI).
220 Early symptoms included depression, fever, anorexia, diarrhea, facial rash, and
221 conjunctivitis. Disease progression continued in all macaques with severely ill animals
222 becoming moribund a day or two prior to death. In the first study, animals were infected
223 with either 10^5 or 10^3 plaque forming units (pfu) of MACV, and the mean time to death
224 (MTD) was 14.3 and 19.5 DPI respectively with a 100% case fatality rate (72). A second
225 report utilizing young (2.5-4kg) and adult (5-8kg) rhesus macaques resulted in mortality
226 rates of 85% and 50% following infection with 10^3 pfu (73). The MTD was similar as
227 with the first study. Survivors developed late neurological disease 26 to 41 days after
228 infection in which 66% of the surviving young macaques and all of the adult macaques
229 succumbed to disease (73). Histopathological examination of infected macaques
230 identified moderate to severe encephalitis with vasculitis and internal hemorrhage.
231 Following SC infection, 100% of cynomolgus monkeys (*Macaca fascicularis*) became
232 viremic at five DPI. Minimal clinical signs were identified in diseased animals when
233 compared to rhesus macaques. Infected cynomolgus animals had a reported 70%
234 mortality rate during the acute phase of the disease(73). The MTD was similar to that of
235 the rhesus monkey along with comparable LNS development in survivors of the initial
236 phase of the disease. Animals which developed LNS had a 50% mortality rate (73).

MACV disease progression has also been studied in the African green monkey (*Cercopithecus aethiops*). Following SC infection, 100% of animal subjects succumbed to MACV infection, 83% to the acute infection and 17% to late neurological development (74). Histopathological samples taken at the time of death identified necrosis and systemic hemorrhage in the kidneys, liver, and spleen of infected animals. Pneumonia was also identified during necropsies in all of the infected African green monkeys. The clinical development of disease was biphasic, similar to that of the rhesus monkeys, but not cynomolgus monkeys or adult marmosets (66, 72-74).

Small Mammals:

Adult small mammals have shown a strong resistance to MACV infection. Inbred adult mice (BALB/C, C3H/HCN, AKR, DBA/2, C57BL/6) challenged by the intracranial (IC) or intraperitoneal (IP) routes had no detectable viremia or illness but developed a strong neutralizing antibody response shown by plaque reducing neutralization test (PRNT) (53). Young and suckling inbred mice, less than two days old, develop a lethal infection following challenge IP or IC but do not develop any hemorrhagic symptoms comparable to BHF described in humans or NHPs (53, 71).

A report utilizing signal transducer and activator of transcription (STAT) -1 knockout mice described the development of lethal disease following IP (MTD = 7.3 days, 100% mortality), SC (MTD=10 days, 66% mortality), and IN (MTD=20, 25% mortality). Virus was detected in the spleen, kidneys, serum, lung, and liver. Clinical

257 development of disease including ruffled fur, hunched back, awkward gait, and lethargy
258 were apparent at 5 DPI (70). (53).

259 An additional mouse model utilizing interferon $\alpha\beta/\gamma$ receptor knockout (IFN- $\alpha\beta/\gamma$
260 R -/-) mice has been reported to develop a lethal disease following challenge with MACV
261 through an IP route of injection (75). Animals were challenged with either wild type
262 MACV or a recombinant MACV virus and were reported to develop two clinical phases
263 of disease. From around 10 to 14 DPI animals were reported to lose a significant percent
264 of body weight when compared to uninfected animals. Peak weight loss observed during
265 the acute phase occurs between 14 to 16 DPI. From this period until severe neurological
266 disease develops, animal bodyweight appears to stabilize, but rarely returns to baseline
267 levels. Starting at 22 DPI, animals developed neurological symptoms including ataxia,
268 rear limb-paralysis, and an awkward gait. One to three days prior to death, infected
269 animals had severe weight and body temperature loss with a MTD around 28 DPI.

270 Adult hamsters, when challenged IN or orally with MACV, did not develop
271 detectable illness. When infected through an IP or IC route at 1,000 pfu with MACV,
272 adult hamsters developed detectable viremia but no observable signs of illness.
273 Neutralizing and complement fixing antibodies are detected 30 days after IC and IP
274 challenge in hamsters (53, 71). Suckling hamsters (less than 6 days old) have been
275 reported to develop a lethal infection following challenge IP, IC, or IN but there are no
276 published reports of disease development or characterization in these animals (53, 71).

277 Both outbred (Hartley) and inbred (C-13) species of adult guinea pigs have been
278 reported to develop a lethal infection following challenge with MACV. The
279 characterization of disease development in either species has not been well reported (53,
280 56, 76). There are no reports utilizing young guinea pigs as an animal model. Other adult
281 animals that have been shown to develop a detectable neutralizing antibody response but
282 no disease are horses, cats, rats, and other outbred wild mice species (71).

283 **THE INNATE IMMUNE RESPONSE TO ARENAVIRUS INFECTION**

284 **The Interferon Response to Viral Infection**

285 The recognition of viral targets and activation of the innate immune response is
286 essential to control viral infection. Initiation of an innate immune response in cells is
287 through pattern recognition receptors (PRRs), which can bind to a large number of
288 pathogen associated molecular patterns (PAMPs) (77). Upon recognition of viral
289 infection, production of type-I interferons (IFN) α and β can be up-regulated leading to
290 the secretion of the IFNs (78-81). Three classes of PRRs associated with induction of
291 type I IFN response to viral infection are retinoic acid-inducible gene-I-like receptors
292 (RLRs), toll-like receptors (TLRs), and nucleotide oligomerization domain (NOD)-like
293 receptors (82-84). The RLRs are further subdivided into retinoic acid-inducible gene-I
294 (RIG-I), melanoma differentiation-associated gene 5 (MDA-5), and laboratory of
295 genetics and physiology 2 (LGP2) cytosolic helicases, all of which are capable of
296 recognizing unique facets of RNA associated with viral infection (77, 85-89).

297 Recognition by any of these three PRRs leads to activation and translocation into
 298 the nucleus of interferon regulatory factors (IRFs) and nuclear factor κ B (NF- κ B) which
 299 stimulate the production of IFN- α/β (84, 90-92). The PRR RIG-I can recognize single
 300 stranded RNA (ssRNA) generated
 301 during viral replication processes with
 302 5'-triphosphates or short double strand
 303 RNA (dsRNA) leading to activation of
 304 IFN- β promoter stimulator-1 (IPS-1)
 305 found on the mitochondrial membrane
 306 (88, 93). IPS-1 acts as a binding
 307 protein leading to the recruitment of
 308 tumor necrosis factor-receptor-
 309 associated factor-3 (TRAF-3) which
 310 can further activate the
 311 serine/threonine kinases I κ B kinase
 312 ϵ /TANK-binding kinase (IKK ϵ /TBK)-
 313 1 complex. Once activated,
 314 IKK ϵ /TBK-1 phosphorylates IFN
 315 regulatory factor (IRF) -3 and -7
 316 which translocates into the nucleus to
 317 initiate IFN expression (82, 92, 94-97).

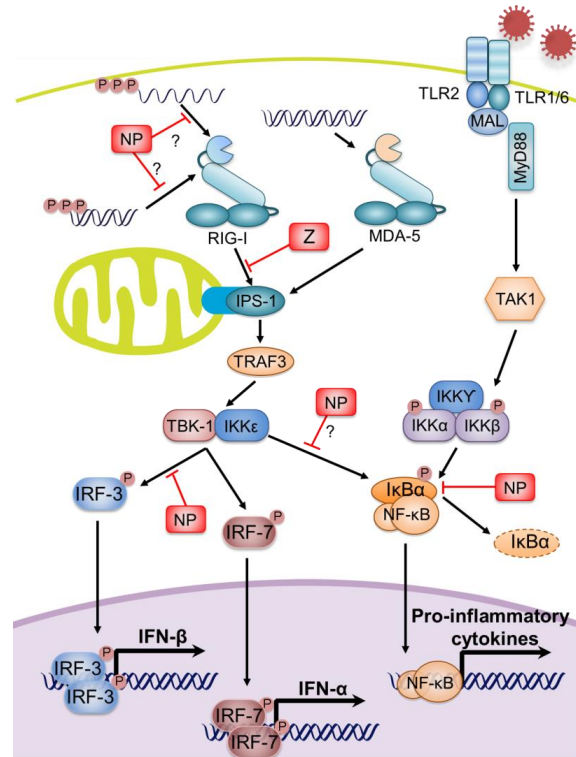


Figure 5: Proposed Mechanisms of Arenavirus Control of the Innate Immune Response.
 Graphical representation of the reported mechanisms which arenaviruses utilize to control the innate immune response and induction of IFN. These mechanisms were primarily identified through plasmid expression of genes of utilizing of infectious arenaviruses other than JUNV and MACV. NP is proposed to have 3'to5' exonuclease activity able to degrade viral ds or ssRNA. Z of NW arenaviruses has been shown to interact with RIG-I inhibiting downstream signaling. NP is also shown to interact with IKK ϵ inhibiting the phosphorylation of IRF-3 and -7. NP also inhibits activation of NF- κ B. Image Copyright Journal of Molecular Biology

318 Upon IFN synthesis, the cytokine is secreted from the cell and binds the cell
319 surface IFN receptors(98). Activation of the IFN receptor leads to downstream activation
320 of the Janus protein kinases (JAKs) Tyk and Jak1 that induce the phosphorylation and
321 activation STAT-1/2, which leads to upregulation of many different IFN stimulated genes
322 (IGSs) and the establishment of an antiviral state in the stimulated cell (87, 99, 100).

323 **Modulation of the Innate Immune Response by Arenaviruses**

324 Reports of LASF describe very low levels of type I IFN, proinflammatory
325 cytokine production, T cell activation, and human dendritic cell activation from a number
326 of *in vitro*, *in vivo*, and clinical data (16, 101-107). In contrast to LASF suppression/lack
327 of activation of the innate immune response, JUNV has been reported to induce strong
328 levels of IFN (2000-64,000 IU/mL) and cytokine production in the serum of patients
329 suffering from AHF (108, 109). High levels of IFN have been linked to disease severity
330 and poor outcome (108, 109). The induction of IFN has also been reported in NHPs
331 infected with MACV or JUNV and from hamsters infected with Pichinde virus (PICV)
332 (110-112). *In vitro* studies have reported that macrophages and monocytes productively
333 infected with JUNV do not induce a cytokine response while infection of A549 cells
334 (human carcinoma epithelial cells) has been shown to induce IFN production through
335 RIG-I recognition resulting in upregulation of ISGs (113, 114).

336 In addition to IFN production and ISG synthesis, cells have the capability to
337 reduce biosynthesis in the cell as one step in developing an antiviral state in the cell with

338 the goal resisting viral infection. The protein kinase R (PKR), an ISG, is capable of
339 recognizing double-stranded RNA (dsRNA), which often is formed during viral
340 replication. Once bound to dsRNA, PKR autophosphorylates to become active (p-PKR).
341 Once activated, p-PKR can phosphorylate eukaryotic translation initiation factor 2
342 (eIF2 α), an essential element for gene translation. Once eIF2 α is phosphorylated, cap
343 dependent translation of genes is severely inhibited as the complex is no longer able
344 recycle bound guanosine diphosphate (100, 115).

345 In recent reports, plasmid driven expression of NP from lymphocytic
346 choriomengitis virus (LCMV), JUNV, PICV, MACV, and LASV inhibited the nuclear
347 translocation of IRF-3 in Vero cells infected with Sendai virus (116). NP has also been
348 shown to prevent the phosphorylation of IRF-3 by binding and blocking IKK ϵ activity
349 (117). As a third proposed mechanism of preventing the establishment of an antiviral
350 state by NP, it has been shown that NP expression can inhibit the activation and
351 therefore, the translocation and transcription activity of nuclear factor kappa B (NF- κ B)
352 (118). Both the GPC and NP of JUNV, expressed transiently in IFN incompetent Vero
353 cells, have been shown to inhibit the phosphorylation of eIF2 α , inhibiting the
354 establishment of an antiviral state in the infected cell (119). Additionally, the plasmid-
355 expressed Z protein from New World arenaviruses (NWAs) but not OWAs has been
356 shown to bind RIG-I in A549 cells, inhibiting the induction of IFN production (120). This
357 evidence suggests that both OWAs and NWAs have multiple mechanisms of controlling

358 the innate immune response but the clinical evidence from AHF and LASF cases
359 suggests a marked difference on the impact of JUNV on IFN production then what is
360 reported in these *in vitro* studies (Fig. 5).

361 **PROPOSAL AIMS:**

362 This dissertation spans three aims regarding the generation and characterization of
363 a rMACV. Each aim and corresponding hypothesis is stated below:

364 Specific Aim 1: Establish a reverse genetics system for the rescue of rMACV and
365 characterize the virus. My hypothesis is that the rescue of a recombinant MACV can be
366 accomplished utilizing a Pol-I/II plasmid system. The rationale for this aim is based upon
367 previous research in the Paessler laboratory, which successfully rescued a recombinant
368 JUNV utilizing the Pol I/II promoter plasmid driven system.

369 Specific Aim 2: Characterization of the innate immune response to MACV
370 infection *in vitro*. My hypothesis is that infection by MACV will induce an innate
371 immune response comparable to that of JUNV. Previous reports in NHP models
372 identified the strong induction of IFN following challenge with MACV comparable to
373 that reported in JUNV clinical patients (111). There are no reported clinical findings of
374 IFN induction in human cases of BHF.

375 Specific Aim 3: Rationally attenuate rMACV and characterize it *in vivo*. The
376 hypothesis for this aim is that a mutation in the F437 amino acid of the transmembrane

377 region of GP2 will attenuate MACV neurovirulence in a mouse model. Previous work
378 has identified a mutation, F427I, in the transmembrane region of GP2 in Candid#1 as a
379 major determinant for attenuation for neurovirulence in mice (121, 122). This
380 transmembrane region is highly conserved in MACV.

381 **SIGNIFICANCE:**

382 The number of cases of Bolivian hemorrhagic fever has increased in recent years
383 (40, 42-44, 123). The increase in the number of at risk individuals living in endemic
384 regions, expansion of farming land, and mechanization of farming equipment are all
385 potential players in the reemergence of MACV. With the newly completed Transoceanic
386 highway there will be increased trade and travel via the southern portion of Bolivia which
387 increases the risk of disease spread and rodent host expansion to other regions of South
388 America. In addition, the continued threat of MACV as a biological terror threat due to
389 easy aerosol generation and high mortality rates makes MACV a viable threat not just to
390 the endemic Bolivian region but to surrounding countries and the United States.

391 While reverse genetic systems for other arenaviruses has been described, there
392 has been no development of a reverse genetics system for the study of MACV (38, 124-
393 127). Once established, it will provide a mechanism to generate genetically identical and
394 stable stocks of MACV that can be shared with other laboratories and increase the quality
395 and comparability of data coming from different sources. Additionally it will provide us
396 the tools to rationally modify the genome of the virus. This eliminates the need for
397 extensive passaging as was used to generate the attenuated strain of JUNV. Using this
398 tool and the knowledge gained from the attenuation of other arenaviruses we can generate

399 the first attenuated strain of MACV. Knowledge gained from this development can be
400 utilized for generating other attenuated arenaviruses, and may assist in the long term goal
401 of developing a pan-NWA vaccine.

402
403 With the completion of these aims this dissertation will describe the first
404 development of a minigenome system for MACV that can be used for replication studies
405 as well as the reverse genetics system to generate infectious MACV from cDNA. The
406 first reports will be generated on the in vitro immune response of human cells to MACV
407 infection, and a novel murine model to study MACV pathogenesis. Finally, to
408 demonstrate the use of the reverse genetics systems I will rationally modify MACV in an
409 attempt to attenuate the virus. The attenuation of the virus can be analyzed utilizing the
410 murine model characterized in the first aim of my dissertation.

411 **CHAPTER 2: RESCUE OF RECOMBINANT MACHUPO VIRUS**

412 **INTRODUCTION:**

413 **Background**

414 Reverse genetics systems have been developed for a number of different viruses
415 in the past decades. The development of such systems allows the rational manipulation
416 and modification of the viral genome without the inherent randomness of passaging virus
417 in different cells or tissues to generate mutations. The first reported reverse genetic
418 system was for the dsDNA simian virus 40 (128). Similarly, systems for rescuing
419 positive ssRNA viruses such the bacteriophage Q β , Sindbis virus, and Semliki forest
420 virus. Reverse genetics systems were developed for these virus by generating viral
421 cDNA, inserting the complete cDNA into a plasmid, and replicating it into infectious
422 mRNA, either through *ex vitro* polymerase or transfection *in vitro* (129-131).

423 The development of such systems for segmented negative- or ambi- sense ssRNA
424 viruses, such as arenaviruses, is more difficult. The first segmented negative sense
425 ssRNA virus to be rescued completely from cDNA was Bunyamwera virus (132). The
426 systems for negative sense ssRNA segmented viruses can be more complicated than
427 systems for DNA or positive sense RNA viruses. These systems require expression

428 plasmids, transfected in trans, containing the genes for the viral proteins necessary for
429 virus transcription, replication, and sometimes packaging. Additionally, plasmids for
430 each segment must be generated and transfected for each segment of the viral genome.

431 To test the functionality and replication of these reverse genetic systems,
432 minigenome assays have been developed concurrent with many reverse genetics systems.
433 These assays replace the viral genes with genes encoding reporter proteins, such as GFP
434 and firefly luciferase, allowing researchers to study the replication processes of a virus
435 without generating virus. In the case of high containment pathogens, such as MACV,
436 minigenome assays allow researchers to study the life cycle of the virus in a lower
437 containment environment which can expand the number of researchers capable of
438 studying aspects of the virus while reducing the costs associated with high containment
439 pathogens. Additionally, these systems have provided insights and screening strategies
440 for identifying antivirals which can affect the replication of the target virus (16, 127, 133-
441 135).

442 The development of a reverse genetics system is a multistep process. A complete
443 sequence of the L and S segments of MACV is necessary to ensure the accurate
444 translation of viable viral proteins and RNA. As previously reported with JUNV, the
445 sequence of the 19 termini nucleotides at the 5' and 3' UTRs might be inaccurate at the 6
446 and 8 base pair position (38). With these inaccuracies, the rescue of a recombinant JUNV
447 was not possible (38). An essential step in the rescue of a rMACV is to confirm that the

448 viral sequence is identical to the published online sequence. The insertion of an L
449 segment into an expression plasmid has been notoriously difficult when establishing
450 reverse genetic systems for other arenaviruses. When inserted, the transfected competent
451 bacterial cells do not grow as efficiently nor is the insertion stable (Personal
452 communication Dr. Paessler, Alexey Seregin). In addition to full segment insertion, the
453 functionality of the RNA dependent RNA polymerase expressed by the expression
454 plasmid has been reported to be problematic (Personal communication Dr. Paessler,
455 Alexey Seregin).

456 The availability of a good animal model for MACV is limited. Adult inbred mice
457 are generally resistant to infection with MACV. Early reports identified suckling
458 hamsters and inbred mice as susceptible following IC challenge (1). Recently,
459 immunoincompetent STAT-1 knockout mice have been reported to develop an acute and
460 lethal infection following intraperitoneal (IP) challenge with MACV, highlighting the
461 importance of an intact IFN pathway in restricting MACV infection but this model did
462 not follow the disease progression which has been reported in BHF cases (70).

463 Guinea pigs have also been reported to succumb to MACV infection following IP
464 challenge but the disease development has not been well characterized (1, 56). Studies
465 utilizing ‘chaired’ NHPs, a method of restraining the NHPs for extended periods which
466 can induce high levels of stress on the animal, reported lethal disease development
467 following intradermal (ID), intramuscular (IM), and IN routes of infection (66, 72, 74,

136). As many of the NHPs utilized for these studies were wild caught, the extended periods of constant restraint could lead to extreme stress in the animals. Interestingly, African green monkeys, rhesus macaques, and cynomolgus monkeys developed a lethal late neurological syndrome (LNS), a disease also reported in guinea pig models infected with JUNV (137). In addition to the neurological involvement identified in serious cases of BHF, both LASV and JUNV have been reported to cause different clinical forms of neurological disease in humans and animal models (65, 138, 139). These clinical signs range from muscle tremors and spasms to delirium, coma, and, in the case of LASF, permanent deafness (55, 140, 141).

Gaps in knowledge

A reverse genetics system for MACV has not been established, nor has a minigenome assay for studying replication kinetics. The lack of a small rodent model, which mimics human disease, also makes it very difficult to study MACV *in vivo* without the increased risk and cost of NHPs. These tools

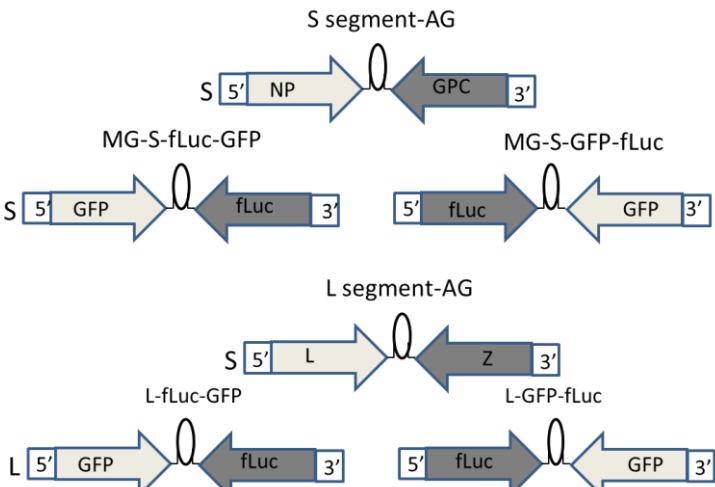


Figure 6: Graphical representation of Six MACV Plasmids. The MACV S and L antigenomic cDNA inserts are shown (S segment AG and L segment AG, respectively) in the orientation of the full segment insertion into the plasmids. Additionally, four MACV MG reporter plasmids (S-fLuc-GFP, S-GFP-fLuc, L-fLuc-GFP and L-GFP-fLuc) were generated with fLuc and GFP genes replacing viral genes in the S and L segments while leaving the UTR and IGR in place. Copyright Journal of Virology

488 are essential for moving forward in studying MACV virulence and the development of
489 antiviral countermeasures.

490 **Hypothesis**

491 Based upon previous research completed within my laboratory developing a
492 JUNV reverse genetics system, I hypothesize that the rescue of a recombinant MACV
493 can be accomplished utilizing a Pol-I/II plasmid system. With the completion of this
494 hypothesis, I expect three novel tools to be established which will further the field of
495 MACV research; a minigenome assay, a reverse genetics system, and a lethal animal
496 model.

497 **Significance**

498 First, the establishment of a reverse genetics system for MACV and subsequent
499 rescue of a rMACV will provide a powerful tool for future studies of the virus.
500 Traditional methods of attenuation would require extensive passaging in different animal
501 and cell types without any control over the mutations, which evolve. The reverse genetics
502 system will provide us the capability to study the genetic determinants of virulence. We
503 will be able to rationally modify entire genes down to specific amino acids. It will also
504 provide us with the ability to generate a genetically stable stock of virus from plasmids,
505 eliminating the need for additional passaging or long term storage of a Select Agent.

506 Second, a minigenome assay will provide us the ability to test the functionality of
507 the MACV NP and L, the proteins essential for viral genome replication, in expressing
508 reporter genes inserted in place of MACV genes in the full segment plasmids (Fig. 6). In
509 addition, the development of a minigenome system would provide a useful tool for
510 studying MACV replication mechanisms outside of the BSL-4 laboratory as has been
511 shown with other arenaviruses (38, 142-148).

512 Third, the modern *in vitro* characterization of MACV and the establishment of a
513 novel murine model would provide the field the knowledge and tools to further study
514 MACV biology. Much of the *in vitro* research characterizing MACV growth kinetics was
515 completed in the 1970s on cell lines, which may no longer be applicable or available.
516 Additionally, the development of a murine model which more closely follows the human
517 disease would be more cost effective, safer, and quicker than utilization of NHPs.

518

519 **METHODS:**

520 **Cells, viruses, and biosafety**

521 Baby hamster kidney (BHK-21) and Vero-CCL81 cells (American Tissue Culture
522 Collection) were maintained in Dulbecco's modified Eagle's medium supplemented with
523 10% fetal calf serum and L-glutamine. The wild-type Carvallo strain of MACV
524 (Genbank accession no. JN794583.1 and JN794584.1) was obtained from Dr. Thomas G.

525 Ksiazek (University of Texas Medical Branch [UTMB]). Viral working stocks of the
526 wild type and recombinant viruses were generated by infecting Vero cells (multiplicity of
527 infection [MOI] =0.01 pfu/cell) and collecting virus containing tissue culture supernatant
528 (TCS) at 96 hours post infection (HPI). Cellular debris was eliminated from the TCS
529 through centrifugation and the viruses were concentrated and purified through Ultra
530 100K Filter Devices (Ultracell 100K centrifugation filter, Amicon) to remove cellular
531 factors, which may affect the immune response. The concentrate containing the virus was
532 diluted with Dulbecco's Modified Eagle Medium (DMEM, Life Technologies 11966-
533 025) containing 2% fetal bovine serum (FBS, Life Technologies 11966-025) to generate
534 a series of working stock aliquots of the virus. All work with infectious MACV and
535 rMACV was performed in the UTMB BSL-4 facility in accordance with institutional and
536 safety guidelines.

537 **Sequencing of Full Length S and L Genomic RNAs from MACV Carvalho**

538 RNA (0.5 to 1.0 mg) was isolated by a RNA purification kit (Zymo Research,
539 DNA-Free RNA kit, R1014) at 96 HPI from MACV-infected Vero cells. Viral cDNA
540 was synthesized by reverse transcription (RT) using either viral specific primers or
541 random primers. Viral specific primers complementary to S and L genome RNAs were
542 used to generate cDNA fragments of each segment. The entire S and L segments were
543 amplified in three and five DNA fragments, respectively, by PCR. PCR products were gel
544 purified (Zymo Research, Zymoclean Gel DNA recovery kit, D4001) and directly

545 sequenced to obtain the corresponding master sequences for the MACV S and L genome
546 RNAs. Sequencing data was analyzed using the program Clone Manager V9.

547 **Determination of 5' and 3' Termini of Both S and L Segments**

548 To determine the sequences of the 5' and 3' 19 terminal regions of the S and L
549 segments, the total RNA was isolated from Vero cells infected with MACV. RNA was
550 treated with RNA 5' Tobacco acid pyrophosphatase (Epicentre) and ligated using T4
551 RNA ligase as I previously described (38). The ligated RNA was reverse transcribed
552 utilizing the primers MACV_SsegR312 (5'-AGGGTGACTGACTGGAACTC-3'),
553 MACV_SsegF3129 (5'- GACATGAGCCTATCCACTTC-3') MACV_LsegR349 (5'-
554 TGTGATGGATGTCGGTAGTG-3'), and MACV_LsegF6917 (5'-
555 AGGCGTGTGCTTCACAGGAC-3') for the S and L segments, respectively. The cDNA
556 was used for amplification through PCR utilizing the same primers. Fragments were gel
557 purified and sequenced.

558 **MACV Minigenome Systems**

559 The plasmids expressing MACV L and S segment minigenome were generated
560 similarly as previously described (38). Briefly, viral genes on the pPol-I-MACVSag and
561 pPol-I-MACVLag template plasmids were replaced by the GFP and firefly Luciferase
562 (fLuc) reporter genes (Fig. 6). BHK-21 cells (6×10^4 /well in a 12-well plate) were
563 transfected with 0.5 μ g of pPol-II-NP, 0.5 μ g of pPol-II-L, and 0.5 μ g of plasmid

564 expressing MACV L or S minigenome segments as indicated. At three days post
565 transfection, cellular lysate was collected and the bioluminescent signal was assayed
566 utilizing a luciferase reporter assay kit (Promega, E1500 or E1910) for luciferase
567 expression.

568 **Rescue of rMACV**

569 The rescue of rMACV was completed in a similar manner as described previously
570 by my laboratory (38). Briefly, equimolar amounts of the two full segment MACV
571 plasmids and the two expression plasmids were transfected into BHK21 cells.
572 Supernatant from these cells was collected at 4 days post transfection. A single passage in
573 Vero cells was performed to generate a higher titer stock of rMACV. The rMACV
574 sequence, including the introduced G1447A gene tag within the NP gene, was confirmed
575 by whole genomic sequence analysis.

576 **Plaque Titrations**

577 All plaque titrations were completed on Vero-CCL81 cell lines, seeded on 6- or
578 12-well plates roughly 16 hours prior to infection. Samples were serially diluted in
579 DMEM with 2% FBS and .5% P/S. Cells were infected with either 200 μ L or 100 μ L
580 respectively and incubated for ~1 hour with shaking every 15 minutes. Wells were then
581 overlayed with a 50:50 warmed mixture of 2% agarose in H₂O and 2X modified eagles
582 medium (MEM) with 10% FBS and .5% Penicillin-Streptomycin Antibiotics (P/S, Life

Technologies, 10378016). The plates were incubated for 8 days post infection (DPI) and fixed with 10% formalin solution. Cells were stained with crystal violet and plaques counted to determine viral load. When calculating the viral load of tissue samples, tissues were weighed prior to homogenization and media was added to the samples consistent to the measured weight, a minimum of 300 μ L to a maximum of 1000 μ L. The volume and organ weight were used to calculate viral loads per gram of tissue for each sample.

Animal Experiments

Six to eight week old interferon (IFN)- $\alpha\beta/\gamma$ receptor double knockout (IFN- $\alpha\beta/\gamma$ R -/-) mice on a C57BL/6 background and wild type C57BL/6 mice were utilized for all studies. All animals were housed in a pathogen free environment. All virus infections were performed in the BSL-4 in the Galveston National Laboratory (GNL), UTMB. All animal studies were reviewed and approved by the Institutional Animal Care and Use Committee at UTMB and were conducted according to the National Institutes of Health guidelines. Animals were anesthetized using an isoflurane precision variable-bypass vaporizer prior to virus inoculation by the IP route with 10⁴ PFU. Telemetric monitoring of body temperature was accomplished throughout the studies. A BMDS IPTT-300 transponder (Bio Medic Data Systems, Inc.) was implanted subcutaneously using a trocar needle assembly. Transponders were read with a DAS-6007 reader (Bio Medic Data Systems, Inc.) and downloaded in accordance with manufacturer's protocol. Body weight measurements were performed throughout the studies by anesthetizing the animals and

weighing them, weights were compared to baseline collected at 0 DPI (38, 149). Scheduled euthanizations occurred at 14 and 14 DPI during the first study. The experimental endpoints of the two studies were both approximately 40 DPI, where surviving animals were humanely euthanized and necropsied.

Histopathological and Immunohistochemical Analysis

Tissue samples were fixed in 10% buffered formalin for a minimum of 4 days and then transferred to 70% ethanol. Samples were embedded in paraffin and cut into 5µm sections to be mounted on slides. Slides were subjected to standard hematoxylin and eosin staining as described previously (38). Immunohistochemistry targeting MACV antigen was accomplished as described previously by my laboratory (38). In brief, cut sections were deparaffinized and rehydrated through xylene and graded ethanol solutions. Endogenous peroxidase activity was blocked with a solution of Tris-buffered saline containing 0.1% Tween 20, 3% hydrogen peroxide, and 0.03% sodium azide for 15 min, followed by heat antigen retrieval in a water bath at 95°C for 40 min in Dako Target Retrieval Solution, pH 6.1 (Dako Corporation). Endogenous biotin reactivity was blocked through incubation with avidin D and biotin solutions (Vector Laboratories).

To detect MACV viral antigen, rabbit anti-peptide primary antibody targeting a 14 amino acid residue starting at amino acid residue 220 (KYPRLKKPTIWHKR, ProSci) was utilized at a dilution of 1:500 and incubated on slides for 60 minutes. Tissue samples from uninfected mice were utilized as a negative control. To prevent nonspecific protein

623 binding, sections were incubated in blocking solution according to the manufacturer's
624 instructions (Histomouse-SP kit; Zymed).

625 **Statistical Analysis**

626 GraphPad Prism v5 was utilized for all data analysis. To determine significance
627 in weight change, a two-way analysis of variance (ANOVA) test was performed
628 comparing a pooled group of infected wild type mice with both MACV and rMACV
629 infected IFN- $\alpha\beta/\gamma$ R^{-/-} mice. Viral growth curve analysis was completed utilizing a two-
630 way ANOVA test comparing all virus and cell culture types over each day. A Kaplan
631 Meier survival curve was generated and statistical Mantel Cox test was completed to
632 determine significant differences in survival between MACV and rMACV infected
633 animals.

634 **RESULTS:**

635 **5' and 3' Terminal Sequences for Machupo Virus:**

636 I designed primers for the purpose of sequencing via PCR the MACV genome.
637 These primers were based on two full segment S and L sequences submitted to Genbank
638 (accession numbers JN794584, JN794583 and AY619643, AY619642). The terminal 19
639 nucleotides of the 5'- and 3'-ends of arenavirus genomic RNAs are highly conserved
640 and have been shown to be important for successful rescue of recombinant virus using
641 reverse genetics systems and the functionality of the arenavirus RNA polymerase (38, 39,

124). I isolated viral RNA from infected Vero cells at 96 HPI and subjected it to sequence analysis by the UTMB Genomics Sequencing Facility. The MACV RNA sequence was found identical to the published JN794583 and JN794584 sequences except at the 5' and 3' ends of the UTRs.

A.

Virus RNA- L Segment	Strain	Accession Number	5' End	3' End
Junin Machupo	Romero	Experimental	CGCACCGGGGATCCTAGGC	GCCTAGGATCCTCGGTGCG
	Carvallo	Experimental	CGCACCGGGGATCCTAGGC	GCCTAGGATCCTCGGTGCG
	Carvallo	JN794583.1	CGCACCGGGGATCCTAGGC	GCCTAGGATCCCTGTGCG
	Carvallo	AY619642	CGCACGGGGATCCTAGGC	GCCTAGGATCCCTGTGCG
Virus RNA- S Segment	Strain	Accession Number	5' End	3' End
Junin Machupo	Romero	Experimental	CGCACCGGGGATCCTAGGC	GCCTAGGATCCACTGTGCG
	Carvallo	Experimental	CGCACCGGGGATCCTAGGC	GCCTAGGATCCACTGTGCG
	Carvallo	JN794584.1	CGCACGGGGATCCTAGGC	GCCTAGGATCCACTGTGC
	Carvallo	AY619643	CGCACGGGGATCCTAGGC	GCCTAGGATCCACTGTGCG

Figure 7: Sequence of the MACV 19 Nucleotide 5' and 3' Genomic Termini.

The terminal 19 nucleotide sequences at the 5' and 3' ends of MACV genomic RNAs were determined in this study (experimental), which are identical to the terminal regions of JUNV. Highlighted are the nucleotide differences in two MACV isolates available from GenBank (accession numbers JN794584, JN794583 and AY619643, AY619642, respectively) Copyright Journal of Virology

Through RNA ligation and amplification through the region, I found the 19 nucleotide sequences at the 5' and 3' termini of the S and L segments identified in this study were identical to that of JUNV (Fig. 7) (38). When compared to the published sequences of MACV S segment (JN794584) and L segment (JN794583), I identified two nucleotide differences at positions 6 and 8 at the 5'-end of the S segment and two nucleotide differences at positions 6 and 8 from the 3'-end of the L segment (Fig. 7). I further identified that there was one extra G present at the 5'-end of L segment for JN794583 and one missing G at the 3'-end of the S segment for JN794584.

654 Comparisons of my sequencing results to other reported MACV sequences
 655 (AY619643 and AY619642) demonstrated the exact same four nucleotide differences
 656 (Fig. 7), which were also reported in the sequences of JUNV (GenBank accession
 657 numbers AY619641 and AY619640) by other groups. These alternative nucleotides at the
 658 6 and 8 positions were determined not
 659 to be viable for the rescue of other
 660 hemorrhagic arenaviruses (38, 124).
 661 There were two additional nucleotide
 662 differences at positions 6 and 8 at the
 663 5'-end of L segment between
 664 AY619642 and the sequence
 665 determined herein (Fig. 7).

Plasmid	gatgggtgggtattccaaactagatgaaggaacaat
Wild Type	gatgggtgggtattccgactagatgaaggaacaat
Passage0	gatgggtgggtattccaaactagatgaaggaacaat
Passage1	gatgggtgggtattccaaactagatgaaggaacaat

Figure 8: Silent Mutation in rMACV.
 Sequencing of the S segment plasmid and rMACV
 confirmed the single genetic marker introduced into the
 GP2 region at nucleotide 1407 (genomic sense) into the
 original plasmid. This marker allows me to distinguish
 MACV from rMACV. Copyright Journal of Virology

666 Construction of Plasmids for MACV Reverse Genetic System

667 To generate the pBSII-S vector plasmid containing the full-length antigenomic
 668 sense MACV S segment, two fragments derived from the S segment with overlapping
 669 restriction sites were amplified by PCR. The cDNA fragments were then digested and
 670 ligated into the vector pBlueScript (pBSII). The vector pBSII-L plasmid containing L
 671 segment was generated in a similar manner using three cDNA fragments. The last two
 672 overlapping fragments of cDNA, from ~2400bp to 7200bp, were generated through PCR
 673 amplification of the viral RNA. For the first portion of the L segment, I was unable to

674 generate a complete insertion of all 3 fragments into a vector plasmid. I ordered the
 675 missing 2600 basepair fragment
 676 to be synthesized and inserted
 677 into a vector plasmid (Gene
 678 Synthesis). Upon receiving the
 679 synthesized fragment and
 680 plasmid, I digested and ligated
 681 the two other fragments to
 682 generate a complete L segment
 683 plasmid.

684 The two full segments
 685 were digested from their vector

686 plasmids and inserted in antigenomic orientation into the murine Pol-I driven pRF42
 687 mPol-I expressing plasmid, generating pPol-I-MACVSag and pPol-I-MACVLag
 688 plasmids, which expressed the full length viral S segment genomic RNA and L segment
 689 genomic RNA, respectively (Fig. 5). A silent G to A mutation at nucleotide 1407 within
 690 the GPC gene was introduced into the S segment as a genetic marker for the recombinant
 691 MACV (Fig. 8).

692 To express the MACV NP and L proteins in *trans*, MACV NP and L genes were
 693 cloned into the Pol-II driven mammalian gene expression plasmid pTriEx-1 to generate

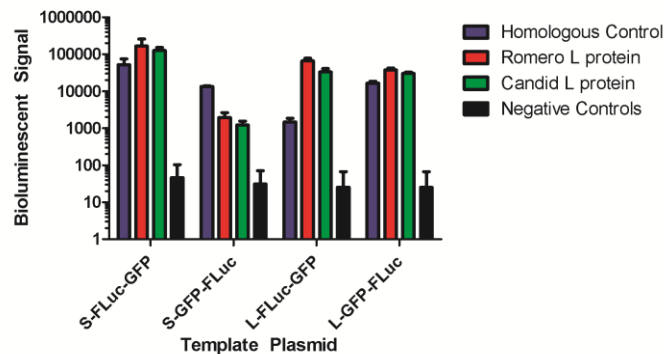


Figure 9: Bioluminescent Signal From Reporter Plasmids. Bioluminescent signal strength from four reporter plasmids transfected with NP and L expression plasmids into BHK cells. Transfections were completed in triplicate. Blue bars denote signal levels from homologous MACV NP and L along with the respective reporter plasmids. Red bars denote signal from reporter plasmids transfected with MACV NP and JUNV L. Green bars denote signal from reporter plasmids transfected with MACV NP and Candid#1 L. Bioluminescent signal from all transfections were stronger than that of the reporter plasmid transfected without the expression plasmids denoting transcription of fLuc occurred and the NP/L expression plasmids are functional. Copyright Journal of Virology

694 plasmids pPol-II-NP and pPol-II-L respectively. An RsrII restriction site was added to
 695 the 5' end of primers corresponding to the ATG codon of each gene, and was utilized for
 696 digestion and ligation of the gene segments into the plasmids. The L polymerase gene
 697 was inserted into pTriEx-1 by three DNA fragment ligation (pPol-II-L) while the NP was
 698 directly inserted as a single fragment (pPol-II-NP). Sequences of all plasmids were
 699 confirmed by sequence analysis by the UTMB Molecular Sequencing Core.

700 **Development of the Machupo Virus Minigenome**

701 To confirm whether the 5' and 3' UTRs of MACV identified in this study were
 702 functional for virus RNA replication and transcription, I developed a MACV minigenome

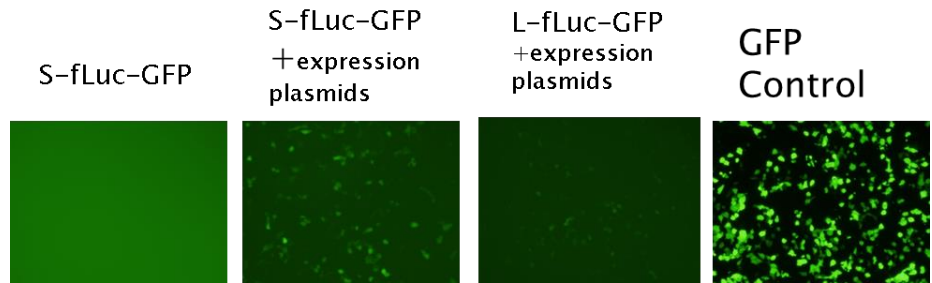


Figure 10: Image of Fluorescent Cells.
 Photographs of BHK cells following transfection. Negative control cells were transfected with only the reporter plasmid. The second two slides present BHK cells transfected with the respective reporter plasmid, MACV NP expression plasmid, and MACV L expression plasmid. GFP control represents cells transfected with a GFP expressing plasmid.

703 system. Minigenome reporter plasmids were generated containing the full UTRs and
 704 IGRs of MACV S and L segments with viral genes replaced by either fLuc or GFP
 705 reporter genes (Fig. 6). Plasmids expressing MACV L and NP in *trans* were generated
 706 by inserting viral NP and L protein genes into a Pol-II-based expression vector (pTriEx-1,
 707 pPol-II-NP and pPol-II-L). Results from my minigenome experiment (n=3 for each

reporter plasmid) confirmed the homologous MACV L and NP provided in *trans* were sufficient to support MACV minigenome RNA replication and transcription (Fig. 9). Cell monolayers visualized under a fluorescent microscope also confirmed the synthesis of GFP in the cells (Fig. 10). These results also confirmed the functionality of the UTR regions I had identified previously. Minigenome-driven fLuc reporter gene expression was substantially stronger for all minigenome constructs in the presence of NP and L protein when compared with samples transfected with the minigenome reporter plasmids only.

To further test the compatibility of MACV minigenome template with heterologous L proteins derived from other NWAs, I tested the relative efficiencies of the L protein of JUNV Romero and JUNV Candid #1 vaccine strain in supporting MACV minigenome replication. I chose the two strains of

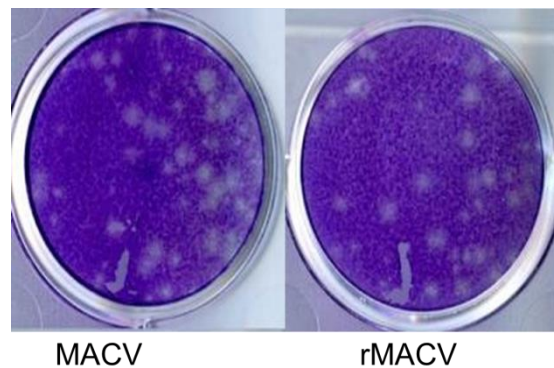


Figure 11: Plaque Morphology of MACV and rMACV. Infected Vero-CCL81 cells were fixed 8 DPI and stained with crystal violet. Size and shape of plaques for MACV and rMACV are similar providing evidence that no phenotypic change has occurred in the rMACV. Copyright Journal of Virology

JUNV, Romero and Candid#1, as they are genotypically similar to MACV. Sequencing comparison of published JUNV virus sequences (accession numbers AY619640, AY619641, AY746353, and AY746354) to MACV (accession numbers JN794583 and JN794584) identified a 69% and 72% nucleotide similarity for the L and S segments

728 respectively. Amino acid similarity between the virus segments were 73% and 87% for
729 the L and S segments.

730 Analysis of the MACV minigenome-driven fLuc expression confirmed that the L
731 protein of both JUNV and Candid#1 were compatible with MACV NP in supporting
732 MACV minigenome RNA replication and transcription (Fig. 9). These data clearly
733 showed that the L protein of JUNV could replace its MACV counterpart in the
734 minigenome systems, suggesting the feasibility of rational design of a modified rMACV
735 by introducing heterogeneous L gene from the attenuated JUNV into MACV genome.

736 Rescue of Recombinant Machupo Virus and *In Vitro* Characterization

737 To generate rMACV
738 from cloned cDNA plasmids, I
739 transfected BHK cells with
740 equimolar concentrations of
741 pPol-I-MACVSag, pPol-I-

742 MACVLag, pPol-II-NP, and
743 pPol-II-L plasmids. I collected
744 TCS at 96 hours post
745 transfection and plaque titrations identified p0 of rMACV had a titer of 8×10^4 pfu/mL.

746 To generate a working stock with higher virus titer, I infected Vero cells at an MOI <
747 0.01. The low MOI was to avoid potential formation of defective interfering particles.

Growth of MACV and rMACV in IFN Competent A549 Cells

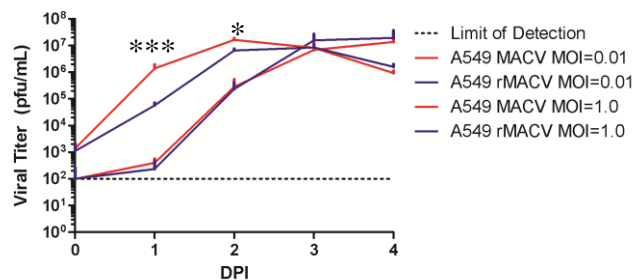


Figure 12: Infection of A549 Cells With MACV and rMACV. A549 Cells were infected with MACV or rMACV at an MOI =0.01 or 1.0 and cellular supernatant was collected every day for four days. Growth and peak virus titers for both viruses at MOI =0.01 was nearly identical. A significant difference at 1 DPI (***P<.001, two-way ANOVA) and 2 DPI (* P<.05 two-way ANOVA) was observed in cells infected at an MOI=1.0. By 3 and 4 DPI no significant difference was observed. Copyright Journal of Virology

748 TCS were harvested at 96 HPI and purified according to manufacturer's protocol
 749 (Millipore Amicon Ultra Centrifugal Filters 100K, UFC910096). Whole genomic RNA
 750 sequence analysis of rMACV confirmed no additional mutations other than the genetic
 751 marker introduced to the rMACV genome RNA (Fig. 8).

752 Plaques formed by both viruses on Vero cells at 8 DPI were similar in their
 753 morphology and size (Fig. 11). TCS collected from rMACV and MACV infected IFN
 754 competent A549 cells

755 demonstrated very similar
 756 growth curve in at MOI=0.01.
 757 A549 cells infected at an
 758 MOI=1.0 with rMACV and

Growth of MACV and rMACV in IFN Incompetent Vero Cells

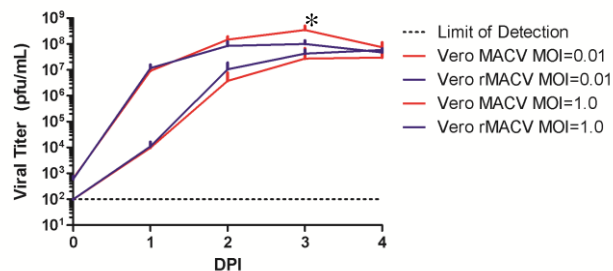


Figure 13: Infection of Vero Cells.

IFN incompetent Vero cells were infected with MACV or rMACV at MOI =0.01 or 1.0 and TCS was collected from 0 to 4 DPI. Cells infected at MOI =0.01 had similar growth titers and peak throughout the days observed. TCS from cells infected at MOI=1.0 had a significant difference in viral load at 3 DPI ($P<.05$, two-way ANOVA) but comparable titers on other days collected. Copyright Journal of Virology

759 MACV had similar growth
 760 pattern and final peak titer but
 761 experienced a significant
 762 difference in titer at 1 and 2 DPI (two-way ANOVA) (Fig. 12). TCS from IFN
 763 incompetent Vero-CCL81 cells infected at MOI=0.01 had similar growth and titers for all
 764 four days observed while cells infected at MOI=1.0 had a significant difference ($p<.05$,
 765 two-way ANOVA) at 3 DPI but had comparable growth titers at other days observed.
 766 (Fig. 13), indicating the rescued rMACV replicated similarly as its parental wild type
 767 MACV in cultured cells.

In vivo Characterization of Machupo Virus in IFN- $\alpha\beta/\gamma$ R^{-/-} Mice

To examine and compare the disease development and pathogenesis caused by the parental and recombinant MACV *in vivo*, I completed two experiments in which C57BL/6 IFN- $\alpha\beta/\gamma$ R^{-/-} (n=25) and wild type C57BL/6 mice (n=10) were challenged IP with 1×10^4 pfu of MACV or rMACV. Two IFN- $\alpha\beta/\gamma$ R^{-/-} mice were mock challenged with PBS as a negative control. Changes in temperature and bodyweight were observed throughout the study. From 10-15 DPI, significant weight loss (P value from <0.05, two-way ANOVA) was identified in the MACV and rMACV infected IFN- $\alpha\beta/\gamma$ R^{-/-} mice when compared to the infected wild type mice (Fig. 14). At 20 DPI, neurological impairment, including partial paralysis, hunched posture, labored breathing, and awkward gait, were observed in IFN- $\alpha\beta/\gamma$ R^{-/-} mice infected with MACV and rMACV. In contrast, the wild type mice infected by either wild type or rMACV did not exhibit any observable symptoms.

From 1 to 20 DPI there was no significant change in temperature observed among any of the mice groups. Starting at 22 DPI the infected IFN- $\alpha\beta/\gamma$ R^{-/-} mice began

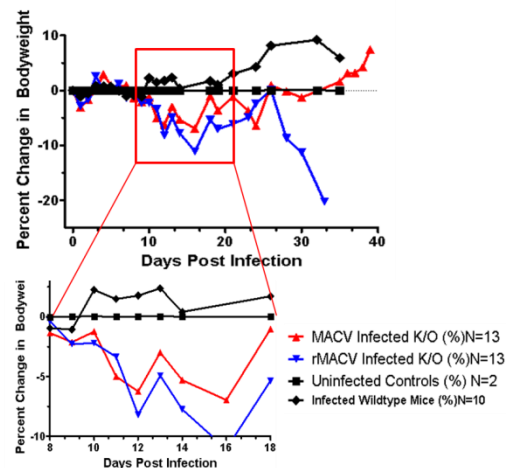


Figure 14: Change in Percent Bodyweight of Infected IFN- $\alpha\beta/\gamma$ R^{-/-} mice. Mice were weighed throughout the study to track disease development. A significant difference was observed between 10-15 DPI in infected -/- when compared to uninfected controls and infected wild type mice (two-way ANOVA, P value ranging from <.05 to <.001. No difference was observed between the two -/- groups infected with rMACV and MACV. Copyright Journal of Virology

788 succumbing to disease (Fig. 15). Significant weight loss (Fig. 14) and temperature
 789 decline (data not shown) were observed 1 to 3 days in all animals prior to death. The
 790 mortality rate for both viruses was 93% with an average time to death of ~31 DPI when
 791 pooling the data from both studies. There was no significant difference in the MTD
 792 between the two viruses (p=0.16,
 793 Log Rank test).

794 Titrations of organ
 795 homogenates confirmed similar
 796 viral load between rMACV and

797 MACV in infected animals (P<.05,
 798 Paired T-Test). A high viral load in
 799 the CNS was observed by 24 DPI
 800 ($\sim 10^8$ pfu/gram) which was

801 maintained until death (Fig. 16, Appendix IV). The single surviving mouse infected with
 802 MACV was euthanized at 40 DPI, and had no detectable viral load in the brain (data not
 803 shown). Titrations of kidney homogenates identified a slight increase from 14 DPI to
 804 clinical endpoint (Fig. 16, Appendix IV). Liver homogenates had a peak titer at 14 DPI
 805 with a generalized downward trend until clinical endpoint (Fig. 16, Appendix IV). Lung
 806 homogenates had a peak titer at 24 DPI (Fig. 16, Appendix IV). Spleen samples had a
 807 peak titer at 14 DPI with a generalized decrease until clinical endpoint (Fig. 16, Appendix

Survival curve of MACV and rMACV infected mice

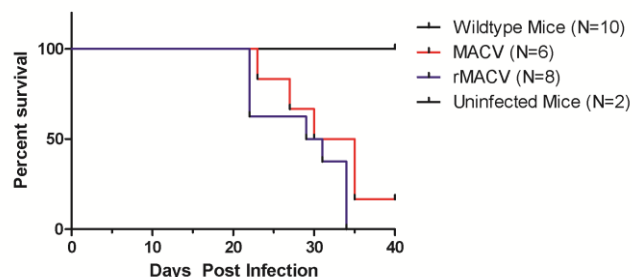


Figure 15: Kaplan Meier Curve of MACV and rMACV Infected Animals.
 Graphical representation of survival data from two pooled studies utilizing IFN $\alpha\beta/\gamma$ R^{-/-} mice. Animals were challenged IP with 1×10^4 pfu of MACV or rMACV in 100 μ L of DPBS and observed for disease development. Animals were euthanized when they reached greater than 20% body weight or became moribund/paralyzed. No significant difference was observed in the time to death (P=.16, Mantel Cox test). One IFN $\alpha\beta/\gamma$ R^{-/-} mice survived challenge with MACV. Copyright Journal of Virology

808 IV). These samples were also most likely to have no viral titer when compared to other
809 organ homogenates. The animals were not perfused prior to necropsy which means blood
810 was collected along with all organs. As virus was identified at 14 and 24 DPI from serum
811 samples, some of these viral loads may be due to viremia and not organ infection as mice
812 were not perfused prior to necropsy (Fig. 16, Appendix IV). Titrations from the organ
813 homogenates of the wild type mice showed no except in a single brain sample from an
814 animal euthanized at 14 DPI confirming previous reports of the resistant nature of the
815 inbred adult mice to MACV (Data not shown). Organ viral loads from mice infected with
816 MACV or rMACV had similar titers (Appendix IV).

817 Histopathology analysis of tissues from infected IFN- $\alpha\beta/\gamma$ R $-/-$ mice
818 demonstrated increasing neuronal damage starting at 14 DPI up to death along with
819 minor vascular and perivascular mononuclear infiltrates in the cortex of the brain
820 (Appendix II). The spleens of IFN- $\alpha\beta/\gamma$ R $-/-$ mice infected with MACV or rMACV
821 showed prominent alterations in microarchitecture with an increase in white pulp volume
822 and expansion of the periarteriolar lymphoid sheath (Appendix 1). The spleen of the
823 uninfected IFN- $\alpha\beta/\gamma$ R $-/-$ mice showed normal white pulp architectures (Appendix II).
824 Immunohistochemical (IHC) staining of the same brain slides confirmed an increasing
825 amount of viral antigen from 14 DPI until death (Appendix III).

826

827 **DISCUSSION:**

828 The sequencing of MACV has clearly shown that the terminal 19 nucleotide
829 sequences at the 5' and 3' UTRs are different from sequences of MACV previously
830 reported in the GenBank. Compared to my new data, the MACV sequences available
831 from GenBank (JN794584 and AY619643) have the C6A and G8U substitutions at the
832 5'-end of the S segment, which predict a perfect base pairing between the 5' and 3' ends
833 of the S segment. My new data suggested two mismatches at positions 6 and 8 in the
834 same region (Fig. 6), which is consistent with the sequences of other arenaviruses such a
835 JUNV, LASV, and Lujo virus (38, 124, 150, 151).

836 The terminal 19 nucleotides at the 5' and 3' ends of L and S genomic RNAs are
837 highly conserved among arenaviruses and play critical roles in viral RNA replication and
838 transcription. Although mutations in positions 6 and 8 are relatively better tolerated than
839 changes in other positions, a previous study using a LASV minireplicon system has
840 demonstrated the same C6A and G8U mutations at the 5'-end of S genomic RNA greatly
841 inhibit LASV viral gene expression by 60% and 90%, respectively (Fig. 17) (150). For
842 JUNV, RNA sequences with the same C6A and G8U substitutions at the 5' terminus of S
843 segment were reported in GenBank (AY619641) and were determined to be non-
844 functional for the rescue of a recombinant JUNV virus (38).

My attempts to rescue MACV with UTRs different from our identified sequence were unsuccessful, highlighting the critical role of these highly conserved sequences at the 5' and 3' termini of viral genomic RNA in viral replication (Data not shown). Additionally, a previous study showed the important role of the 3' terminal sequence of the MACV S segment in MACV RNA polymerase recruitment (39). The difficulty in generating the entire L segment plasmid has been reported in our laboratory for MACV, JUNV, and LASV. The reason for this difficulty is not yet understood. It is possible the complete insertion plasmid is unstable or has a cytotoxic effect on the competent cell. Once I had the first fragment generated and ligated the entire segment together into the plasmid, I did not identify a loss of the segment within the plasmid. The extended incubation time to grow the plasmid in competent cells when compared to the S segment leads me to believe the insertion has a deleterious effect on the growth of the cell, and that this effect is localized to first 2600 basepairs of the L segment. It is not known if this deleterious effect has an influence in normal host infections.

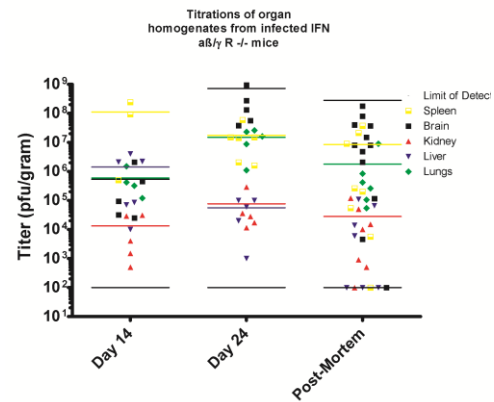


Figure 16: Titration of Organ Samples. Brain homogenate samples (red) show an increase in viral titer from 14 DPI. Kidney homogenate (blue) has a gradual decrease in titer from 14 DPI to death. Liver homogenate (green) had a peak titer at 14 and 24 DPI with a decrease at time of death. Lung homogenate (yellow) had a high viral load in a single animal at time of death. Spleen homogenate (purple) had a peak titer at 14 DPI with a decrease until time of death. Modified from an image copyrighted Journal of Virology

865 The minigenome was utilized to confirm that the MACV L protein and NP were
 866 sufficient to support efficient viral RNA transcription and replication of the MACV
 867 minigenome genome. The establishment of a MACV derived minigenome will provide
 868 an additional tool to study the molecular biology of new-world arenaviruses. Minigenome
 869 assays of other arenaviruses have been proven as useful tools in dissecting the role of

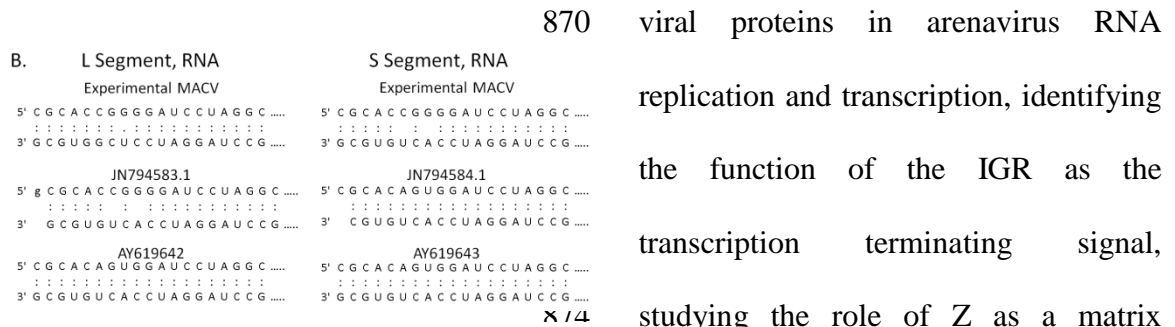


Figure 17: MACV Segment Termini Alignment.
 The alignment of the 19 bp alignment at the 5' and 3' termini
 ends of the S and L segment are vital for virus transcription.
 Sequencing of MACV confirmed a nearly 100% alignment in
 the L segment while the S segment had two distinct mismatch
 bps at the 6 and 8 position. When compared to published
 sequences online of the S segment of MACV, these
 mismatches are not found. Copyright Journal of Virology ,

878 MACV could assist in studying the replication of this virus in the BSL-2 environment or
 879 as a tool for testing antivirals as it has been shown for the Lassa minigenome assay (152).

880 My studies with the minigenome also provided preliminary evidence for the
 881 compatibility of Romero and Candid#1 L protein with MACV NP for replication of the
 882 MACV template. This evidence, in combination with availability of the reverse genetics
 883 system, might allow for the generation of chimeric viruses containing genetic sequence
 884 from both MACV and Candid#1. The generation of a Lassa/Mopeia reassortment virus as

885 a method of attenuation has been proven effective with OWAs, but never with NWAs
886 (153). The introduction of an attenuating sequence or the insertion of entire genes from
887 Candid#1 into the MACV backbone may allow for the rational generation of a live-
888 attenuated vaccine candidate for MACV.

889 My *in vitro* studies have proved similar growth patterns between wild type
890 MACV and rMACV. The similar growth and peak curves helps to confirm the two
891 viruses are phenotypically similar. Furthermore, *in vivo* studies provide additional
892 evidence that rMACV is similar to MACV. Challenge with rMACV and MACV led to
893 similar disease development, weight loss, neurological symptoms, and death in IFN- $\alpha\beta/\gamma$
894 R -/- mice. Viral invasion of the brain appears to have occurred in a similar manner in
895 both groups of mice with comparable peak viral loads. The findings in this study,
896 utilizing the IFN- $\alpha\beta/\gamma$ R -/- mice, identified the development of a biphasic disease with an
897 acute weight loss occurring 10 to 15 DPI and LNS between 20 to 34 DPI. Previously, a
898 lethal model of MACV infection was reported using STAT-1 -/- adult mice, which
899 succumbed rapidly to disease without developing LNS (70).

900 However, the biphasic disease described in my study is similar to some of the
901 reports of BHF in humans as well as in multiple species of NHPs experimentally infected
902 with MACV (53, 72-74). The neurological disease in the late stages of BHF in humans
903 can be correlated to the development of awkward gait, labored breathing, and partial
904 paralysis observed in my murine model (55, 154). Approximately 10% of AHF patients

905 treated with immune plasma develop a late neurological disease which has been lethal in
906 one reported case (61). In NHPs, the development of LNS has been reported in multiple
907 species with mortality near 100%, which is highly comparable to the IFN- $\alpha\beta/\gamma$ R^{-/-}
908 model reported here.

909 One of the most common complications in humans after infection with various
910 hemorrhagic arenaviruses, including Machupo and Junin virus, is the presence of
911 neurological disease, which can be lethal or result in transient or permanent neurological
912 sequelae (61, 140, 155). In addition, a portion of patients who have recovered from
913 LASF develop long term hearing loss showing a potential neurological impact of OWAs.
914 Further investigation into the pathogenesis of arenavirus neurologic disease may provide
915 key insights for multiple diseases. As the animal model I described here also progresses
916 into a lethal neurological disease, it may be an ideal tool for studying this aspect of
917 arenavirus disease compared to other rodent models.

918 The lack of disease development in the wild type C57BL/7 mice corresponds to
919 previously reported data. The gain in weight and the 100% survival rate when compared
920 to the IFN- $\alpha\beta/\gamma$ R^{-/-} mice suggests a potential and important role that the innate immune
921 response plays in BHF progression, which will need to be further elucidated. When
922 compared to the short but fatal disease that has been reported in STAT-1^{-/-} mice, with a
923 MTD of ~8 days, it may provide a better model for studying the neurological disease
924 which develops in human cases (70). Additionally, the impact of removing either the IFN

925 receptors or STAT-1, confirms the importance of the early innate immune response to
926 viral infection.

927 The experimental development of neurological disease for MACV has only been
928 described in NHPs so far, which are costly and not easy to handle in the BSL-4
929 laboratory. Utilizing mice instead of NHPs for neurological disease modeling has
930 multiple benefits. For example, many immunological and imaging tools are available for
931 further elucidation of neurological disease development, and working with mice in the
932 BSL-4 environment is considered to be safer, faster, and more cost effective than
933 research with NHPs.

934

935 **CHAPTER SUMMARY:**

936 My research has identified functional 19-nucleotide sequences at the 5'- and 3'-
937 ends of the MACV S and L genomic RNAs. I have generated a minigenome assay for
938 analyzing the replication and transcription of the S and L segments of the MACV
939 template. This new system was used to demonstrate the compatibility of L and NP
940 between MACV and two different Junin viruses. The establishment of a minigenome for
941 MACV provides a powerful tool for studying the replication kinetics and necessary
942 proteins for MACV replication within a BSL2 environment. It may also allow for future
943 studies investigating antivirals which can impact virus replication. I have successfully

944 rescued rMACV and have reported *in vitro* characterization of its growth in Vero and
945 A549 cells. I also report that MACV and rMACV cause similar disease development *in*
946 *vivo*. Following challenge in IFN- $\alpha\beta/\gamma$ R $-/-$ mice I have identified the first murine model
947 for MACV-induced neurological disease, which is similar to the severe disease reported
948 in human cases and NHPs studies. This model will be useful for future studies on the
949 virulence of MACV *in vivo*.

950 **CHAPTER 3: CHARACTERIZATION OF THE INNATE IMMUNE**
951 **RESPONSE TO MACV INFECTION *IN VITRO*.**

952 **INTRODUCTION:**

953 **Background**

954 The innate immune response plays a vital role in early recognition and cellular
955 response to viral infection. Recognition of PAMPs by PRRs initiates downstream
956 pathways leading to the establishment of an antiviral state in infected cells (78, 84, 86,
957 98, 100). Many viruses have evolved mechanisms for evading this response; prevention
958 of PRR detection, control of downstream pathways, and inhibition of immune modulator
959 synthesis are just a few mechanisms that ensure the virus has the time and environment to
960 replicate (78, 84, 156). The outcome of the back and forth interactions between a virus
961 and the innate immune response can be a helpful predictor in how a disease develops and
962 its severity.

963 Arenaviruses can cause severe disease through mechanisms not well elucidated.
964 Both NWAs and OWAs have been reported to cause lethal hemorrhagic disease but the
965 clinical presentation can vary drastically between the two complexes (5, 6, 8, 55, 71, 139-

966 141, 155, 157). OWAs, such as LASV and LCMV, are associated with low levels of IFN
967 while the NWA JUNV has been associated with extremely high levels of IFN in human
968 cases of AHF (108, 109, 139-141). In addition, a number of arenaviruses cause minimal
969 to no clinical disease in humans but are genotypically similar to those viruses that cause
970 hemorrhagic disease (158-160).

971 A comparison of these distinct viruses can be difficult, especially considering that
972 the research involving hemorrhagic viruses requires a high containment facility. Much of
973 what is known about arenaviruses, MACV in particular, was learned using less virulent
974 arenaviruses, such as LCMV, or through plasmid expressed viral proteins. Without live
975 virus infection modeling or analyzing the effect of a disease can be very difficult.
976 Utilization of these tools has provided a better understanding of the basic interactions
977 with a host system, and important insight into the human innate immune response.
978 However, utilization of these model systems could have provided results that do not
979 represent the entire arenavirus population, especially that of the hemorrhagic NWAs. The
980 expansion of national high security biosafety facilities provides us better opportunities to
981 study the virulent viruses and their pathological effect directly without requiring the
982 utilization of attenuated or non-virulent models.

983 Infection of dendritic cells and macrophages by LASV have been reported to have
984 low levels of type I IFNs and other proinflammatory cytokines corresponding to the
985 clinical description of LASF (105, 106). Arenaviruses have been reported to impact the

innate immune response in a number of different ways at different targets along the IFN induction pathway. It has also been reported that LASV infected dendritic cells are unable to activate CD4⁺ and CD8⁺ T cells efficiently (107). The NP of LCMV has been shown to bind IRF3 interfering with IFN induction following coinfection with Sendai virus (161). The NP from LCMV, LASV, JUNV, and MACV has been reported to interfere with NF- κ B translocation and initiation of gene transcription (118). The 3' to 5' exonuclease activity of LASV and Tacaribe virus of plasmid expressed NP has also been reported as a method of evading viral recognition by the cell (162, 163). The LCMV NP and plasmid expressed NP from JUNV, MACV, LASV, Whitewater Arroyo virus, and Latino virus have all been reported to inhibit IRF-3 phosphorylation and translocation (116, 117, 164). The plasmid expressed Z protein from JUNV, MACV, and other NWAs has been shown to bind with RIG-I, inhibiting signaling with downstream IPS-1 and preventing IFN induction (120).

Gaps in knowledge

The utilization of plasmid expression systems and arenaviruses other than hemorrhagic NWAs as prototypical models, has led to the formation of two dogmas within the field. The first dogma is that pathogenic arenaviruses evade the cellular immune response and do not induce IFN production. The second dogma is that infection with pathogenic arenaviruses does not lead to the phosphorylation of PKR or eIF2 α . The data, which led to these dogmas, was acquired primarily through models and not through

1006 research with infectious hemorrhagic NWAs such as JUNV and MACV. These dogmas
1007 do not correspond with known clinical data from patients with AHF or animals infected
1008 with JUNV and MACV (111, 165). Further illumination of the impact of MACV
1009 infection on host protein biosynthesis and the corresponding innate immune response can
1010 be an important step in developing therapies and therapeutics that can decrease mortality
1011 rates during an outbreak. In addition, correctly categorizing JUNV and MACV as distinct
1012 modulators of the innate immune response from other arenaviruses is necessary to further
1013 progress within the research field.

1014 **Hypothesis**

1015 Based upon the reports of AHF, the data from animals infected with MACV or
1016 JUNV, and the data recently published from our laboratory on JUNV infection inducing
1017 IFN, I hypothesize that infection by MACV will induce an innate immune response
1018 comparable to that of JUNV. I expect my results to identify an uninhibited IFN induction
1019 and downstream signaling pathway in cells infected with MACV.

1020 **Significance**

1021 Characterization of the impact of MACV infection on the innate immune response
1022 will benefit the field of arenavirus research, as it will provide further evidence for the
1023 separation of pathogenic NWAs from other arenaviruses. It will provide further evidence
1024 that utilizing plasmids expression systems or nonpathogenic arenaviruses as prototypical

1025 models does not always provide accurate data. Finally, identification of how MACV
1026 impacts the innate immune response may provide key insights into developing antivirals
1027 which can prevent disease development.

1028 **METHODS:**

1029 **Cells, Viruses, and Biosafety**

1030 Baby hamster kidney (BHK-21) and Vero cells (American Tissue Culture
1031 Collection) were maintained in Dulbecco's modified Eagle's medium supplemented with
1032 10% fetal calf serum and L-glutamine. The wild-type Carvallo strain of MACV
1033 (Genbank accession no. JN794583.1 and JN794584.1) was obtained from Dr. Thomas G.
1034 Ksiazek (University of Texas Medical Branch [UTMB]). Viral working stocks of the
1035 wild type and recombinant virus was generated by infecting Vero cells (multiplicity of
1036 infection [MOI] = 0.01 plaque forming unit (PFU)/cell) and collecting virus containing
1037 tissue culture supernatant (TCS) at 96 hours post infection (HPI). Cellular debris was
1038 eliminated from the TCS through centrifugation and the viruses were concentrated and
1039 purified through Ultra 100K Filter Devices (Ultracell 100K centrifugation filter, Amicon)
1040 to remove cellular factors, which may affect the immune response. All work with
1041 infectious MACV and rMACV was performed in the UTMB BSL-4 facility in
1042 accordance with institutional and safety guidelines.

1043

1044 **Knockdown of RIG-I in A549 Cells**

1045 A549 cells with a knockdown of RIG-I gene expression were provided by Dr.
1046 Tseng (UTMB) and the description on how they were generated can be found in a recent
1047 publication from our laboratory (114). In brief, ON-TARGET plus SMART pool siRNA
1048 targeting RIG-I or a Non-targeting Pool (Thermo Fisher Scientific Inc.), were transfected
1049 into A549 cells by electroporation Amaxa Cell Line Nucleofector Kit T (Lonza
1050 Walkersville, Inc.) according to manufacturer's protocols.

1051 **Plaque Titrations**

1052 All plaque titrations were completed on Vero-CCL81 cell lines, seeded on 12-well
1053 plates ~16 hours prior to infection. Samples were serially diluted in DMEM with 2% FBS
1054 and .5% P/S. Cells were infected with 100µl of diluent and incubated for ~1 hour with
1055 agitation every 15 minutes. Wells were then overlayed with a 50:50 warmed mixture of
1056 2% agarose in H₂O and 2X MEM with 10% FBS and .5% P/S. The plates were incubated
1057 for 8 days post infection (DPI) and fixed with 10% formalin solution. Cells were stained
1058 with crystal violet and plaques were counted to determine viral load.

1059 **Western Blots and Antibodies:**

1060 Cellular lysate samples were collected by removing supernatant, washing the cells
1061 with PBS, and incubating the cells for ~3 minutes with sample lysate buffer (BioRad, 2x
1062 Laemmli Sample Buffer). Samples were frozen at -80°C until they were removed from

1063 the BSL-4 following GNL sample removal guidelines. Samples were heated to 95°C for 5
1064 minutes prior to being loading onto the gel. Samples were resolved on 4-20% SDS-PAGE
1065 gels (Bio-Rad Precast gels, Catalog #4561093 and 4561096) using a Mini Trans-Blot
1066 Electrophoretic Transfer Cell apparatus (Bio-Rad, Catalog #170-3930). Samples were
1067 then transferred to PVDF membranes using a Trans-Blot SD Semi-Dry Transfer Cell
1068 apparatus (Bio-Rad, Catalog #170-3940) according to manufacturer's recommended
1069 protocol. Membranes were incubated overnight at 4°C with the primary antibody.
1070 Membranes were washed and the appropriate secondary antibody was incubated for 1
1071 hour at room temperature.

1072 Proteins were visualized using ECL Western blotting Detection Reagents (GE,
1073 NJ) according to the manufacturer's instruction. Primary antibodies used for Western
1074 blotting analysis were rabbit anti-phosphorylated STAT1 antibody (#9171, Cell
1075 Signaling), mouse anti-STAT-1 antibody (WH0006772M1, Sigma), rabbit anti-IRF 3
1076 antibody (ab76409, Abcam), rabbit anti-PKR (#3079, Cell Signaling), rabbit anti-
1077 phosphorylated PKR (#2283-1, Epitomics), rabbit anti-eIF2 α (#9722, Cell Signaling),
1078 rabbit anti-phosphorylated eIF2 α (#9721, Cell Signaling), monoclonal anti-Junin
1079 immunoglobulin G targeting NP of MACV (BEI Resources, NA05-AG12), and goat anti-
1080 human β actin antibody (sc-1616, Santa Cruz Biotechnology). Secondary antibodies used
1081 were HRP conjugated goat anti-rabbit IgG (#7074, Cell Signaling), HRP conjugated Goat
1082 anti-mouse IgG (115-035-146, Jackson Immunology) and HRP-conjugated donkey anti-

1083 goat IgG (sc-2020, Santa Cruz). These methods are described in previous publications
1084 from our laboratory (114).

1085 **Statistics:**

1086 GraphPad Prism V5.0 was used for all statistical calculations. Viral growth curve
1087 analysis was completed utilizing a two-way ANOVA test comparing all virus and cell
1088 culture TCS over each day.

1089 **RESULTS:**

1090 **Effect of RIG-I Knockdown on MACV Growth**

1091 The cytoplasmic PRR
1092 RIG-I plays a pivotal role in
1093 recognizing JUNV infection and
1094 initiating induction of IFN
1095 production (114). To identify if

1096 RIG-I also has an effect on
1097 MACV infection, I seeded
1098 twelve well plates ~16 hours
1099 prior to infection with either A549 Control cells, cells containing an inserted Non-
1100 Targeting siRNA, or A549 RIG-I-K/D cells with siRNA targeting RIG-I. I infected cells
1101 with MACV (MOI=0.01) and collected TCS at 0, 24, 48, 72, and 96 HPI. Titration of

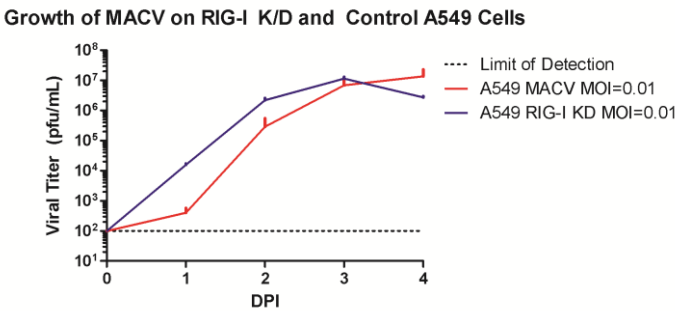


Figure 18: Effect of RIG-I Knockdown on MACV Growth in A549 Cells.
The TCS from A549 cells, either K/D or control transfected, infected at an MOI=0.01 with MACV was collected for 4 DPI. While virus growth followed a similar pattern a significant difference was observed at 1, 2 and 4 DPI (P<.001, <.01, <.01 respectively, two-way ANOVA). Cell monolayer by 4 DPI was badly damaged in wells infected with both viruses.

1102 samples confirmed significant impact on virus growth at 1(P<.001), 2(P<.01), and
 1103 4(P<.01) DPI (two-way ANOVA) (Fig. 18).

1104 **Effect of Infection on IFN Competent Cells**

1105 To elucidate the impact of MACV infection on IFN competent A549 cells, I
 1106 infected A549 cells with MACV (MOI=0.01) and collected cellular lysate at 24, 48, and
 1107 72 HPI. Uninfected control A549 samples
 1108 were collected concurrently with infected
 1109 lysates for the Western blot analysis.
 1110 Phosphorylation of STAT-1 (pSTAT-1)
 1111 occurs following induction of interferon
 1112 production, which activates JAK leading to
 1113 phosphorylation of STAT-1. In the case of
 1114 type I IFNs, pSTAT-1 complexes with
 1115 pSTAT-2 and IRF-9. The complex
 1116 translocates into the nucleus, binding to
 1117 interferon stimulated response element and
 1118 inducing transcription of ISGs, such as
 1119 ISG15 and STAT-1. Cellular lysate samples
 1120 were collected from IFN competent A549
 1121 cells at 24, 48, and 72 HPI and a notable difference was detected in protein concentration

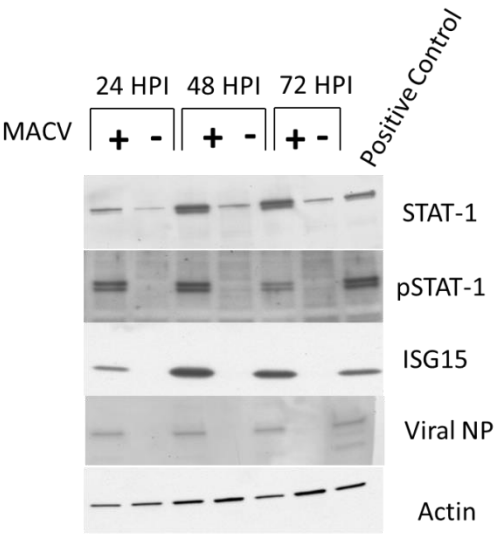


Figure 19: Activation of the JAK/STAT Pathway in IFN Competent A549 Cells Infected With MACV. A549 cells were mock-infected or infected with MACV at MOI=1.0. Cellular lysates were prepared and resolved by Western blot. Analysis identified increasing levels of the ISG STAT-1 for all time points resolved when compared to uninfected controls. The presence of pSTAT-1 was confirmed in all infected cellular lysates with a peak at 48 HPI. ISG15 production was also confirmed with a peak at 48 HPI. A positive control of cells infected with Candid#1 was utilized as it has been previously shown to induce IFN production in A549 cells within my laboratory.

1122 of pSTAT-1 when compared to uninfected A549 cells. The increase in pSTAT-1
 1123 provides direct evidence of type I IFN signaling (Fig. 19) with high levels of pSTAT-1
 1124 when compared to uninfected controls through 72 HPI.

1125 To provide further evidence of type I IFN synthesis, I analyzed downstream
 1126 protein production linked to IFN signaling, specifically interferon stimulated genes
 1127 (ISGs). I detected an increase in STAT-1 concentration when compared to the controls in
 1128 all time points collected with a peak
 1129 concentration at 48 HPI (Fig. 19).

1130 Additionally, total ISG15 concentration was
 1131 increased when compared to control samples
 1132 with a peak at 48 HPI (Fig. 19). To confirm
 1133 that MACV had generated a viable infection
 1134 in the A549 cells, I utilized an anti-NP
 1135 MACV/JUNV monoclonal antibody to detect

1136 production of this viral protein. As a loading
 1137 control, I analyzed concentration levels of
 1138 actin in all samples. My positive control was
 1139 a cellular lysate sample of A549 cells
 1140 infected with Candid#1 collected at 48 HPI
 1141 (Fig. 19).

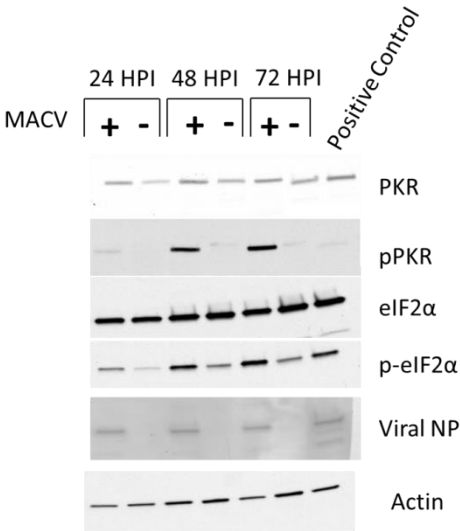


Figure 20: Recognition of MACV Infection by PKR in A549 Cells.
 A549 cells were mock-infected or infected with MACV at MOI=1.0. Cellular lysates were prepared and resolved by Western blot. Analysis identified increasing and higher levels of the ISG PKR when compared to mock-infected cells. Resolution also identified high levels of p-eIF2α when compared to mock infected cells. Interestingly A549 cells infected with Candid#1 as a positive control experienced increased levels of p-eIF2α but not pPKR.

1142 **Effect of MACV Infection on Cellular Protein Biosynthesis**

1143 To investigate the impact of MACV infection on cellular protein biosynthesis, I
1144 looked at phosphorylation of PKR and eIF2 α . Samples collected from IFN competent
1145 A549 cells at 24, 48, and 72 hours were resolved by Western blot. I detected an increase
1146 in PKR and phosphorylated PKR (p-PKR) concentrations starting at 24 HPI and peaking
1147 at 72 HPI (Fig. 20). I identified no discernable change in eIF2 α levels at any time point
1148 between infected or uninfected cells (Fig. 20). Levels of phosphorylated eIF2 α (p-eIF2 α)
1149 in infected cells were detected at all time points collected. Uninfected cells also showed
1150 an increasing level of p-eIF2 α but with markedly lower concentrations than infected cells
1151 (Fig. 20).

1152 **DISCUSSION:**

1153 The paucity of clinical data from patients infected with MACV has made it very
1154 difficult to describe the host innate immune response. Unlike JUNV, where high levels of
1155 IFN in clinical cases has been well described, the only published data relevant to MACV
1156 and IFN production is a NHP model which investigated the potential of Polyinosinic:
1157 polycytidylic acid (poly I:C), a synthetic dsRNA analog and toll-like receptor 3 agonist,
1158 treatment (108, 111). This study reported detectable IFN by 3 to 5 DPI with a peak level
1159 of around 700 units of IFN in infected untreated animals. Stephen *et al.* also showed that
1160 treatment with poly I:C lead to earlier detection of viremia and higher titers in treated
1161 NHPs (111). There was no significant difference in late stage disease, or a decrease in

1162 mortality rate when compared to untreated animals. These published results correspond to
1163 my *in vitro* data presented in Chapter 2 in which peak titer of MACV in IFN competent
1164 cells was not significantly affected, as seen with MACV growth in IFN incompetent Vero
1165 cells. While a significant difference in the virus growth curve was identified at 1 DPI, no
1166 significance was identified at any other time point collected (Fig. 18).

1167 While no clinical data exists from MACV infected patients, recent studies
1168 utilizing plasmid over expression of MACV or JUNV NP *in vitro* identified an inhibition
1169 of IRF-3 translocation (116). In contrast, recent work by Cheng *et al.* reported strong IFN
1170 production in cells infected with JUNV (114). My data further supports the distinction
1171 between NWA vs OWA and infectious virus vs plasmid protein expression.

1172 My results support that MACV infection in IFN competent cells induces
1173 upregulation of interferon production leading to expression of ISGs (Fig. 19). Previous
1174 publications that reported an inhibition of IFN induction in Vero cells could be correct as
1175 Vero cells are IFN deficient (166-168). Additionally, overexpression of NP by plasmid
1176 instead of through viral replication, as was used in these studies, could result in higher
1177 concentrations of NP than what is seen during an infection. The higher levels of NP may
1178 exaggerate the proteins capability to control the innate immune response. While clinical
1179 data and *in vitro* data supports the rational that low levels of IFN are induced during
1180 LASV infection, reports human cases of AHF identify high levels of endogenous IFN- α
1181 (109). Due to the variances reported in human cases of AHF and LASF, a case can be

1182 made that a distinction between NWAs and OWAs should be made, especially as it
1183 relates to induction of innate immune response in human cells. However, considering the
1184 extended incubation period of both MACV and JUNV, some mechanism of controlling
1185 the innate immune response is reasonable and must be addressed.

1186 A correlation between high levels of IFN with severe outcome in patients with
1187 AHF has been reported (109). My data also clearly demonstrates that the infection with
1188 MACV can affect cellular protein biosynthesis, which is in contrast with the model of
1189 LCMV cell infection. When compared to the extended incubations and persistent
1190 infections, which are reported in JUNV, MACV, and LCMV, this data is intriguing.
1191 Many viruses that cause persistent infection have evolved mechanisms to avoid
1192 impacting cellular protein biosynthesis (156). Infection by LCMV does not induce eIF2 α
1193 phosphorylation in Huh 7 cells, but does lead to disassociation of BiP from ATF6, an
1194 essential mediator of endoplasmic reticulum (ER) stress (169). This disassociation
1195 commonly occurs in the presence of high concentrations of misfolded proteins (16, 169,
1196 170). The paper by Pasqual *et al.* also reported that the disassociation of ATF6 played an
1197 important role in viral titers during acute but not persistent infection of LCMV.

1198 Further investigations on the effect of MACV on the innate immune response can
1199 follow a number of paths. First, the cytoplasmic PRR responsible for recognizing MACV
1200 infection must be confirmed. While MACV is very similar to JUNV and it is reasonable

1201 to assume that the RIG-I is the primary PRR for recognizing MACV, it must be
1202 confirmed.

1203 The next step to further elucidate the impact of MACV and mechanism of
1204 immune modulation on cell protein biosynthesis is to identify activation of PKR. There
1205 are multiple mechanisms for PKR activation; recognition of dsRNA, interaction with the
1206 protein PACT (PKR activating protein), or overexpression of ISG15, all of which can
1207 lead to phosphorylation of PKR (171, 172). The primary method of activation of PKR is
1208 recognition of viral dsRNA, which is believed to be generated during the viral replication
1209 cycle. Interestingly, arenaviruses have been reported to induce discrete cytosolic
1210 structures where replication can take place potentially sequestering any dsRNA
1211 intermediates from PKR recognition (173). While PACT has been shown to activate
1212 PKR, it also has been shown that this activation does not play a role in an antiviral
1213 response (174). As my results confirm upregulation of ISG15 following infection, I
1214 would propose investigating if it plays a role in PKR activation. This can be
1215 accomplished utilizing the siRNA-transfected cell line targeting the PRRs described
1216 previously or utilizing siRNA targeting ISG15 specifically. If PKR activation continues
1217 without expressed ISG15, it would be reasonable to assume dsRNA is the primary
1218 instigator of activation.

1219 In addition to reports of LCMV induction of ER stress through ATF6, and in
1220 contrast to previous reports of negligible eIF2 α phosphorylation, my data supports that

1221 MACV infection leads to strong phosphorylation of eIF2 α in IFN competent cells. My
1222 data suggests the phosphorylation of eIF2 α does not affect virus growth. While inhibition
1223 of PKR activation by viral proteins is well described, descriptions of how viruses
1224 overcome phosphorylation of eIF2 α appears to be less common. Poliovirus has been
1225 shown to cleave eIF5B to rescue biosynthesis through an eIF2 α independent mechanism
1226 (175). Alternatively, human T-cell leukemia virus type 1 has been shown to upregulate
1227 and stabilize the suppressor of cytokine signaling (SOCS) 1 that acts as a negative
1228 regulator of JAK/STAT signaling (176). MACV infection of A549 cells causes the
1229 phosphorylation of eIF2 α , yet the cell continues to produce infectious virus. The
1230 mechanism of virus replication must be identified as it appears MACV can still grow in
1231 cells with by phosphorylated eIF2 α .

1232 Interestingly, the Western blot data (Fig. 19 and 20) also confirmed there was no
1233 significant change in concentration of actin in the cellular lysate, even though eIF2 α had
1234 been phosphorylated for more than 48 HPI. Further investigation is necessary to
1235 determine if MACV is capable of restoring cell protein biosynthesis completely. This
1236 could be accomplished utilizing radiolabeled S³⁵ or P³² in a Pulse-Chase experiment
1237 model in future experiments. A variant of pulse-chase experimentation, utilizing mass
1238 spectrometry with radio labeled amino acids, could also be utilized to identify a change in
1239 whole cell protein synthesis (177). This methodology would allow us to determine at

1240 different time points when synthesis is being impacted and if there is a specific period at
1241 which MACV is able to overcome eIF2 α phosphorylation.

1242 **CHAPTER SUMMARY:**

1243 In this chapter I present data demonstrating that the MACV infection can induce
1244 an innate immune response in IFN competent cells. I showed that STAT-1
1245 phosphorylation and ISG upregulation occurs within 1 DPI in A549 cells. Finally, I
1246 showed that both PKR and eIF2 α are phosphorylated, which commonly occurs in cells
1247 entering an antiviral state leading to downregulation of cellular protein biosynthesis. This
1248 data contradicts commonly held dogma of arenavirus innate immune evasion and their
1249 impact on cellular biosynthesis. These dogmas have been established utilizing plasmid
1250 expression systems or nonpathogenic NWAs. My data is similar to IFN induction in
1251 A549 cells following JUNV infection and corresponds with clinical samples of IFN
1252 induction in patients with AHF. This data is significant as it provides evidence that
1253 nonpathogenic models and expression systems may not be accurate representations of
1254 hemorrhagic NWAs and this must be considered for all future research within the
1255 arenavirus field. Additionally, further elucidation of how cells detect MACV and the
1256 mechanisms of evading biosynthesis shutdown MACV utilizes are necessary to form a
1257 more complete description of BHF, and to potentially develop novel therapeutics.

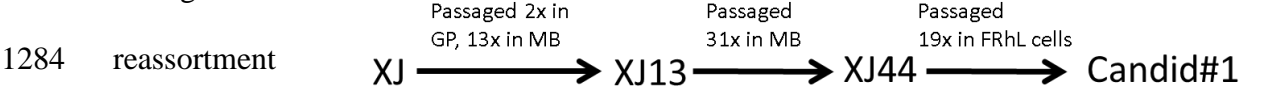
1258 **CHAPTER 4: RATIONAL ATTENUATION OF MACV***

1259 **INTRODUCTION:**

1260 **Background**

1261 With the reemergence of MACV in Bolivia and the lack of proven
1262 countermeasures, additional research must investigate methods of controlling future
1263 outbreaks. Transfusion of immune plasma has proven effective in preventing lethal AHF,
1264 if administered within eight days of disease development (65). Successful treatment
1265 through transfusion of immune plasma has been reported in a limited number of BHF
1266 cases, but there have been no clinical trials to confirm efficacy (55). Utilization of
1267 plasma requires rapid recognition of disease, available health professionals in the region,
1268 consistent collection and storage of the plasma, and the infrastructure to support these
1269 endeavors. This would be potentially difficult to achieve in the remote Beni district of
1270 Bolivia (178, 179). Preliminary studies utilizing ribavirin have had positive results in
1271 cases of both BHF and AHF, but there has been no clinical efficacy testing (67, 180,
1272 181). With the limitations of infrastructure and cost of therapeutics, a protective vaccine
1273 may prove the most effective method of preventing further outbreaks of BHF, as has been
1274 reported with Candid#1 in Argentina.

1275 The generation of a novel arenavirus vaccine candidate through reassortment has
 1276 been reported for LASV (182, 183). The novel virus, ML29, contains the L segment of
 1277 Mopeia virus (MOPV) and the S segment of LASV. It was generated through co-
 1278 infection of Vero cells with both LASV and MOPV and was selected following
 1279 identification of plaque phenotype change in cell culture. ML29 protects against lethal
 1280 LASV challenge in both guinea pig and NHP animal models providing strong evidence
 1281 for its potential as a vaccine candidate (153). However, the mechanism of reassortment
 1282 and selection brings up questions of stock purity and safety. One risk factor is that
 1283 through the



1285 process, it is possible a small portion of the virus population maintains the L segment of LASV. With the L segment
 1286 still present, it is possible to generate virulent LASV from a vaccine seed stock. These
 1287 small virus populations would need to be completely eliminated prior to clinical trials.

Figure 21: Passage History of Candid#1.
 Candid#1 has had 65 passages in different cells. The F437I mutation occurred in the last 19 passages in FRhL cells. GP-Guinea Pig, MB-Mouse Brain, FRhL- Fetal rhesus lung

1290 The generation of the attenuated vaccine strain for JUNV, Candid#1, was
 1291 accomplished through passaging the virulent XJ strain in guinea pigs, mouse brains, and
 1292 a fetal rhesus monkey lung cell line (FRhL-2) for a total of 65 different passages (Fig. 21)
 1293 (155, 184). Comparison of the amino acid sequence of Candid#1 NP, GPC, and Z
 1294 proteins to the XJ13 strain proteins has identified a number of genetic changes which
 1295 have occurred following these passages (185). Recent analysis of these mutations has

identified the F427I mutation in the GP2 transmembrane region as having an attenuating role in murine neurovirulence following challenge with the single mutant JUNV (121, 122). This region is highly conserved between MACV and JUNV (Fig. 22). Additional research is required to better elucidate the genetic mechanisms of attenuation and stability of these mutations prior to licensing within the U.S. or Bolivia.

Gaps in knowledge

While unsubstantiated reports have identified Candid#1 as protecting NHPs against MACV challenge, there is no published evidence of protection. Additionally, the reports of an increase in liver enzymes in challenged guinea pigs vaccinated with MOPV, when compared to those vaccinated with ML29, indicated that the presence of homologous antigens against the target virus may be necessary for complete protection

(153). This report of improved protection through heterologous vaccination provides evidence for the importance of a MACV derived vaccine instead of utilizing Candid#1 within Bolivia (153). The availability of MACV

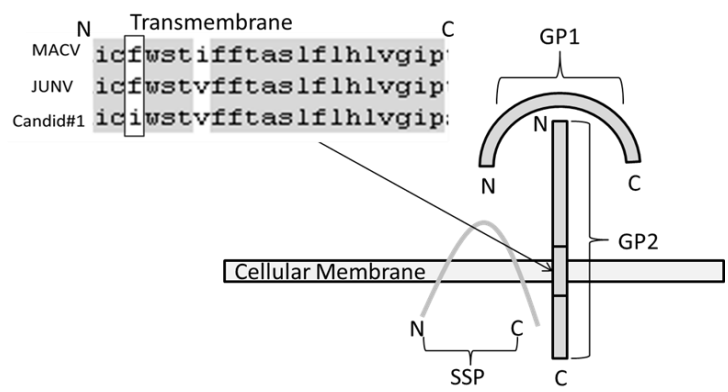


Figure 22: Transmembrane Region of MACV and JUNV. Textual and graphical representation of the transmembrane region of GPC. The alignment of amino acids making up the transmembrane region for MACV, JUNV, and Candid#1 show significant similarity with only one amino acid difference a the MACV I441 and JUNV/Candid#1 V43I residues. The highlighted residue identifies the single mutation found in Candid#1.

1316 isolates is extremely limited and there have been no reports of an attenuated strain of
1317 MACV from which to identify the genetic determinants of attenuation.

1318 **Hypothesis**

1319 The reverse genetics system developed in Aim 1 of this dissertation is an ideal
1320 tool to investigate the impact of a single mutation in MACV at the F437 amino acid
1321 residue. I hypothesize that utilizing my reverse genetics system I can introduce a
1322 mutation at the F437 amino acid position of the transmembrane region of GP2 to
1323 attenuate MACV neurovirulence in a mouse model. The lethal murine model I
1324 characterized in Aim 1 can be used to study changes in MACV virulence to determine if
1325 the mutation attenuates the virus. I expect from my results that rMACV-F437I will be
1326 attenuating *in vivo*.

1327 **Significance**

1328 The proposed modification of rMACV would be the first report of an attenuated
1329 MACV. It would provide useful insight into how NWAs other than JUNV can be
1330 rationally attenuated. It would also be the first step towards the development of a design
1331 vaccine for MACV.

1332

1333

1334 **METHODS:**

1335 **Cells, viruses, and biosafety**

1336 Baby hamster kidney (BHK-21) and Vero cells (American Tissue Culture
1337 Collection) were maintained in Dulbecco's modified Eagle's medium supplemented with
1338 10% fetal calf serum and L-glutamine. Viral working stocks of rMACV-F437I were
1339 generated by infecting Vero cells (MOI =0.01 PFU/cell) and collecting virus containing
1340 TCS at 96 HPI. Cellular debris was eliminated from the TCS through centrifugation and
1341 the viruses were concentrated and purified through Ultra 100K Filter Devices to remove
1342 cellular factors, which may affect the immune response. All work with infectious virus
1343 was performed in the UTMB BSL-4 facility in accordance with institutional and safety
1344 guidelines.

1345 **Construction of the F437I Mutant S Plasmid**

1346 To generate an S segment plasmid containing the identical amino acid change
1347 found in Candid#1, I modified the wild-type MACV S segment plasmid generated in
1348 Chapter 2 through PCR mutagenesis. To accomplish this, I designed two overlapping and
1349 reverse direction primers which contained the nucleotide change. This base pair change
1350 would cause a change from phenylalanine at residue 437 to an isoleucine (GP2-F437I-
1351 R1v2, CACATTAGTTGATATATTTGTATCTGGAGCACAAATTTTCTTC and GP2-
1352 F437I-F2v2, GAAGAAAATTGTGCTCCAGATACAAATATCAACTAATGTG).

1353 Additionally I generated two primers located downstream and upstream of the
 1354 transmembrane region (GP2-F437I-F1v2 and GP2-F437I-R2v2) that would be used to

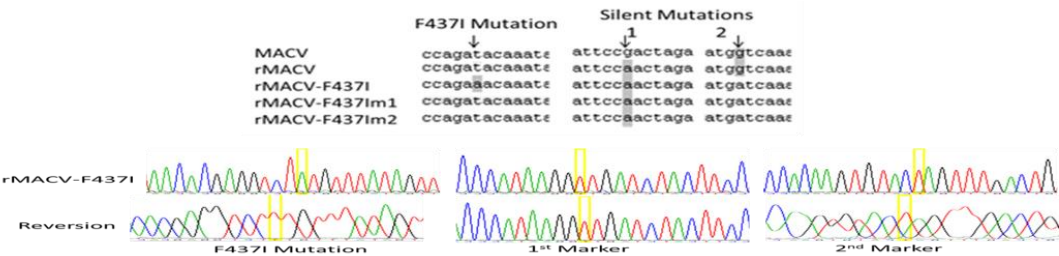


Figure 23: Sequence Analysis of rMACV-F437I.
 Graphical sequence analysis and comparison of cDNA generated from MACV, rMACV, and rMACV-F437I isolates. rMACV and MACV maintain the wild type genotype at the nucleotide coding for F437. The nucleotide change coding for I437 is present in the stock of rMACV-F437I while a reversion has occurred in the viral RNA isolated from mouse 1 and 2. The presence of the second silent marker confirms that both animals were challenged with rMACV-F437I. Chromatography analysis of sequenced viral cDNA confirming the reversion of the mutation in the consensus sequence and the presence of both silent markers.

1355 amplify the two fragments.

1356 Utilizing these four primers, I synthesized two cDNA fragments, 1.2kb and .9kb

1357 each, utilizing a high fidelity polymerase (NEB, Q5 Hot Start # M0493S). I then

1358 generated a single cDNA fragment from both smaller fragments by amplifying through

1359 the overlapping region utilizing the external forward and reverse primers. I digested the

1360 whole cDNA fragment and the original S segment plasmid inclusive of the F437I

1361 mutation and second gene marker to distinguish rMACV-F437I from rMACV, ligated the

1362 insert into the plasmid, and transfected the new plasmid into competent cells to generate a

1363 working stock of plasmid. In order to differentiate rMACV from rMACV-F437I, I

1364 introduced an additional silent mutation at the 808 nucleotide, G to A (Fig. 23). The new

1365 plasmid was sequenced by the UTMB Molecular Genetics Core to ensure the single
1366 mutation and two gene markers were present within the plasmid with no additional
1367 mutations.

1368 **Rescue of rMACV-F437I**

1369 The rescue of rMACV-F437I was completed in a similar manner as described
1370 previously by my laboratory and in Chapter 2 of this dissertation (38). Equimolar
1371 amounts of the wild type L full segment MACV plasmid and the S segment single mutant
1372 plasmid and the two expression plasmids were transfected into BHK21 cells.
1373 Supernatant from these cells was collected at 4 days post transfection. A single passage in
1374 Vero cells was performed to generate a high titer stock of rMACV-F437I. The rMACV-
1375 F437I sequence, including the introduced G808A and G1447A gene tags within the GP
1376 gene which were inserted to distinguish rMACV-F437I from rMACV and MACV, were
1377 confirmed by whole genomic sequence analysis.

1378 **Sequencing of Full Length S and L Genomic RNAs from rMACV-F437I**

1379 RNA (0.5 to 1.0 mg) was isolated by a RNA purification kit (Zymo Research,
1380 DNA-Free RNA kit, R1014) at 96 HPI from rMACV-F437I infected Vero cells. Viral
1381 cDNA was synthesized by reverse transcription (RT) using random primers. Viral
1382 specific primers complementary to S and L genome RNAs were used to generate cDNA
1383 fragments of each segment. The entire S and L segments were amplified in three and five

1384 DNA fragments, respectively. PCR products were gel purified (Zymo Research,
1385 Zymoclean Gel DNA recovery kit, D4001) and directly sequenced to obtain the
1386 corresponding master sequences for the MACV S and L genome RNAs. Sequencing data
1387 was analyzed using the program Clone Manager V9. The sequencing of RNA isolated
1388 from tissue samples follows this same procedure except Trizol sample (Zymo Research,
1389 DNA-Free RNA kit, R1014) is utilized to homogenize samples.

1390 **Plaque Titrations**

1391 All plaque titrations were completed on Vero-CCL81 cell lines, seeded on 12-well
1392 plates ~16 hours prior to infection. Samples were serially diluted in DMEM with 2% FBS
1393 and .5% P/S. Cells were infected with 100µl of diluted virus and incubated for ~1 hour
1394 with shaking every 15 minutes. Wells were then overlayed with a 50:50 warmed mixture
1395 of 2% agarose in sterile H₂O and 2X MEM with 10% FBS and .5% P/S. The plates were
1396 incubated for 8 DPI and fixed with 10% formalin solution. Cells were stained with crystal
1397 violet and plaques counted to determine viral load. When calculating the viral load of
1398 tissue samples, tissues were weighed prior to homogenization and media was added to the
1399 samples consistent to the measured weight. Utilizing these values, viral loads per gram of
1400 tissue was calculated for each sample.

1401

1402

1403 **Animal Experiments**

1404 Six-to-eight-week old IFN- $\alpha\beta/\gamma$ R $-/-$ mice on a C57BL/6 background were
1405 utilized for all studies. All animals were housed in a pathogen-free environment. All
1406 virus infections were performed in the BSL-4 in the GNL, UTMB. All animal studies
1407 were reviewed and approved by the UTMB Institutional Animal Care and Use
1408 Committee, and were completed according to the National Institutes of Health guidelines.
1409 Animals were anesthetized using an isoflurane precision variable-bypass vaporizer prior
1410 to virus inoculation by the IP route with 10^4 PFU. Telemetric monitoring of body
1411 temperature was accomplished throughout the studies. A BMDS IPTT-300 transponder
1412 (Bio Medic Data Systems, Inc.) was implanted subcutaneously using a trocar needle
1413 assembly. Transponders were read with a DAS-6007 reader (Bio Medic Data Systems,
1414 Inc.) and downloaded in accordance with manufacturer's protocol. Body weight
1415 measurements were performed throughout the studies by anesthetizing the animals and
1416 weighing them, weights were compared to baseline collected at 0 DPI (38, 149). The
1417 experimental endpoints of the studies were ~40 DPI, where surviving animals were
1418 humanely euthanized and necropsied.

1419

1420

1421

Statistical Analysis

GraphPad Prism v5 was utilized for all data analysis. To determine significance in weight and temperature change, two-way ANOVA tests were performed comparing pooled data from the infected rMACV or rMACV-F437I IFN- $\alpha\beta/\gamma$ R^{-/-} mice. Viral growth curve analysis was completed utilizing a two-way ANOVA test comparing all virus and cell culture types over each day. A Kaplan Meier survival curve was generated and statistical Mantel Cox test was completed to determine significance between rMACV and rMACV-F437I.

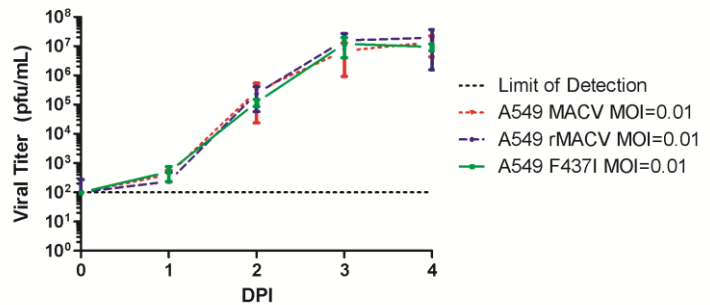


Figure 24: Infection of IFN Competent A549 Cells with MACV, rMACV, and rMACV-F437I. A549 cells were infected at an MOI=0.01 with MACV, rMACV, and rMACV-F437I. TCS was collected from 0 to 4 DPI in triplicate from infected cells and plaque titrated. No significant difference ($P>.05$, two-way ANOVA) was observed on any day between the three viruses. All three viruses had similar growth kinetics and peak titers.

RESULTS:

In Vitro Characterization of rMACV-F437I

The rescue of rMACV-F437I was accomplished in a manner similar to rMACV presented in Chapter 2 and as described in the methods of this chapter. A working stock of rMACV-F437I with a titer of 4e7pfu/mL was generated following a single passage of

1441 Vero cells. Sequencing confirmed no additional mutations were generated during the
 1442 passage. To characterize the *in vitro* growth kinetics of rMACV-F437I, I infected IFN
 1443 competent A549 cells at an MOI = 0.01. I collected TCS at 0, 1, 2, 3, and 4 DPI in
 1444 triplicate and completed plaque titrations on all samples (Fig. 24). Additionally, I infected
 1445 IFN incompetent Vero cells at an MOI=0.01 and collected TCS at 0, 1, 2, 3, and 4 DPI
 1446 (Fig. 25). Both growth curves corresponded closely with MACV and rMACV in the same
 1447 cell lines.

1448 ***In Vivo* Characterization of rMACV-F437I**

1449 To investigate the impact of the single mutation on rMACV virulence, I utilized
 1450 the IFN- $\alpha\beta/\gamma$ R^{-/-} murine model I characterized previously in Chapter 2. I hypothesized
 1451 that the introduction of

1452 the single mutation would
 1453 alter the virulence and
 1454 disease development in
 1455 infected animals. I
 1456 completed two

1457 experiments from which
 1458 the pooled data is
 1459 presented. C57BL/6 IFN-

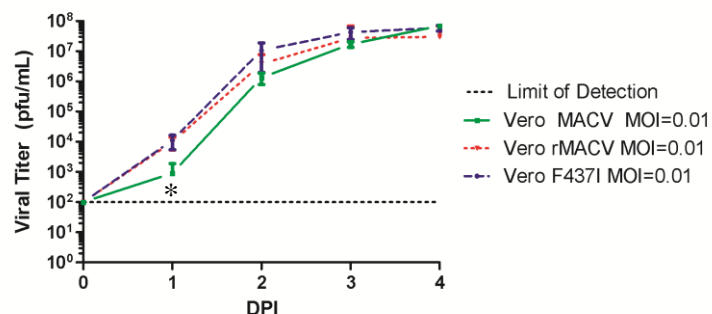


Figure 25: Infection of IFN Incompetent Vero-CLL81 Cells with MACV, rMACV, and rMACV-F437I.

Vero cells were infected at an MOI=0.01 and TCS was collected from 0 to 4 DPI. A significant difference was observed at 1 DPI between the titers of MACV and rMACV/rMACV-F437I ($P < .01$, two-way ANOVA). No significant difference was observed from 2 to 4 DPI ($P > .05$, two-way ANOVA). All three viruses grew similarly with comparable titers after 2 DPI.

1460 $\alpha\beta/\gamma$ R^{-/-} mice were challenged IP with 1×10^4 pfu of rMACV (N=9) or rMACV-F437I
1461 (N=7).

1462 Mice infected with rMACV became hunched-but-active as early as 9 DPI and I
1463 observed progressive weight loss from 10-15 DPI. Between 15 to 20 DPI all animals had
1464 no discernable disease. Starting at 20 DPI, rMACV infected mice began to develop
1465 neurological impairments. These impairments included partial to full paralysis, hunched
1466 posture, labored breathing, and ataxia. All rMACV infected animals developed lethal
1467 disease or were humanely euthanized after reaching disease endpoints defined within the
1468 study protocols (Fig. 26).

1469 In contrast,
1470 rMACV-F437I infected
1471 mice could be classified
1472 into two separate groups
1473 based upon their clinical
1474 outcome. The first group,
1475 five of the seven mice,
1476 developed no discernable
1477 disease throughout the
1478 period of the two studies.

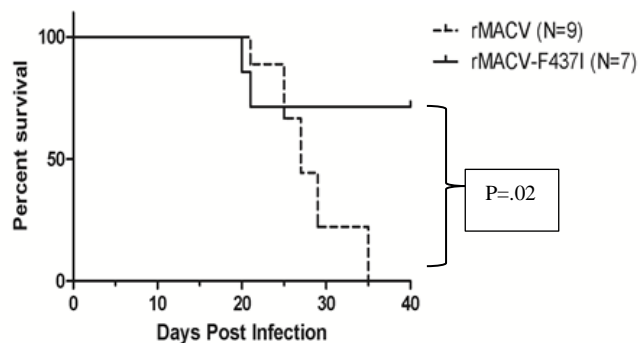


Figure 26: Kaplan Meier Curve of rMACV and rMACV-F437I Infected IFN- $\alpha\beta/\gamma$ R^{-/-} Mice.

Data is representative of two pooled studies. Mice were challenged with rMACV and rMACV-F437I through the IP route with 1×10^4 pfu/mL and observed for clinical disease. All animals challenged with rMACV reached endpoints defined by the study or were found dead with a MTD of ~27 DPI. Two of the seven animals challenged with rMACV-F437I develop endpoints defined by the study protocol, the other five developed no observable disease symptoms and were euthanized at the end of the study. A significant difference ($P=0.02$, Mantel Cox test) was observed between the two groups of animals survival rates. The two mice infected with rMACV-F437I which reached disease endpoints had a MTD of 20.5 DPI.

1479 No significant changes in temperature or weight were reported in these animals. The

1480 second group was comparable to the first group for the first 18 DPI. Starting at 18 DPI
1481 the second group became hunched-but-active and/or ataxic. By 20 DPI both animals in
1482 the second group were losing body weight and were paralyzed or moribund. One animal
1483 was euthanized at 20 DPI, and the other at 21 DPI (Fig. 26).

1484 Temperature and bodyweight data was collected throughout the two studies. At
1485 10, 14, and 15 DPI I identified significant weight loss ($p < 0.05$, Two-way ANOVA) in
1486 the rMACV infected IFN- $\alpha\beta/\gamma$ R^{-/-} mice when compared to the infected rMACV-F437I
1487 mice (Fig. 27). Additionally, a significant difference in weight change was identified at
1488 22, 24, and 27 DPI, corresponding to 1-3 days prior to individual animals succumbing to
1489 disease. There was minimal change in body temperature throughout most of the study
1490 between the rMACV and rMACV-F437I infected mice. These days correspond to the
1491 death of two animals in the rMACV pool, both of which developed hypothermia at the
1492 final temperature collection prior to death/euthanizations (Fig. 28).

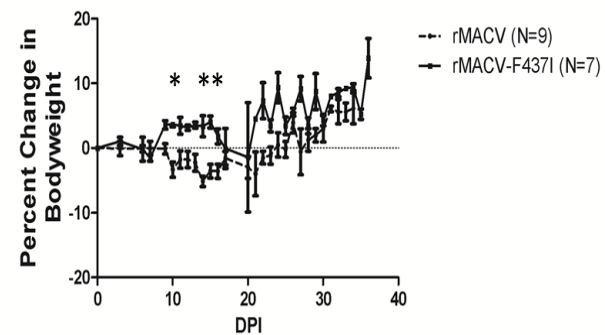
1493 Organ samples were collected and homogenized for titration from infected
1494 animals. Animals challenged with rMACV-F437I which survived until the end of the
1495 study had no detectable virus in their brains, kidneys, lungs, livers, or spleen (Data not
1496 shown). Interestingly, only the brain homogenates from the two mice which develop
1497 lethal infection showed titerable plaques with viral loads at 2×10^6 and 2×10^5 pfu/mL
1498 respectively, there was no sign of infectious virus within the peripheral organs.

1499

1500

1501 **Isolation of Viral RNA from Two rMACV-F437I Infected Mice**

1502 To investigate if the two
1503 distinct outcomes in IFN- $\alpha\beta/\gamma$ R $-/-$
1504 mice infected by rMACV-F437I was
1505 driven by a change in the virus, I
1506 isolated and sequenced viral RNA
1507 collected from organ homogenate
1508 from the two animals. Brains, livers,



1509 lungs, spleens, and kidneys were
1510 collected in thirds during necropsy
1511 with one part, around 0.1 grams added
1512 to 1mL of Trizol (Life Technologies,

Figure 27: Weight Change of IFN- $\alpha\beta/\gamma$ R $-/-$ Mice infected with rMACV and rMACV-F437I. Observations of weight change of rMACV and rMACV-F437I infect mice were collected throughout the study. A significant difference ($P<.05$, two-way ANOVA) was observed during the acute phase of disease between the two groups, at 10, 14, and 15 DPI. Weight loss was observed at 20 DPI and later 1 to 2 days prior to death or the animal reaching the defined study end point.

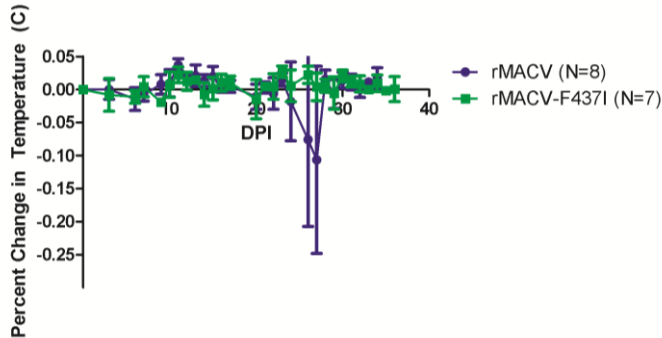
1513 #15596-026). Samples were homogenized and centrifuged with the aqueous layer
1514 transferred to a clean vial. Fresh Trizol was added to the aqueous layer and the samples
1515 were removed from the BSL-4 following approved GNL protocols.

1516 RNA was isolated from the Trizol lysate according to the manufacturer's protocol
1517 as described in the methods section. I completed RT-PCR utilizing random primers on
1518 the samples and amplified the entire MACV genome utilizing the primers I had
1519 previously designed to sequence MACV. Amplified fragments from the brains, lungs,

1520 and kidneys were sequenced by the UTMB Sequencing Core. Analysis of the sequence
 1521 identified the two silent mutations, confirming the virus as rMACV-F437I. However, at
 1522 the single mutation F437I, there was a reversion to the original phenylalanine 437 amino
 1523 acid (Fig. 23). This residue reversion was confirmed in viral RNA isolated from the
 1524 organs collected from both mice.

1525 **DISCUSSION:**

1526 The data presented in this chapter confirms the reverse genetics system described
 1527 in Chapter 2 as a powerful tool for studying rMACV biology. The highly conserved
 1528 nature of the GP2
 1529 transmembrane region of
 1530 MACV and JUNV makes
 1531 targeting the single F437
 1532 residue an ideal target for
 1533 modification of MACV.



1534 Introduction and subsequent
 1535 rescue of the virus with the
 1536 single mutation confirms the
 1537 viability of the virus with this single mutation, as reported with LASV and JUNV (122).
 1538 This is the first report of the attenuation of MACV *in vivo*.

Figure 28: Change in Temperature in rMACV and rMACV-F437I Infected Mice.
 Collection of body temperature from rMACV and rMACV-F437I infected animals was completed throughout the study through the subcutaneous implantation of a BMDS transponder chip. No development of febrile disease was observed throughout the studies. Drastic loss in temperature was observed in animals 1 to 3 days prior to death or reaching defined study end point.

1539 Initial rescue and concentration of rMACV-F437I resulted in a similar peak titer
1540 as seen with rMACV. Characterization of viral growth kinetics in IFN incompetent Vero
1541 cells confirmed similar growth curves and peaks as the wild type virus. Similar growth
1542 analysis in IFN competent A549 cells confirmed that the single mutant virus grew and
1543 peaked at similar titers as MACV and rMACV. This data is comparable to results
1544 reported from the single mutant rXJ13-F427I, a passaged strain of JUNV with the single
1545 mutation (121). rXJ13-F427I also exhibited similar growth characteristics when
1546 compared to wild type XJ13 (121). In comparison, the addition of the single mutation in
1547 rLASV greatly reduced viral growth when compared to the wild-type virus (121).
1548 Following two passages in Vero cells, additional spontaneous mutations developed in the
1549 rLASV single mutant virus that allowed for robust growth of the single mutant virus
1550 comparable to that of the wild-type virus. The characteristics identified from *in vitro*
1551 analysis of rMACV provide further evidence of the distinct natures of NWAs when
1552 compared to OWAs.

1553 Challenge of IFN- $\alpha\beta/\gamma$ R -/- mice with rMACV-F437I resulted in a significant
1554 difference ($p=.02$) in mortality rate when compared to mice infected with rMACV.
1555 Disease presentation also was drastically distinct between the majority of the rMACV-
1556 F437I infected and rMACV infected animals. The periods of weight loss and
1557 neurological disease present in rMACV infected animals in these two studies were
1558 identical to what I previously reported in Chapter 2. The period of acute disease and

1559 weight loss was not present in mice infected with rMACV-F437I, even when looking at
1560 the two mice that did succumb following viral challenge.

1561 Interestingly, both mice which developed lethal disease following challenge with
1562 rMACV-F437I had a gain in weight at 10 to 14 DPI comparative to the rMACV infected
1563 animals. Both animals developed neurological disease, albeit 2-3 days earlier than
1564 previously reported in rMACV- and MACV-infected animals. The mortality rate I
1565 identified in the murine model challenged with rMACV-F437I is comparable to the
1566 reported mortality rate of mice challenged with XJ13-F427I but it is not known if a
1567 reversion occurred in the animals challenged with XJ13-F427I (121). The MTD for the
1568 two mice which developed lethal disease following rMACV-F437I infection was 20.5
1569 DPI. When compared to the ~28 DPI MTD reported in animals challenged with rMACV,
1570 this initial data suggests the reversion may result in more rapid disease progression than
1571 infection with the wild type virus. Without further study it is not possible to confirm this
1572 phenomenon statistically.

1573 In an attempt to determine why infection with rMACV-F437I resulted in such
1574 variable outcomes for a significant portion of the experimental animals, I investigated if
1575 any genetic mutations had occurred in rMACV-F437I following challenge. The
1576 sequencing I completed from viral RNA isolated from different organs of the two mice
1577 confirmed that the mice had been infected with the single mutant virus, but that the single
1578 mutation was no longer present. All RNA isolates from organ homogenates presented

1579 with an identical reversion of the single nucleotide at the I437F residue resulting in a
1580 wild-type genotype.

1581 The F427I mutation appeared in the final series of passaging during the
1582 generation of Candid#1; it was not present in XJ44 or any previous passage strain (121).
1583 It has been proposed that this mutation alters the pH requirements for fusion allowing for
1584 more relaxed environmental requirements for fusogenic transformation and entry into
1585 cells (122). This alteration of fusion phenotype could have a number of different effects
1586 on the virus. It has been shown that Candid#1 has a greater dependence upon human
1587 transferrin receptor (hTfR) 1 than wild-type JUNV but this is linked to mutations in GP1
1588 and not GP2 or F437I (121).

1589 A change in MACV ability to fuse to the early or late endosome following
1590 invagination caused by the F437I mutation may lead to a change in cell tropism. With the
1591 fusion to the endosome occurring earlier, it may be possible the virus is injecting into a
1592 different location within the cytoplasm compared to where it normally occurs, impacting
1593 the replication of the virus. This could greatly alter disease progression and severity. As
1594 my murine model has shown, late-stage disease and death occurs when the titer of
1595 MACV in the brain is at its peak. It is possible the reversion of rMACV-F437I and
1596 subsequent rapid decline of the animals is due to a more rapid dissemination leading to
1597 faster invasion of the central nervous system by the single mutant followed by the
1598 reversion to a more virulent genotype. The *in vitro* characterization of the single mutant

1599 virus showed no significant change in growth kinetics compared to rMACV, but this is in
1600 cell culture with only a single cell type. Further characterization in different cell lines and
1601 *in vivo* studies are warranted to determine if the presence of the single mutation changes
1602 the rate of infection or type of cell normally targeted by MACV. It would also be
1603 interesting to identify if the virus enters the cytoplasm earlier, fusing through the early
1604 endosome instead of the late endosome, forcing the virus to replicate in a different
1605 manner or location within the cell.

1606 An alternative method of attenuation could be that F437I mutation causes a
1607 decrease in virus infectivity due to a change in virion stability. The mutation might not
1608 change the cellular tropism but could change the rate or efficiency of cellular entry by
1609 MACV. This was not seen in the *in vitro* characterization but may be cell type dependent.
1610 As reported previously, this mutation could lead to a conformational change at neutral pH
1611 prior to the low pH reported to be necessary for virus fusion (186, 187). It has been
1612 shown that the GP of LASV undergoes irreversible conformational changes at pH 6.0,
1613 potentially shedding GP1 following binding to the cell receptor and endocytosis. A
1614 conformational change at neutral pH might lead to the shedding of GP1, preventing
1615 rMACV-F437I from binding the cellular receptor correctly and entering the cell. The
1616 mutation might also lead to early shedding or a conformational change within the
1617 endosome prior to reaching the low pH required for normal fusion; this could expose the
1618 viral proteins and RNA to a low pH environment earlier than normal. To determine if this

1619 is occurring I recommend investigating if conformational changes occur in the GP-1/2
1620 spike in different pH environments, potentially utilizing the expression plasmids
1621 generated in Chapter 2. If changes occur, I would investigate at what pH to determine if it
1622 is occurring prior to binding the receptor, within the early endosome, or at the late
1623 endosome. Finally, further characterization of cellular tropism is necessary to understand
1624 the route and method of infection, not just for MACV but for many arenaviruses as
1625 knowledge of primary cell targets is extremely limited for hemorrhagic NWAs.

1626 **CHAPTER SUMMARY:**

1627 The research presented in this chapter describes the rational modification and
1628 attenuation of rMACV. The modification and generation of an attenuated rMACV proves
1629 the usefulness of the tools developed in Chapter 2, and demonstrates areas of interest for
1630 further studies to elucidate the genetic mechanisms of attenuation. I have presented the *in*
1631 *vitro* characterization of rMACV-F437I on two different cell lines, IFN competent and
1632 incompetent, showing that the mutation in the transmembrane region does not greatly
1633 affect virus growth kinetics in cell culture. I have also shown *in vivo* that rMACV-F437I
1634 is attenuated in the IFN- $\alpha\beta/\gamma$ R $-/-$ mouse model when compared to rMACV. Finally, I
1635 have shown that the single F437I mutation, on its own, appears to be unstable with a
1636 reversion rate of 28% in the two studies completed. Further studies are necessary to
1637 determine how this single mutation is causing attenuation and what pressures are leading
1638 to the reversion to wild-type genotype.

CHAPTER 5: DISSERTATION SUMMARY

In Chapter 1, I provide a comprehensive review of MACV based upon published articles and conference presentations dating back to the original outbreak in 1959. I also provide the three aims from my original dissertation proposal, my hypotheses, and a brief rationale for my hypotheses. I provide a summary of all the published information on MACV, including details on all reported outbreaks, the genomic makeup of arenaviruses, a clinical description of BHF, and a list of all published animal models utilized for studying BHF. I also detail the recent discoveries made from models utilizing plasmid expression of MACV protein or other arenaviruses which have been ascribed to what can occur with infectious MACV.

In Chapter 2, I discuss the development of the reverse genetics system I utilized for rescuing rMACV. To ensure the viability of the virus I completed a full sequence of the viral genome, including the UTRs, and identified the correct 5' and 3' terminal regions of the S and L segments. During this process I generated a minigenome assay that allowed me to identify the functional NP and L proteins in the BSL-2. Additionally, I showed that the L protein from Candid#1 and Romero were able to replicate the MACV genome. Following rescue of rMACV, I completed growth curve analysis at different MOIs in different cell lines. This analysis allowed me to compare the wild-type virus to

1657 the recombinant virus, ensuring they were similar. I characterized a novel murine model,
1658 IFN- $\alpha\beta/\gamma$ R $-/-$ mice, which developed a biphasic disease following IP challenge with
1659 MACV or rMACV.

1660 The identification of the 5' and 3' termini regions of MACV is an important step
1661 in the development of the reverse genetics system and it also confirms the conservation of
1662 this region across multiple arenaviruses. This is the fourth report of a hemorrhagic
1663 arenavirus with identical termini sequence, the other three being Lujo virus, JUNV, and
1664 LASV (38, 124, 150). Confirmation of this sequence may assist in future attempts at
1665 rescuing hemorrhagic arenaviruses. The development of the novel minigenome assay was
1666 essential for confirming the functionality of the plasmid-expressed viral proteins and the
1667 termini regions of MACV. Other groups have utilized similar assays to elucidate viral
1668 replication kinetics and to test antivirals (122, 143-148, 152). I utilized this assay to show
1669 that two different JUNV L proteins could replicate the reporter genes, providing evidence
1670 that a chimeric virus with JUNV and MACV genes could be generated. The development
1671 of the reverse genetics system is the tool necessary for such a project. Unlike ML29,
1672 which was generated through *in vitro* co-infection and reassortment of the two viruses,
1673 my reverse genetics system could be used to rationally generate chimeric viruses (153,
1674 182). Additionally, my system can be utilized to modify specific regions of the MACV
1675 genome to better elucidate the genetic determinants of attenuation as comparable systems
1676 have been utilized for other arenaviruses (38, 124-126, 151, 188, 189).

1677 In Chapter 3, I provide evidence that RIG-I knockdown in A549 cells had
1678 minimal impact on viral growth or peak titer at 3 and 4 DPI when compared to control
1679 cells. The reduced growth at 1 and 2 DPI may imply that MACV is inhibited by IFN
1680 induction early in infection but is able to overcome the inhibiting factor at later stages of
1681 infection. I show that MACV infection of A549 cells leads to activation of STAT-1,
1682 induction of STAT-1, and induction of ISG15. All three of these steps are correlated with
1683 PRR recognition of the virus infection leading to synthesis of IFN and IFN signaling. The
1684 evidence I provide identifies activation of PKR and phosphorylation of eIF2 α , which is
1685 also contradictory to the commonly held dogma within the arenavirus field, that these
1686 viruses do not impact cellular biosynthesis.

1687 The indication that MACV is affected by but may overcome the activity of IFN is
1688 very intriguing especially as early tests utilizing therapeutic poly I:C in MACV
1689 challenged NHPs reported no clinical benefit. However, it did identify a more rapid
1690 detection of viremia in treated compared to untreated animals (111). While poly I:C
1691 failed to elicit a beneficial response, Ribavirin has been reported to reduce the NWA
1692 virulence in infected animals and, in a very limited number of cases, humans (67, 70,
1693 112, 179-181). The identification that MACV infection of A549 induces an IFN signaling
1694 response is contradictory to the accepted arenavirus dogma, which is primarily based
1695 upon plasmid-expressed proteins and non-pathogenic arenaviruses (117, 118, 120, 164).
1696 Previous research identified no phosphorylation of eIF2 α following infection of cells Huh

1697 7 cells with the prototypical arenavirus LCMV (169). The existence of these dogmas can
1698 be a detriment to the field as it may encourage scientific pursuits based upon incorrect
1699 evidence. Clinical data from JUNV-infected patients have clearly identified IFN
1700 induction, as have reports from MACV infected NHPs and JUNV infected guinea pigs
1701 (108, 111, 165). The clinical data from LASV infected patients clearly identify a
1702 suppression of IFN induction (139, 140, 190). The distinctions between pathogenic
1703 NWAs and OWAs must be clarified to allow further unconstrained progress within the
1704 field. Based upon this data, I propose MACV and JUNV both induce IFN early in
1705 infection and the production of IFN is maintained throughout the infection within the
1706 host. The ability of MACV to propagate within an IFN inducing cell and the role of IFN
1707 in MACV infection must be further elucidated, especially if, at late stages of severe
1708 disease, IFN is pathogenic instead of protective as seen with Severe acute respiratory
1709 syndrome and Influenza A (191-193).

1710 In Chapter 4 I utilized the reverse genetics system and mouse model I
1711 characterized in Chapter 2 to study the impact of a single mutation in the glycoprotein
1712 membrane of MACV at residue F437. This mutation has been identified in Candid#1 and
1713 shown to play a significant role in attenuating JUNV in a murine neurovirulence model.
1714 After generating the rMACV-F437I, I confirmed that the single mutant virus had similar
1715 growth curves and peaks compared to the wild type virus. After challenging IFN- $\alpha\beta/\gamma$ R
1716 -/- mice with rMACV and rMACV-F437I, I identified a significant reduction in

1717 morbidity and mortality between the two viruses. Reversion to wild type sequence was
1718 identified in the two of seven rMACV-F437I-infected animals, both of which succumbed
1719 to disease with a MTD of 20.5 DPI.

1720 The role of the F437I substitution, while significant in its attenuation, is not well
1721 characterized. The mutation has been shown to play a role in cell-to-cell fusion at more
1722 neutral pH, reducing infectivity in cell culture (122). The mutation also plays a critical
1723 role in attenuating the neurovirulence of JUNV in a murine model (121). My data further
1724 exemplify the attenuating role, but does not characterize the molecular mechanism of
1725 attenuation. The identical reversion of the single mutation confirms the importance of the
1726 residue, but does not identify the role of the residue.

1727 Looking towards the future of this project, further investigation needs to be
1728 completed to determine the role of IFN induction on hemorrhagic NWAs to determine if
1729 the IFN response plays an antiviral or pathogenic role in the outcome of the patient. As a
1730 correlation of high IFN levels to more severe outcomes has already been published
1731 relating to JUNV, early identification of high levels of endogenous IFN may provide an
1732 ideal marker to identify critical cases of BHF prior to severe disease development (109). I
1733 also propose investigating the role of phosphorylated PKR to identify if there is an impact
1734 on cellular and viral protein biosynthesis or if MACV has a method of evading cap-
1735 dependent translation shutdown. If MACV is able to overcome cap-dependent translation
1736 shutdown within an infected cell, it avoids an essential antiviral cell response. If the

1737 mechanistic target can be identified, there are two distinct opportunities for antiviral
1738 development. The first would be to identify which MACV protein plays a critical role in
1739 the process and possibly target the protein-protein interaction restoring the shutdown of
1740 translation. The second would be to identify which part of the translation pathway is
1741 being affected and develop therapeutics, which could possibly restore the antiviral state.
1742 Both of these targets would aim to restore the shutdown of translation within infected
1743 cells, inhibiting MACV replication and slowing infection.

1744 Another direction is to investigate the single mutation F437I, to determine if it can
1745 be stabilized similar to Candid#1 and the role it plays in attenuating the MACV.
1746 Elucidation of this mutation may play a key role in the development of a future vaccine,
1747 especially if attenuation of other hemorrhagic NWAs can be achieved in a similar
1748 manner. The reverse genetics system I developed and the lethal animal model I
1749 characterized in this dissertation will play a vital role in further elucidation of MACV
1750 virulence and the future development of an attenuated rMACV.

1751

Appendix:

I: TABLE OF MACV ANIMAL EXPERIMENTS

Animal/Models	Route of Challenge (Dose)	Disease Symptoms	Mean time to death	Late Neurological Syndrome (Mortality %)	Neutralizing Antibodies
Non-Human Primates	Adult Marmosets (Saguinus oeffroyi)	<u>SC, SS, Cr, IN, Or</u>	1-3 days prior to death; refuse food, huddled, inattentive, weakness, hypothermia	11-21 DPI	N/A
	Adult Rhesus macaques (Macaca mulatta)	<u>SC</u> (10 ⁵ pfu, 10 ⁹ pfu)	Biphasic disease identified ~7 DPI. Skin petechiae, facial rash, nasal discharge, fever, and anorexia. Moribund ~2 before death.	13-17, 17-25 (50%)	Yes (100%)
	Young Rhesus macaques (Macaca mulatta)	<u>SC</u> (10 ⁹ pfu)	Biphasic disease identified ~7 DPI. Skin petechiae, facial rash, nasal discharge, fever, and anorexia. Moribund ~2 before death.	19 DPI (86%)	Yes (50%)
	Cynomolgus monkeys (Macaca fascicularis)	<u>SC</u> (10 ⁹ pfu)	Sudden death with disease reported 1-3 days prior to death	17 DPI (71%)	Yes (50%)
	African green monkey (Cercopithecus aethiops)	<u>SC</u> (10 ⁹ pfu)	Fever, Anorexia, Shock, Hemorrhage, Pneumonia	15 DPI (83%)	Yes (100%)
Murine	Adult inbred white mice	<u>IC, IP, IN, Or</u>	No Disease	N/A	Yes
	Young (<2 days old) inbred white mice	<u>IC, IP</u>	Growth retardation, tremors, convulsions	9-16 DPI	N/A
	STAT-1-/-	<u>IP</u> (10 ⁹ pfu), <u>SC</u> (10 ⁹ pfu)	Ruffled, hunched, and lethargic	7-30 DPI, 10-5 DPI	N/A
	IFN- α /R-/-	<u>IP</u> (10 ⁹ pfu)	Biphasic disease- acute weight loss, neurological- ataxia, awkward gait, loss of balance, paralysis, death	30 DPI	Yes (100%)
	Adult Guinea pigs	<u>IP</u>	N/A	N/A	Yes
Other Animals	C-13 Guinea pigs	<u>IP</u>	N/A	N/A	N/A
	Young Guinea pigs	<u>IP, IC</u>	N/A	N/A (87%)	N/A
	Adult hamsters	<u>IC, IP, IN, Or</u>	No Disease	N/A	Yes
	Young hamsters (<5 days)	<u>IC, IP</u>	Neurological	N/A	N/A
	Cats	<u>IC, IP, IV, Or</u>	No Disease	N/A	Yes
Other Animals	Chickens	N/A	No Disease	N/A	No
	Swine	N/A	No Disease	N/A	No
	Equine	N/A	No Disease	N/A	Yes
	Rabbit	N/A	No Disease	N/A	Yes

Table 1: Table of published animal models from the 1960s to present.

When available, data of clinical development, routes of exposure, and doses are reported. Routes of exposure which are underlined represent lethal challenges. Acronyms: Sub-cutaneous (SC), Scarified skin (SS), Corneal instillation (Cr), Intra-nasal (IN), Oral (Or), Plaque forming unit (pfu), Intracranial (IC), Intravenous (IV), and intraperitoneal (IP). Copyright Current Opinions in Virology

II: BRAIN AND SPLEEN HISTOLOGY FROM INFECTED MICE

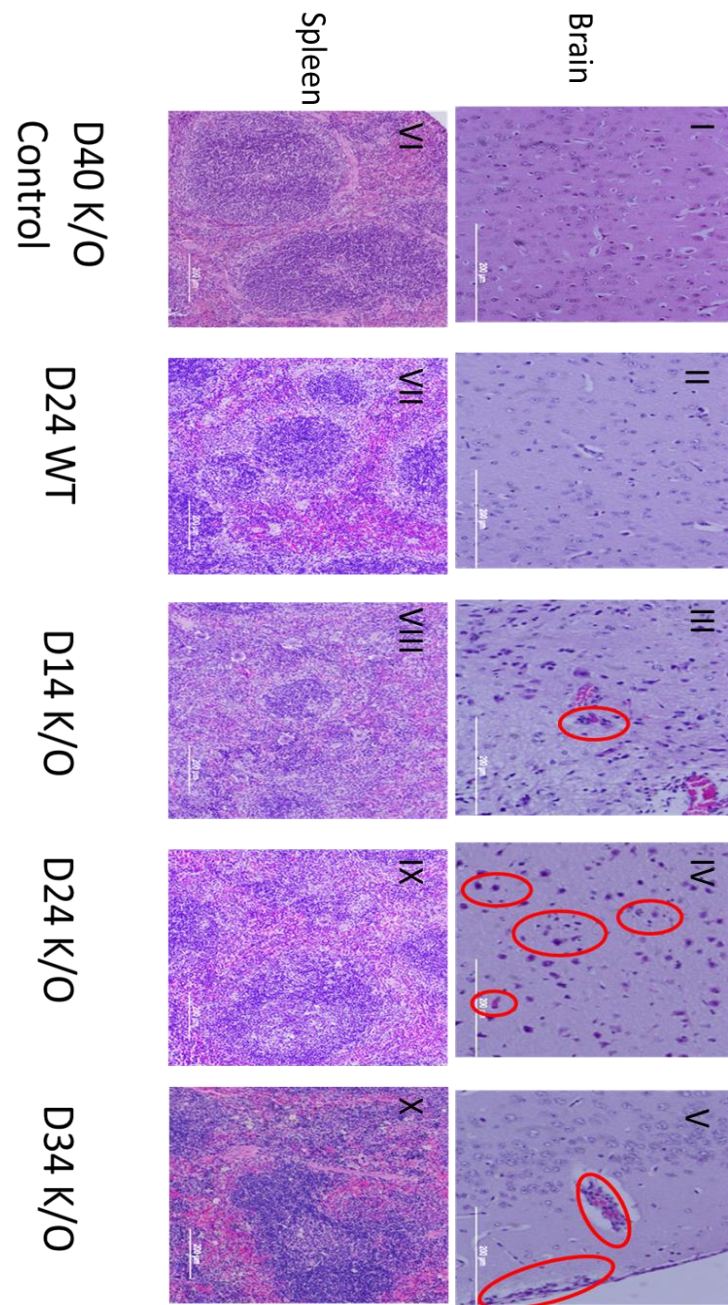


Figure 29: Histopathology Staining of Brain and Spleen Tissues.

Sections I and VI are from an uninfected IFN- $\alpha\beta/\gamma$ R/mouse showing no neuronal death and good spleen structure. Sections II and VII are from a C57BL/6 mouse infected with MACV with no visible neuron death or inflammation and good spleen structure. Sections III and VIII are from an IFN- $\alpha\beta/\gamma$ R/mouse euthanized at 14 dpi, the red circle identifying vascular infiltrates. Sections IV and IX are from IFN- $\alpha\beta/\gamma$ R/mice euthanized at 24 dpi; red circles identify microglial cells and cellular debris from dead neuronal cells. Sections V and X are from an IFN- $\alpha\beta/\gamma$ R/mouse that died at 34 dpi; red circles identify increased vascular and perivascular cellular infiltrates.

III: IMMUNOHISTOCHEMISTRY FROM INFECTED MICE

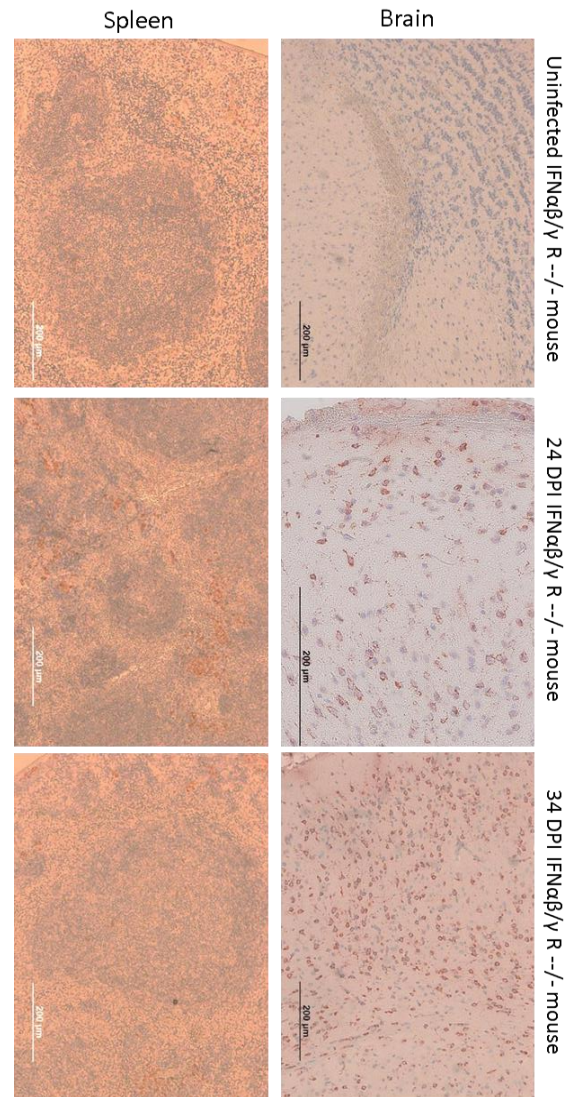


Figure 30: Immunohistochemistry of Brain and Spleen Tissue Slides from IFN $\alpha\beta/\gamma$ R^{-/-} Mice.

Tissue slides made from Brain and Spleen organs collected at 24 and 34 DPI with accompanying control. By 34 DPI a large percentage of neuronal cells are infected while spleens have minimal signs of viral antigen and have started to regain normal architecture.

IV: VIRAL LOAD OF DIFFERENT ORGANS FROM INFECTED MICE

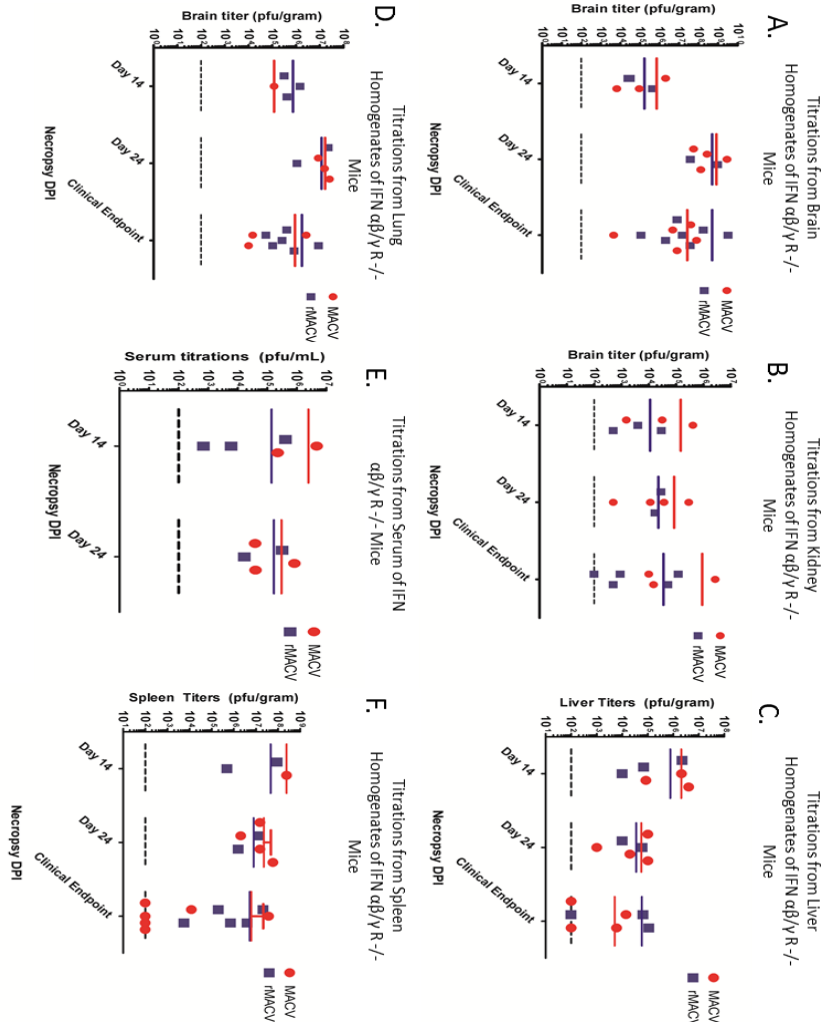


Figure 31: Titrations From Organ Homogenates of Infected IFN $\alpha\beta\gamma$ R^{-/-} Mice. Organs from infected animals were weighed and homogenized in 2% FBS DMEM. Plaque titrations on Vero-CCL81 cells were completed and corresponding titrations are shown above. No significant difference ($P > .05$, two-way ANOVA) was identified between the two viruses in any homogenate sample. A high viral load in the CNS was observed by 24 DPI ($\sim 10^8$ pfu/gram) and was maintained until death. The single surviving mouse infected with MACV was euthanized at 40 DPI, and had no detectable viral load in the brain (data not shown). Titrations of kidney homogenates identified a slight increase from 14 DPI to clinical endpoint. Liver homogenates had a peak titer at 14 DPI with a generalized downward trend until clinical endpoint. Lung homogenates had a peak titer at 24 DPI. Serum samples confirmed the presence of viremia at 14 and 24 DPI. Spleen samples had a peak titer at 14 DPI with a generalized decrease until clinical endpoint.

PERMISSION TO PUBLISH

FROM THE JOURNAL OF VIROLOGY:

“Authors may republish/adapt portions of their articles

ASM also grants the authors the right to republish discrete portions of his/her article in any other publication (including print, CD-ROM, and other electronic formats) of which he or she is author or editor, provided that proper credit is given to the original ASM publication. “Proper credit” means either the copyright lines shown on the top of the first page of the PDF version, or “Copyright © American Society for Microbiology, [insert journal name, volume number, year, page numbers and DOI]” of the HTML version. For technical questions about using Rightslink, please contact Customer Support via phone at (877) 622-5543 (toll free) or (978) 777-9929, or e-mail Rightslink customer care at customercare@copyright.com.

From the Elsevier website

How authors can use their own journal articles

Authors can use their articles for a wide range of scholarly, non-commercial purposes as outlined below. These rights apply for all Elsevier authors who publish their article as either a subscription article or an open access article.

We require that all Elsevier authors always include a full acknowledgement and, if appropriate, a link to the final published version hosted on Science Direct.

Authors can use either their accepted author manuscript or final published article for:

Use at a conference, meeting or for teaching purposes

Internal training by their company

Sharing individual articles with colleagues for their research use* (also known as 'scholarly sharing')

Use in a subsequent compilation of the author's works

Inclusion in a thesis or dissertation

Reuse of portions or extracts from the article in other works

Preparation of derivative works (other than for commercial purposes)”

The permission to utilize my publication in the Journal of Virology,

Patterson M, Seregin A, Huang C, Kolokoltsova O, Smith J, Miller M, Smith J, Yun N, Poussard A, Grant A, Tigabu B, Walker A, Paessler S. 2013. Rescue of a Recombinant Machupo Virus from Cloned cDNAs and In Vivo Characterization in Interferon ($\alpha\beta/\gamma$) Receptor Double Knockout Mice. Journal of Virology,

applies to all sections of Chapter 2, a portion of the Chapter 4 methods, Appendix I and II, and Figures 5, 6, 7, 8, 10, 11, 12, 13, 14, and 16.

FROM THE JOURNAL CURRENT OPINIONS IN VIROLOGY:

<http://www.elsevier.com/journal-authors/author-rights-and-responsibilities>

How authors can use their own journal articles

Authors can use their articles for a wide range of scholarly, non-commercial purposes as outlined below. These rights apply for all Elsevier authors who publish their article as either a subscription article or an open access article.

We require that all Elsevier authors always include a full acknowledgement and, if appropriate, a link to the final published version hosted on Science Direct.

For open access articles these rights are separate from how readers can reuse your article as defined by the author's choice of Creative Commons user license options.

Authors can use either their accepted author manuscript or final published article for:

Use at a conference, meeting or for teaching purposes

Internal training by their company

Sharing individual articles with colleagues for their research use* (also known as 'scholarly sharing')

Use in a subsequent compilation of the author's works

Inclusion in a thesis or dissertation

Reuse of portions or extracts from the article in other works

Preparation of derivative works (other than for commercial purposes)

This copyright applies to the entirety of Chapter 1 except the Innate Immune subsection, Figures 1, 2, 3, and Table 1.

FROM THE JOURNAL OF MOLECULAR BIOLOGY

This is a License Agreement between Michael Patterson ("You") and Elsevier ("Elsevier") provided by Copyright Clearance Center ("CCC"). The license consists of your order details, the terms and conditions provided by Elsevier, and the payment terms and conditions.

All payments must be made in full to CCC. For payment instructions, please see information listed at the bottom of this form.

Supplier

Elsevier Limited

The Boulevard, Langford Lane

Kidlington, Oxford, OX5 1GB, UK

Registered Company Number

1982084

Customer name

Michael Patterson

Customer address

301 University Blvd

Galveston, TX 77555

License number

3327790452926

License date

Feb 14, 2014

Licensed content publisher

Elsevier

Licensed content publication

Journal of Molecular Biology

Licensed content title

Innate Immune Response to Arenaviral Infection: A Focus on the Highly
Pathogenic New World Hemorrhagic Arenaviruses

Licensed content author

Takaaki Koma, Cheng Huang, Olga A. Kolokoltsova, Allan R. Brasier, Slobodan
Paessler

Licensed content date

13 December 2013

Licensed content volume number

425

Licensed content issue number

24

Number of pages

11

Start Page

4893

End Page

4903

Type of Use

reuse in a thesis/dissertation

Portion

figures/tables/illustrations

Number of figures/tables/illustrations

1

Format

electronic

Are you the author of this Elsevier article?

No

Will you be translating?

No

Title of your thesis/dissertation

THE DEVELOPMENT OF A REVERSE GENETICS SYSTEM FOR
MACHUPO VIRUS

Expected completion date

Mar 2014

Estimated size (number of pages)

120

Elsevier VAT number

GB 494 6272 12

Permissions price

0.00 USD

VAT/Local Sales Tax

0.00 USD / 0.00 GBP

Total

0.00 USD

This applies to Figure 4 of my dissertation

REFERENCES

1. **Webb PA.** 1965. Properties of Machupo Virus. *Am J Trop Med Hyg* **14**:799-802.
2. **Johnson KM, Kuns ML, Mackenzie RB, Webb PA, Yunker CE.** 1966. Isolation of Machupo Virus from Wild Rodent *Calomys callosus*. *Am J Trop Med Hyg* **15**:103-106.
3. **Parodi AS, Rugiero HR, Greenway DJ, Mettler N, Martinez A, Boxaca M, De La Barrera JM.** 1959. [Isolation of the Junin virus (epidemic hemorrhagic fever) from the mites of the epidemic area (*Echinolaelaps echidninus*, Barlese).]. *Prensa Med Argent* **46**:2242-2244.
4. **Terezinha Lisieux M Coimbra, Elza S Nassar, Marcelo N Burattini, Luiza Terezinha Madia de Souza, Ivani B Ferreira, Iray M Rocco, Amelia PA Travassos da Rosa, Pedro FC Vasconcelos, Francisco P Pinheiro, James W LeDuc, Rebeca Rico-Hesse, Jean-Paul Gonzalez, Peter B Jahrling, Tesh RB.** 1994. New arenavirus isolated in Brazil. *Lancet*. **343**:391-392.
5. **Salas R, de Manzione N, Tesh RB, Rico-Hesse R, Shope RE, Betancourt A, Godoy O, Bruzual R, Pacheco ME, Ramos B, et al.** 1991. Venezuelan haemorrhagic fever. *Lancet* **338**:1033-1036.
6. **Delgado S, Erickson BR, Agudo R, Blair PJ, Vallejo E, Albariño CG, Vargas J, Comer JA, Rollin PE, Ksiazek TG, Olson JG, Nichol ST.** 2008. Chapare Virus, a Newly Discovered Arenavirus Isolated from a Fatal Hemorrhagic Fever Case in Bolivia. *PLoS Pathog* **4**:e1000047.
7. **Buckley SM, Casals J.** 1970. Lassa Fever, a New Virus Disease of Man from West Africa. *Am J Trop Med Hyg* **19**:680-691.
8. **Briese T, Paweska JT, McMullan LK, Hutchison SK, Street C, Palacios G, Khristova ML, Weyer J, Swanepoel R, Egholm M, Nichol ST, Lipkin WI.** 2009. Genetic Detection and Characterization of Lujo Virus, a New Hemorrhagic Fever–Associated Arenavirus from Southern Africa. *PLoS Pathog* **5**:e1000455.
9. **Fulhorst CF, Bowen MD, Ksiazek TG, Rollin PE, Nichol ST, Kosoy MY, Peters CJ.** 1996. Isolation and Characterization of Whitewater Arroyo Virus, a Novel North American Arenavirus. *Virology* **224**:114-120.
10. **Mackenzie RB, Beye HK, Valverde Ch L, Garron H.** 1964. Epidemic Hemorrhagic Fever in Bolivia: I. A Preliminary Report of the Epidemiologic and Clinical Findings in a New Epidemic Area in South America. *Am J Trop Med Hyg* **13**:620-625.

11. **Kuns ML.** 1965. Epidemiology of Machupo Virus Infection. *Am J Trop Med Hyg* **14**:813-816.
12. **Johnson KM.** 1965. Epidemiology of Machupo Virus Infection. *Am J Trop Med Hyg* **14**:816-818.
13. **Johnson KM, Wiebenga NH, Mackenzie RB, Kuns ML, Tauraso NM, Shelokov A, Webb PA, Justines G, Beye HK.** 1965. Virus Isolations from Human Cases of Hemorrhagic Fever in Bolivia. *Proc Soc Exp Biol Med. Society for Experimental Biology and Medicine (New York, N.Y.)* **118**:113-118.
14. **Johnson KM, Mackenzie RB, Webb PA, Kuns ML.** 1965. Chronic infection of rodents by Machupo virus. *Science* **150**:1618-1619.
15. **Centers for Disease Control and Prevention.** 2013, posting date. Select Agents and Toxins List. [Online.]
16. **Buchmeier M, de la Torre J, Peters C.** 2007. Arenaviridae: The Viruses and Their Replication, p. 1791-1827. *In* Knipe HP (ed.), *Field's Virology*, vol. 5. Wolter Kluwer Lippincott Williams & Wilkins, Philadelphia, PA, USA.
17. **Murphy FA, Webb PA, Johnson KM, Whitfield SG, Chappell WA.** 1970. Arenoviruses in Vero Cells: Ultrastructural Studies. *J Virol* **6**:507-518.
18. **O Poch, I Sauvaget, M Delarue, Tordo N.** 1989. Identification of four conserved motifs among the RNA-dependent polymerase encoding elements. *EMBO* **8**:3867-3874.
19. **Salvato M, Shimomaye E, Oldstone MBA.** 1989. The primary structure of the lymphocytic choriomeningitis virus L gene encodes a putative RNA polymerase. *Virology* **169**:377-384.
20. **Perez M, Craven RC, de la Torre JC.** 2003. The small RING finger protein Z drives arenavirus budding: Implications for antiviral strategies. *Proc Natl Acad Sci U S A* **100**:12978-12983.
21. **Strecker T, Eichler R, Meulen Jt, Weissenhorn W, Dieter Klenk H, Garten W, Lenz O.** 2003. Lassa Virus Z Protein Is a Matrix Protein Sufficient for the Release of Virus-Like Particles. *J Virol* **77**:10700-10705.
22. **Djavani M, Lukashevich IS, Sanchez A, Nichol ST, Salvato MS.** 1997. Completion of the Lassa Fever Virus Sequence and Identification of a RING Finger Open Reading Frame at the L RNA 5' End. *Virology* **235**:414-418.
23. **Salvato MS, Shimomaye EM.** 1989. The completed sequence of lymphocytic choriomeningitis virus reveals a unique RNA structure and a gene for a zinc finger protein. *Virology* **173**:1-10.
24. **Salvato MS, Schweighofer KJ, Burns J, Shimomaye EM.** 1992. Biochemical and immunological evidence that the 11 kDa zinc-binding protein of lymphocytic choriomeningitis virus is a structural component of the virus. *Virus Research* **22**:185-198.

25. **Buchmeier MJ, Oldstone MBA.** 1979. Protein structure of lymphocytic choriomeningitis virus: Evidence for a cell-associated precursor of the virion glycopeptides. *Virology* **99**:111-120.
26. **Beyer WR, Pöplau D, Garten W, von Laer D, Lenz O.** 2003. Endoproteolytic Processing of the Lymphocytic Choriomeningitis Virus Glycoprotein by the Subtilase SKI-1/S1P. *J Virol* **77**:2866-2872.
27. **Lenz O, ter Meulen J, Klenk H-D, Seidah NG, Garten W.** 2001. The Lassa virus glycoprotein precursor GP-C is proteolytically processed by subtilase SKI-1/S1P. *Proc Natl Acad Sci USA* **98**:12701-12705.
28. **York J, Nunberg JH.** 2006. Role of the stable signal peptide of Junin arenavirus envelope glycoprotein in pH-dependent membrane fusion. *J Virol* **80**:7775-7780.
29. **York J, Romanowski V, Lu M, Nunberg JH.** 2004. The signal peptide of the Junin arenavirus envelope glycoprotein is myristoylated and forms an essential subunit of the mature G1-G2 complex. *J Virol* **78**:10783-10792.
30. **York J, Nunberg JH.** 2007. Distinct requirements for signal peptidase processing and function in the stable signal peptide subunit of the Junin virus envelope glycoprotein. *Virology* **359**:72-81.
31. **Eichler R, Lenz O, Strecker T, Eickmann M, Klenk H-D, Garten W.** 2003. Identification of Lassa virus glycoprotein signal peptide as a trans-acting maturation factor. *EMBO Rep* **4**:1084-1088.
32. **Riviere Y, Ahmed R, Southern PJ, Buchmeier MJ, Dutko FJ, Oldstone MB.** 1985. The S RNA segment of lymphocytic choriomeningitis virus codes for the nucleoprotein and glycoproteins 1 and 2. *J Virol* **53**:966-968.
33. **Morin B, Coutard B, Lelke M, Ferron F, Kerber R, Jamal S, Frangeul A, Baronti C, Charrel R, de Lamballerie X, Vonnrhein C, Lescar J, Bricogne G, Gunther S, Canard B.** 2010. The N-terminal domain of the arenavirus L protein is an RNA endonuclease essential in mRNA transcription. *PLoS Pathog* **6**:e1001038.
34. **Tortorici MA, Albarino CG, Posik DM, Ghiringhelli PD, Lozano ME, Rivera Pomar R, Romanowski V.** 2001. Arenavirus nucleocapsid protein displays a transcriptional antitermination activity in vivo. *Virus Res* **73**:41-55.
35. **Meyer BJ, Southern PJ.** 1994. Sequence heterogeneity in the termini of lymphocytic choriomeningitis virus genomic and antigenomic RNAs. *J Virol* **68**:7659-7664.
36. **Auperin DD, Compans RW, Bishop DHL.** 1982. Nucleotide sequence conservation at the 3' termini of the virion RNA species of new World and Old World arenaviruses. *Virology* **121**:200-203.
37. **Auperin DD, McCormick JB.** 1989. Nucleotide sequence of the Lassa virus (Josiah strain) S genome RNA and amino acid sequence comparison of the N and GPC proteins to other arenaviruses. *Virology* **168**:421-425.

38. **Emonet SF, Seregin AV, Yun NE, Poussard AL, Walker AG, de la Torre JC, Paessler S.** 2011. Rescue from cloned cDNAs and in vivo characterization of recombinant pathogenic Romero and live-attenuated Candid #1 strains of Junin virus, the causative agent of Argentine hemorrhagic fever disease. *J Virol* **85**:1473-1483.
39. **Kranzusch PJ, Schenk AD, Rahmeh AA, Radoshitzky SR, Bavari S, Walz T, Whelan SP.** 2010. Assembly of a functional Machupo virus polymerase complex. *Proc Natl Acad Sci U S A* **107**:20069-20074.
40. **Aguilar PV CW, Vargas J, Guevara C, Roca Y, Felices V, et al.** 2009, posting date. Reemergence of Bolivian hemorrhagic fever, 2007–2008. [Online.]
41. **Kilgore PE, Peters CJ, Mills JN, Rollin PE, Armstrong L, Khan AS, Ksiazek TG.** 1995. Prospects for the control of Bolivian hemorrhagic fever. *Emerg Infect Dis* **1**:97-100.
42. **ProMED-email.** 2013. Bolivian Hemorrhagic Fever - Bolivia: (Beni). ProMED-email **20130317.1590121**.
43. **ProMED-email.** 2013. Bolivian hemorrhagic fever - Bolivia (02): (BE). ProMED-email **20130420.1660132**.
44. **ProMED-email.** 2012. Bolivian Hemorrhagic Fever - Bolivia (05): (Beni). ProMED-email **20120730.1220842**.
45. **Olds N.** 1988. Dissertation: A revision of the genus *Calomys* (Rodentia: Muridae). City University of New York, New York.
46. **J.W. Drago, J. Salazar-Bravo, L.J. Layne, Yates TL.** 2002. Relationships within the *Calomys callosus* species group based on amplified fragment length polymorphisms. *Biochem Syst Ecol* **31**:703–713.
47. **Sabattini MS, Gonzalez LE, de Rios Diaz G, Vega VR.** 1977. Infection natural y experimental de roedores con virus Junin. *Medicina* **37**:149-161.
48. **Sabattini MS, Contigiani MS.** 1982. Ecological and biological factors influencing the maintenance of arenaviruses in nature, with special reference to the agent of Argentine hemorrhagic fever. . *Acad. Brasil. Cienc.*:261-262.
49. **Kravetz F, Percich R, Zuleta GA, Caleb MA, Weissenbacher MC.** 1986. Distribution of Junin virus and its reservoirs: A tool for Argentine hemorrhagic fever risk evaluation in non-endemic areas. . *Interciencia* **11**:185-188.
50. **Salazar-Bravo J, Ruedas LA, Yates TL.** 2002. Mammalian reservoirs of arenaviruses. *Curr Top Microbiol Immunol* **262**:25-63.
51. **Pan American Health Organization.** 2003. Machupo Hemorrhagic Fever, vol. II. [Online]
52. **Justines G, Johnson KM.** 1969. Immune Tolerance in *Calomys callosus* infected with Machupo Virus. *Nature* **222**:1090-1091.
53. **Webb PA, Justines G, Johnson KM.** 1975. Infection of wild and laboratory animals with Machupo and Latino viruses. *Bull World Health Organ* **52**:493–499.

54. **Douglas R, Wiebenga N, Couch R.** 1965. Bolivian hemorrhagic fever probably transmitted by personal contact. *Am J Epidemiol* **82**:8591.
55. **Stinebaugh BJ, Schloeder FX, Johnson KM, Mackenzie RB, Entwisle G, De Alba E.** 1966. Bolivian hemorrhagic fever: A report of four cases. *The American journal of medicine* **40**:217-230.
56. **Peters CJ, Kuehne RW, Mercado RR, Le Bow RH, Spertzel RO, Webb PA.** 1974. Hemorrhagic Fever in Cochabamba, Bolivia, 1971. *Am J Epidemiol* **99**:425-433.
57. **McKee KT, Jr., Mahlandt BG, Maiztegui JI, Green DE, Peters CJ.** 1987. Virus-specific factors in experimental Argentine hemorrhagic fever in rhesus macaques. *J Med Virol* **22**:99-111.
58. **American Society of Pediatrics.** 2009. Viral Hemorrhagic Fevers Caused by Arenaviruses. *Red Book* **2009**:325-334.
59. **Cajimat MNB, Milazzo ML, Rollin PE, Nichol ST, Bowen MD, Ksiazek TG, Fulhorst CF.** 2009. Genetic diversity among Bolivian arenaviruses. *Virus Research* **140**:24-31.
60. **Weissenbacher MC, Laguens RP, Coto CE.** 1987. Argentine hemorrhagic fever. *Curr Top Microbiol Immunol* **134**:79-116.
61. **Enria DA, de Damilano AJ, Briggiler AM, Ambrosio AM, Fernandez NJ, Feuillade MR, Maiztegui JI.** 1985. [Late neurologic syndrome in patients with Argentinian hemorrhagic fever treated with immune plasma]. *Medicina (B Aires)* **45**:615-620.
62. **Eddy G, Wagner F, Scott S, Mahlandt B.** 1975. Protection of monkeys against Machupo virus by the passive administration of Bolivian haemorrhagic feverimmunoglobulin (human origin). *Bull World Health Organ* **52**.
63. **Enria DA, Briggiler AM, Fernandez NJ, Levis SC, Maiztegui JI.** 1984. Importance of dose of neutralising antibodies in treatment of Argentine haemorrhagic fever with immune plasma. *Lancet* **2**:255-256.
64. **Mahanty S, Bausch DG, Thomas RL, Goba A, Bah A, Peters CJ, Rollin PE.** 2001. Low Levels of Interleukin-8 and Interferon-Inducible Protein-10 in Serum Are Associated with Fatal Infections in Acute Lassa Fever. *J Infect Dis* **183**:1713-1721.
65. **Maiztegui JI, Fernandez NJ, de Damilano AJ.** 1979. Efficacy of immune plasma in treatment of Argentine haemorrhagic fever and association between treatment and a late neurological syndrome. *Lancet* **2**:1216-1217.
66. **C. G. Mcleod, J. L. Stookey, G. A. Eddy, Scott K.** 1976. Pathology of chronic Bolivian hemorrhagic fever in the rhesus monkey. *Am J Pathol* **84**:211-224.
67. **Kilgore PE, Ksiazek TG, Rollin PE, Mills JN, Villagra MR, Montenegro MJ, Costales MA, Paredes LC, Peters CJ.** 1997. Clin Infect Dis. Clinical Infectious Diseases **24**:718-722.

68. **McCormick JB, King IJ, Webb PA, Scribner CL, Craven RB, Johnson KM, Elliott LH, Belmont-Williams R.** 1986. Lassa fever. Effective therapy with ribavirin. *N Engl J Med* **314**:20-26.
69. **Jahrling P, Trotter R, Barrero O.** 1988. Proceedings of the second international conference on the impact of viral diseases on the development of Latin American countries and the Caribbean Region Mar del Plata, Argentina.
70. **Bradfute S, Stuthman K, Shurtleff A, Bavari S.** 2011. A STAT-1 knockout mouse model for Machupo virus pathogenesis. *Virology Journal* **8**:300.
71. **Webb PA, Johnson KM, Mackenzie RB, Kuns ML.** 1967. Some Characteristics of Machupo Virus, Causative Agent of Bolivian Hemorrhagic Fever. *Am J Trop Med Hyg* **16**:531-538.
72. **Kastello MD, Eddy GA, Kuehne RW.** 1976. A Rhesus Monkey Model for the Study of Bolivian Hemorrhagic Fever. *Journal of Infectious Diseases* **133**:57-62.
73. **Eddy G, Scott S, Wagner F, Brand O.** 1975. Pathogenesis of Machupo virus infection in primates. *Bull World Health Organ* **52**.
74. **McLeod CG, Stookey JL, White JD, Eddy GA, Fry GA.** 1978. Pathology of Bolivian Hemorrhagic Fever in the African Green Monkey. *Am J Trop Med Hyg* **27**:822-826.
75. **Patterson M, Seregin A, Huang C, Kolokoltsova O, Smith J, Miller M, Yun N, Poussard A, Grant A, Tigabu B, Walker A, Paessler S.** 2014. Rescue of a Recombinant Machupo Virus from Cloned cDNAs and In Vivo Characterization in Interferon (alphabeta/gamma) Receptor Double Knockout Mice. *J Virol* **88**:1914-1923.
76. **Syromiatnikova SI, Khmelev AL, Pantiukhov VB, Shatokhina IV, Pirozhkov AP, Khamitov RA, Markov VI, Birisevich IB, Bondarev VP.** 2009. [Chemotherapy for Bolivian hemorrhagic fever in experimentally infected guinea pigs]. *Vopr Virusol* **54**:37-40.
77. **Medzhitov R.** 2007. Recognition of microorganisms and activation of the immune response. *Nature* **449**:819-826.
78. **Versteeg GA, Garcia-Sastre A.** 2010. Viral tricks to grid-lock the type I interferon system, p. 508-516, *Curr Opin Microbiol*, vol. 13. 2010 Elsevier Ltd, England.
79. **Diamond MS, Gale M, Jr.** 2012. Cell-intrinsic innate immune control of West Nile virus infection. *Trends Immunol* **33**:522-530.
80. **Borden EC, Sen GC, Uze G, Silverman RH, Ransohoff RM, Foster GR, Stark GR.** 2007. Interferons at age 50: past, current and future impact on biomedicine, p. 975-990, *Nat Rev Drug Discov*, vol. 6, England.
81. **Bowie AG, Unterholzner L.** 2008. Viral evasion and subversion of pattern-recognition receptor signalling, p. 911-922, *Nat Rev Immunol*, vol. 8, England.

82. **Honda K, Yanai H, Negishi H, Asagiri M, Sato M, Mizutani T, Shimada N, Ohba Y, Takaoka A, Yoshida N, Taniguchi T.** 2005. IRF-7 is the master regulator of type-I interferon-dependent immune responses. *Nature* **434**:772-777.
83. **Loo YM, Fornek J, Crochet N, Bajwa G, Perwitasari O, Martinez-Sobrido L, Akira S, Gill MA, Garcia-Sastre A, Katze MG, Gale M, Jr.** 2008. Distinct RIG-I and MDA5 signaling by RNA viruses in innate immunity. *J Virol* **82**:335-345.
84. **Takeuchi O, Akira S.** 2009. Innate immunity to virus infection. *Immunol Rev* **227**:75-86.
85. **Beutler B, Eidenschenk C, Crozat K, Imler JL, Takeuchi O, Hoffmann JA, Akira S.** 2007. Genetic analysis of resistance to viral infection. *Nat Rev Immunol* **7**:753-766.
86. **Kato H, Takeuchi O, Sato S, Yoneyama M, Yamamoto M, Matsui K, Uematsu S, Jung A, Kawai T, Ishii KJ, Yamaguchi O, Otsu K, Tsujimura T, Koh CS, Reis e Sousa C, Matsuura Y, Fujita T, Akira S.** 2006. Differential roles of MDA5 and RIG-I helicases in the recognition of RNA viruses, p. 101-105, *Nature*, vol. 441, England.
87. **Fujita T, Onoguchi K, Onomoto K, Hirai R, Yoneyama M.** 2007. Triggering antiviral response by RIG-I-related RNA helicases. *Biochimie* **89**:754-760.
88. **Kato H, Takahashi K, Fujita T.** 2011. RIG-I-like receptors: cytoplasmic sensors for non-self RNA. *Immunol Rev* **243**:91-98.
89. **Satoh T, Kato H, Kumagai Y, Yoneyama M, Sato S, Matsushita K, Tsujimura T, Fujita T, Akira S, Takeuchi O.** 2010. LGP2 is a positive regulator of RIG-I- and MDA5-mediated antiviral responses. *Proc Natl Acad Sci U S A* **107**:1512-1517.
90. **Akira S, Takeda K.** 2004. Toll-like receptor signalling, p. 499-511, *Nat Rev Immunol*, vol. 4, England.
91. **Finberg RW, Wang JP, Kurt-Jones EA.** 2007. Toll like receptors and viruses. *Rev Med Virol* **17**:35-43.
92. **Fitzgerald KA, McWhirter SM, Faia KL, Rowe DC, Latz E, Golenbock DT, Coyle AJ, Liao SM, Maniatis T.** 2003. IKKepsilon and TBK1 are essential components of the IRF3 signaling pathway. *Nat Immunol* **4**:491-496.
93. **Kato H, Sato S, Yoneyama M, Yamamoto M, Uematsu S, Matsui K, Tsujimura T, Takeda K, Fujita T, Takeuchi O, Akira S.** 2005. Cell type-specific involvement of RIG-I in antiviral response. *Immunity* **23**:19-28.
94. **Kawai T, Takahashi K, Sato S, Coban C, Kumar H, Kato H, Ishii KJ, Takeuchi O, Akira S.** 2005. IPS-1, an adaptor triggering RIG-I- and Mda5-mediated type I interferon induction. *Nat Immunol* **6**:981-988.
95. **Tang ED, Wang CY.** 2009. MAVS self-association mediates antiviral innate immune signaling. *J Virol* **83**:3420-3428.

96. **Baril M, Racine ME, Penin F, Lamarre D.** 2009. MAVS dimer is a crucial signaling component of innate immunity and the target of hepatitis C virus NS3/4A protease. *J Virol* **83**:1299-1311.
97. **Honda K, Taniguchi T.** 2006. IRFs: master regulators of signalling by Toll-like receptors and cytosolic pattern-recognition receptors. *Nat Rev Immunol* **6**:644-658.
98. **de Weerd NA, Samarajiwa SA, Hertzog PJ.** 2007. Type I interferon receptors: biochemistry and biological functions. *J Biol Chem* **282**:20053-20057.
99. **Samuel CE.** 2001. Antiviral Actions of Interferons. *Clin Microbiol Rev* **14**:778-809.
100. **Onomoto K, Jogi M, Yoo JS, Narita R, Morimoto S, Takemura A, Sambhara S, Kawaguchi A, Osari S, Nagata K, Matsumiya T, Namiki H, Yoneyama M, Fujita T.** 2012. Critical role of an antiviral stress granule containing RIG-I and PKR in viral detection and innate immunity. *PLoS One* **7**:e43031.
101. **Geisbert TW, Jahrling PB.** 2004. Exotic emerging viral diseases: progress and challenges. *Nat Med* **10**:S110-121.
102. **Yun NE, Poussard AL, Seregin AV, Walker AG, Smith JK, Aronson JF, Smith JN, Soong L, Paessler S.** 2012. Functional interferon system is required for clearance of lassa virus. *J Virol* **86**:3389-3392.
103. **Peters CJ, Liu CT, Anderson GW, Jr., Morrill JC, Jahrling PB.** 1989. Pathogenesis of viral hemorrhagic fevers: Rift Valley fever and Lassa fever contrasted. *Rev Infect Dis* **11 Suppl 4**:S743-749.
104. **Baize S, Kaplon J, Faure C, Pannetier D, Georges-Courbot MC, Deubel V.** 2004. Lassa virus infection of human dendritic cells and macrophages is productive but fails to activate cells. *J Immunol* **172**:2861-2869.
105. **Baize S, Pannetier D, Faure C, Marianneau P, Marendat I, Georges-Courbot MC, Deubel V.** 2006. Role of interferons in the control of Lassa virus replication in human dendritic cells and macrophages. *Microbes Infect* **8**:1194-1202.
106. **Mahanty S, Hutchinson K, Agarwal S, McRae M, Rollin PE, Pulendran B.** 2003. Cutting edge: impairment of dendritic cells and adaptive immunity by Ebola and Lassa viruses. *J Immunol* **170**:2797-2801.
107. **Pannetier D, Reynard S, Russier M, Journeaux A, Tordo N, Deubel V, Baize S.** 2011. Human dendritic cells infected with the nonpathogenic Mopeia virus induce stronger T-cell responses than those infected with Lassa virus. *J Virol* **85**:8293-8306.
108. **Levis SC, Saavedra MC, Ceccoli C, Falcoff E, Feuillade MR, Enria DAM, Maiztegui JI, Falcoff R.** 1984. Endogenous Interferon in Argentine Hemorrhagic Fever. *J Infect Dis* **149**:428-433.
109. **Levis SC, Saavedra MC, Ceccoli C, Feuillade MR, Enria DA, Maiztegui JI, Falcoff R.** 1985. Correlation between endogenous interferon and the clinical

- evolution of patients with Argentine hemorrhagic fever. *J Interferon Res* **5**:383-389.
110. **Kenyon RH, McKee KT, Jr., Zack PM, Rippy MK, Vogel AP, York C, Meegan J, Crabbs C, Peters CJ.** 1992. Aerosol infection of rhesus macaques with Junin virus. *Intervirology* **33**:23-31.
 111. **Stephen EL, Scott SK, Eddy GA, Levy HB.** 1977. Effect of interferon on togavirus and arenavirus infections of animals. *Tex Rep Biol Med* **35**:449-454.
 112. **Gowen BB, Smee DF, Wong MH, Hall JO, Jung KH, Bailey KW, Stevens JR, Furuta Y, Morrey JD.** 2008. Treatment of late stage disease in a model of arenaviral hemorrhagic fever: T-705 efficacy and reduced toxicity suggests an alternative to ribavirin. *PLoS One* **3**:e3725.
 113. **Groseth A, Hoenen T, Weber M, Wolff S, Herwig A, Kaufmann A, Becker S.** 2011. Tacaribe virus but not junin virus infection induces cytokine release from primary human monocytes and macrophages, p. e1137, *PLoS Negl Trop Dis*, vol. 5, United States.
 114. **Huang C, Kolokoltsova OA, Yun NE, Seregin AV, Poussard AL, Walker AG, Brasier AR, Zhao Y, Tian B, de la Torre JC, Paessler S.** 2012. Junín Virus Infection Activates the Type I Interferon Pathway in a RIG-I-Dependent Manner. *PLoS Negl Trop Dis* **6**:e1659.
 115. **Pindel A, Sadler A.** 2011. The role of protein kinase R in the interferon response. *J Interferon Cytokine Res* **31**:59-70.
 116. **Martínez-Sobrido L, Giannakas P, Cubitt B, García-Sastre A, de la Torre JC.** 2007. Differential Inhibition of Type I Interferon Induction by Arenavirus Nucleoproteins. *J Virol* **81**:12696-12703.
 117. **Pythoud C, Rodrigo WW, Pasqual G, Rothenberger S, Martinez-Sobrido L, de la Torre JC, Kunz S.** 2012. Arenavirus nucleoprotein targets interferon regulatory factor-activating kinase IKKepsilon. *J Virol* **86**:7728-7738.
 118. **Rodrigo WW, Ortiz-Riano E, Pythoud C, Kunz S, de la Torre JC, Martinez-Sobrido L.** 2012. Arenavirus nucleoproteins prevent activation of nuclear factor kappa B. *J Virol* **86**:8185-8197.
 119. **Linero FN, Thomas MG, Boccaccio GL, Scolaro LA.** 2011. Junin virus infection impairs stress-granule formation in Vero cells treated with arsenite via inhibition of eIF2alpha phosphorylation. *J Gen Virol* **92**:2889-2899.
 120. **Fan L, Briese T, Lipkin WI.** 2010. Z Proteins of New World Arenaviruses Bind RIG-I and Interfere with Type I Interferon Induction. *J. Virol.* **84**:1785-1791.
 121. **Albariño CG, Bird BH, Chakrabarti AK, Dodd KA, Flint M, Bergeron É, White DM, Nichol ST.** 2011. The Major Determinant of Attenuation in Mice of the Candid1 Vaccine for Argentine Hemorrhagic Fever Is Located in the G2 Glycoprotein Transmembrane Domain. *J virol* **85**:10404-10408.
 122. **Droniou-Bonzom ME, Reignier T, Oldenburg JE, Cox AU, Exline CM, Rathbun JY, Cannon PM.** 2011. Substitutions in the glycoprotein (GP) of the

- Candid#1 vaccine strain of Junin virus increase dependence on human transferrin receptor 1 for entry and destabilize the metastable conformation of GP. J virol.
123. **ProMED-email**. 2011. Bolivian hemorrhagic fever - Bolivia: (BE) ProMED-email **20111202.3514**.
 124. **Bergeron É, Chakrabarti AK, Bird BH, Dodd KA, McMullan LK, Spiropoulou CF, Nichol ST, Albariño CG**. 2012. Reverse Genetics Recovery of Lujo Virus and Role of Virus RNA Secondary Structures in Efficient Virus Growth. J Virol **86**:10759-10765.
 125. **Flatz L, Berghaler A, de la Torre JC, Pinschewer DD**. 2006. Recovery of an arenavirus entirely from RNA polymerase I/II-driven cDNA. Proc Natl Acad Sci U S A **103**:4663-4668.
 126. **Sánchez AB, de la Torre JC**. 2006. Rescue of the prototypic Arenavirus LCMV entirely from plasmid. Virology **350**:370-380.
 127. **de la Torre JC**. 2008. Reverse genetics approaches to combat pathogenic arenaviruses, p. 239-250, Antiviral Res, vol. 80, Netherlands.
 128. **Goff SP, Berg P**. 1976. Construction of hybrid viruses containing SV40 and lambda phage DNA segments and their propagation in cultured monkey cells. Cell **9**:695-705.
 129. **Liljestrom P, Garoff H**. 1991. A new generation of animal cell expression vectors based on the Semliki Forest virus replicon. Biotechnology (N Y) **9**:1356-1361.
 130. **Rice CM, Levis R, Strauss JH, Huang HV**. 1987. Production of infectious RNA transcripts from Sindbis virus cDNA clones: mapping of lethal mutations, rescue of a temperature-sensitive marker, and in vitro mutagenesis to generate defined mutants. J Virol **61**:3809-3819.
 131. **Taniguchi T, Palmieri M, Weissmann C**. 1978. QB DNA-containing hybrid plasmids giving rise to QB phage formation in the bacterial host. Nature **274**:223-228.
 132. **Bridgen A, Elliott RM**. 1996. Rescue of a segmented negative-strand RNA virus entirely from cloned complementary DNAs. Proc Natl Acad Sci U S A **93**:15400-15404.
 133. **Dittmann J, Stertz S, Grimm D, Steel J, Garcia-Sastre A, Haller O, Kochs G**. 2008. Influenza A virus strains differ in sensitivity to the antiviral action of Mx-GTPase. J Virol **82**:3624-3631.
 134. **Janzen C, Kochs G, Haller O**. 2000. A Monomeric GTPase-Negative MxA Mutant with Antiviral Activity. J Virol **74**:8202-8206.
 135. **Habjan M, Penski N, Wagner V, Spiegel M, Overby AK, Kochs G, Huiskonen JT, Weber F**. 2009. Efficient production of Rift Valley fever virus-like particles: The antiviral protein MxA can inhibit primary transcription of bunyaviruses. Virology **385**:400-408.

136. **Klein HJ.** 1995. Part C. – Restraint, p. 292. *In Benneter TB, Abee CR, Henrickson R* (ed.), *Nonhuman Primates in Biomedical Research*. Elsevier
137. **Kenyon RH, Green DE, Eddy GA, Peters CJ.** 1986. Treatment of Junin virus-infected guinea pigs with immune serum: development of late neurological disease. *J Med Virol* **20**:207-218.
138. **Johnson KM, J. B. McCormick, P. A. Webb, E. S. Smith, L. H. Elliott, and I. J. King.** 1987. Clinical virology of Lassa fever in hospitalized patients. *J Infect Dis* **155**:456-464.
139. **McCormick JB, Fisher-Hoch SP.** 2002. Lassa fever. *Curr Top Microbiol Immunol* **262**:75-109.
140. **Yun NE, Walker DH.** 2012. Pathogenesis of Lassa fever. *Viruses* **4**:2031-2048.
141. **Charrel RN, Lamballerie Xd.** 2003. Arenaviruses other than Lassa virus. *Antiviral Research* **57**:89-100.
142. **Wang J, Danzy S, Kumar N, Ly H, Liang Y.** 2012. Biological Roles and Functional Mechanisms of Arenavirus Z Protein in Viral Replication. *J Virol* **86**:9794-9801.
143. **Cornu TI, de la Torre JC.** 2001. RING finger Z protein of lymphocytic choriomeningitis virus (LCMV) inhibits transcription and RNA replication of an LCMV S-segment minigenome. *J Virol* **75**:9415-9426.
144. **Hass M, Golnitz U, Muller S, Becker-Ziaja B, Gunther S.** 2004. Replicon system for Lassa virus. *J Virol* **78**:13793-13803.
145. **Lee KJ, Novella IS, Teng MN, Oldstone MB, de La Torre JC.** 2000. NP and L proteins of lymphocytic choriomeningitis virus (LCMV) are sufficient for efficient transcription and replication of LCMV genomic RNA analogs. *J Virol* **74**:3470-3477.
146. **Lopez N, Jacamo R, Franze-Fernandez MT.** 2001. Transcription and RNA replication of tacaribe virus genome and antigenome analogs require N and L proteins: Z protein is an inhibitor of these processes. *J Virol* **75**:12241-12251.
147. **Pinschewer DD, Perez M, de la Torre JC.** 2005. Dual role of the lymphocytic choriomeningitis virus intergenic region in transcription termination and virus propagation. *J Virol* **79**:4519-4526.
148. **Lelke M, Brunotte L, Busch C, Gunther S.** 2010. An N-terminal region of Lassa virus L protein plays a critical role in transcription but not replication of the virus genome. *J Virol* **84**:1934-1944.
149. **Kolokoltsova OA, Yun NE, Poussard AL, Smith JK, Smith JN, Salazar M, Walker A, Tseng C-TK, Aronson JF, Paessler S.** 2010. Mice Lacking Alpha/Beta and Gamma Interferon Receptors Are Susceptible to Junin Virus Infection. *J Virol* **84**:13063-13067.
150. **Hass M, Westerkofsky M, Müller S, Becker-Ziaja B, Busch C, Günther S.** 2006. Mutational Analysis of the Lassa Virus Promoter. *J Virol* **80**:12414-12419.

151. **Albariño CG, Bergeron É, Erickson BR, Khristova ML, Rollin PE, Nichol ST.** 2009. Efficient Reverse Genetics Generation of Infectious Junin Viruses Differing in Glycoprotein Processing. *J Virol* **83**:5606-5614.
152. **Muller S, Gunther S.** 2007. Broad-spectrum antiviral activity of small interfering RNA targeting the conserved RNA termini of Lassa virus. *Antimicrob Agents Chemother* **51**:2215-2218.
153. **Lukashevich IS, Patterson J, Carrion R, Moshkoff D, Ticer A, Zapata J, Brasky K, Geiger R, Hubbard GB, Bryant J, Salvato MS.** 2005. A Live Attenuated Vaccine for Lassa Fever Made by Reassortment of Lassa and Mopeia Viruses. *J Virol* **79**:13934-13942.
154. **Child PL, MacKenzie RB, Valverde LR, Johnson KM.** 1967. Bolivian hemorrhagic fever. A pathologic description. *Arch Pathol* **83**:434-445.
155. **Grant A, Seregin A, Huang C, Kolokoltsova O, Brasier A, Peters C, Paessler S.** 2012. Junín Virus Pathogenesis and Virus Replication. *Viruses* **4**:2317-2339.
156. **Taylor KE, Mossman KL.** 2013. Recent advances in understanding viral evasion of type I interferon. *Immunology* **138**:190-197.
157. **Parodi AS, Coto CE, Boxaca M, Lajmanovich S, Gonzalez S.** 1966. Characteristics of Junin virus. Etiological agent of Argentine hemorrhagic fever. *Arch Gesamte Virusforsch* **19**:393-402.
158. **MC Weissenbacher CC, MA Calello, SN Rondinone, EB Damonte, MJ Frigerio.** 1982. Cross-protection between Tacaribe complex viruses. Presence of neutralizing antibodies against Junin virus (Argentine hemorrhagic fever) in guinea pigs infected with Tacaribe virus. *Infect Immun* **35**:425-430.
159. **Aronson JF, Herzog NK, Jerrells TR.** 1994. Pathological and virological features of arenavirus disease in guinea pigs. Comparison of two Pichinde virus strains. *Am J Pathol* **145**:228-235.
160. **Waggoner JJ, Soda EA, Deresinski S.** 2013. Rare and emerging viral infections in transplant recipients. *Clin Infect Dis* **57**:1182-1188.
161. **Zhou S, Cerny AM, Zacharia A, Fitzgerald KA, Kurt-Jones EA, Finberg RW.** 2010. Induction and Inhibition of Type I Interferon Responses by Distinct Components of Lymphocytic Choriomeningitis Virus. *J. Virol.* **84**:9452-9462.
162. **Jiang X, Huang Q, Wang W, Dong H, Ly H, Liang Y, Dong C.** 2013. Structures of arenaviral nucleoproteins with triphosphate dsRNA reveal a unique mechanism of immune suppression. *J Biol Chem* **288**:16949-16959.
163. **Qi X, Lan S, Wang W, Schelde LM, Dong H, Wallat GD, Ly H, Liang Y, Dong C.** 2010. Cap binding and immune evasion revealed by Lassa nucleoprotein structure. *Nature* **468**:779-783.
164. **Martínez-Sobrido L, Zúñiga EI, Rosario D, García-Sastre A, de la Torre JC.** 2006. Inhibition of the Type I Interferon Response by the Nucleoprotein of the Prototypic Arenavirus Lymphocytic Choriomeningitis Virus. *J Virol* **80**:9192-9199.

165. **Dejean CB, Ayerra BL, Teyssie AR.** 1987. Interferon response in the guinea pig infected with Junin virus. *J Med Virol* **23**:83-91.
166. **Emeny JM, Morgan MJ.** 1979. Regulation of the interferon system: evidence that Vero cells have a genetic defect in interferon production. *J Gen Virol* **43**:247-252.
167. **Desmyter J, Melnick JL, Rawls WE.** 1968. Defectiveness of interferon production and of rubella virus interference in a line of African green monkey kidney cells (Vero). *J Virol* **2**:955-961.
168. **Chew T, Noyce R, Collins SE, Hancock MH, Mossman KL.** 2009. Characterization of the interferon regulatory factor 3-mediated antiviral response in a cell line deficient for IFN production. *Mol Immunol* **46**:393-399.
169. **Pasqual G, Burri DJ, Pasquato A, de la Torre JC, Kunz S.** 2011. Role of the host cell's unfolded protein response in arenavirus infection. *J Virol* **85**:1662-1670.
170. **Shen J, Snapp EL, Lippincott-Schwartz J, Prywes R.** 2005. Stable binding of ATF6 to BiP in the endoplasmic reticulum stress response. *Mol Cell Biol* **25**:921-932.
171. **Patel RC, Sen GC.** 1998. PACT, a protein activator of the interferon-induced protein kinase, PKR. *Embo j* **17**:4379-4390.
172. **Okumura F, Okumura AJ, Uematsu K, Hatakeyama S, Zhang D-E, Kamura T.** 2013. Activation of Double-stranded RNA-activated Protein Kinase (PKR) by Interferon-stimulated Gene 15 (ISG15) Modification Down-regulates Protein Translation. *J Biol Chem* **288**:2839-2847.
173. **Baird NL, York J, Nunberg JH.** 2012. Arenavirus Infection Induces Discrete Cytosolic Structures for RNA Replication. *J Virol* **86**:11301-11310.
174. **Marques JT, White CL, Peters GA, Williams BR, Sen GC.** 2008. The role of PACT in mediating gene induction, PKR activation, and apoptosis in response to diverse stimuli. *J Interferon Cytokine Res* **28**:469-476.
175. **White JP, Reineke LC, Lloyd RE.** 2011. Poliovirus switches to an eIF2-independent mode of translation during infection. *J Virol* **85**:8884-8893.
176. **Strebovsky J, Walker P, Dalpke AH.** 2012. Suppressor of cytokine signaling proteins as regulators of innate immune signaling. *Front Biosci (Landmark Ed)* **17**:1627-1639.
177. **Fierro-Monti I, Racle J, Hernandez C, Waridel P, Hatzimanikatis V, Quadroni M.** 2013. A novel pulse-chase SILAC strategy measures changes in protein decay and synthesis rates induced by perturbation of proteostasis with an Hsp90 inhibitor. *PLoS One* **8**:e80423.
178. **Enria DA, Maiztegui JI.** 1994. Antiviral treatment of Argentine hemorrhagic fever. *Antiviral Res* **23**:23-31.
179. **Enria DA, Briggiler AM, Sanchez Z.** 2007. Treatment of Argentine hemorrhagic fever. *Antiviral Research* **78**:132-139.

180. **Salazar M, Yun NE, Poussard AL, Smith JN, Smith JK, Kolokoltsova OA, Patterson MJ, Linde J, Paessler S.** 2012. Effect of Ribavirin on Junin Virus Infection in Guinea Pigs. *Zoonoses and Public Health* **59**:278-285.
181. **Enria DA, Briggiler AM, Levis S, Vallejos D, Maiztegui JI, Canonico PG.** 1987. Tolerance and antiviral effect of ribavirin in patients with Argentine hemorrhagic fever. *Antiviral Res* **7**:353-359.
182. **Lukashevich IS.** 1992. Generation of reassortants between African arenaviruses. *Virology* **188**:600-605.
183. **Lukashevich IS, Vasiuchkov AD, Stel'makh TA, Scheslenok EP, Shabanov AG.** 1991. [The isolation and characteristics of reassortants between the Lassa and Mopeia arenaviruses]. *Vopr Virusol* **36**:146-150.
184. **Contigiani M, Medeot S, Diaz G.** 1993. Heterogeneity and stability characteristics of Candid 1 attenuated strain of Junin virus. *Acta Virol* **37**:41-46.
185. **Goni SE, Iserte JA, Ambrosio AM, Romanowski V, Ghiringhelli PD, Lozano ME.** 2006. Genomic features of attenuated Junin virus vaccine strain candidate. *Virus Genes* **32**:37-41.
186. **Cuevas CD, Lavanya M, Wang E, Ross SR.** 2011. Junín Virus Infects Mouse Cells and Induces Innate Immune Responses. *J Virol* **85**:11058-11068.
187. **Cosset FL, Marianneau P, Verney G, Gallais F, Tordo N, Pecheur EI, ter Meulen J, Deubel V, Bartosch B.** 2009. Characterization of Lassa virus cell entry and neutralization with Lassa virus pseudoparticles. *J Virol* **83**:3228-3237.
188. **Albariño CG, Bird BH, Chakrabarti AK, Dodd KA, Erickson BR, Nichol ST.** 2011. Efficient Rescue of Recombinant Lassa Virus Reveals the Influence of S Segment Noncoding Regions on Virus Replication and Virulence. *J Virol* **85**:4020-4024.
189. **Albariño CG, Bird BH, Chakrabarti AK, Dodd KA, White DM, Bergeron É, Shrivastava-Ranjan P, Nichol ST.** 2011. Reverse Genetics Generation of Chimeric Infectious Junin/Lassa Virus Is Dependent on Interaction of Homologous Glycoprotein Stable Signal Peptide and G2 Cytoplasmic Domains. *J Virol* **85**:112-122.
190. **McCormick JB, King IJ, Webb PA, Scribner CL, Craven RB, Johnson KM, Elliott LH, Belmont-Williams R.** 1986. Lassa Fever. *N Engl J Med* **314**:20-26.
191. **Huang KJ, Su IJ, Theron M, Wu YC, Lai SK, Liu CC, Lei HY.** 2005. An interferon-gamma-related cytokine storm in SARS patients. *J Med Virol* **75**:185-194.
192. **Baharoon SA.** 2010. H1N1 infection-induced thyroid storm. *Ann Thorac Med* **5**:110-112.
193. **Gao R, Bhatnagar J, Blau DM, Greer P, Rollin DC, Denison AM, Deleon-Carnes M, Shieh WJ, Sambhara S, Tumpey TM, Patel M, Liu L, Paddock C, Drew C, Shu Y, Katz JM, Zaki SR.** 2013. Cytokine and chemokine profiles in

lung tissues from fatal cases of 2009 pandemic influenza A (H1N1): role of the host immune response in pathogenesis. *Am J Pathol* **183**:1258-1268.

Name: Michael Patterson, PhD MPH

Present Position and Contact Information

Graduate Research Assistant (03/2014)
University of Texas Medical Branch (UTMB)
301 University Ave, Galveston National Laboratory
Galveston, TX 77555-0609
Michaelpattersonphd@gmail.com
(916) 899-9164

Biographical:

Home Address: 1401 Merrill Creek Pkwy Apt 5032, Everett WA 98203
Citizenship: USA

Education:

2014	Doctor of Philosophy: Experimental Pathology, University of Texas Medical Branch, Galveston, TX, USA
2013	Master of Public Health: Infectious Disease Epidemiology, University of Texas Medical Branch, Galveston, TX, USA
2008	B.A.: Biochemistry, Biophysics and Molecular Biology. Whitman College, Walla Walla, WA, USA
2007	National University of Galway, Galway, Ireland

Professional Experience:

2008-Present	Graduate Assistant at UTMB, Galveston, TX
2008	Organic Chemistry laboratory assistant, Whitman College, Walla Walla, WA: Assisted in preparing experiments and teaching classes of 30+ students bi-weekly
2007	Summer Undergraduate Research Program (SURP), UTMB, Galveston, TX: Studied the effects of drug and exercise treatment on protein expression in recovering burn patients.
2006	Summer Intern at PASCO Electronics, Roseville CA: Worked with the experiment design team developing high school and undergraduate level protocols and documentation. Additional work included troubleshooting newly designed equipment and software.

Peer Reviewed Publications:

1. **Patterson M**, Grant A, Paessler S. 2014. Epidemiology and pathogenesis of Bolivian hemorrhagic fever. *Curr Opin Virol* **5c**:82-90.
2. **Patterson M**, Seregin A, Huang C, Kolokoltsova O, Smith J, Miller M, Yun N, Poussard A, Grant A, Tigabu B, Walker A, Paessler S. 2014. Rescue of a Recombinant Machupo Virus from Cloned cDNAs and In Vivo Characterization in Interferon (alphabeta/gamma) Receptor Double Knockout Mice. *J Virol* **88**:1914-1923
3. Poussard, A.*, **Patterson, M.***, et al., In vivo imaging systems (IVIS) detection of a neuro-invasive encephalitic virus. *J Vis Exp*, 2012(70): p. e4429.*co-first authors
4. **Patterson, M.**, Poussard, A., Taylor, K., et al. Rapid, non-invasive imaging of alphaviral brain infection: Reducing animal numbers and morbidity to identify efficacy of potential vaccines and antivirals. *Vaccine* 2011;29:9345-51.
5. Salazar, M., Yun, N., Poussard, A., et al. Effect of Ribavirin on Junin Virus Infection in Guinea Pigs. *Zoonoses and Public Health* 2012;59:278-85.
6. Taylor, K., Kolokoltsova, O., **Patterson, M.**, et al. Natural killer cell mediated pathogenesis determines outcome of central nervous system infection with Venezuelan equine encephalitis virus in C3H/HeN mice. *Vaccine* 2012;30:4095-105.

Other:

1. **Patterson, M.** Dissertation for Doctor in Philosophy: The Development of a Reverse Genetics System for Machupo virus. March 2014. University of Texas Medical Branch, Galveston Texas 77555
2. **Patterson, M.** Masters of Public Health Capstone: *A Review of the Government Sponsored Offensive Biological Programs, Weaponized Biological Pathogens and their Countermeasures*. August 2013. University of Texas Medical Branch, Galveston Texas 77555

Research:

Research Fields/Key Words:

Molecular biology, biochemistry, immunology, viral pathogenesis, disease modeling, vaccine development, recombinant genetics, *in vivo* imaging, infectious disease epidemiology, biodefense, biosecurity, bioweapons

Clearance:

CDC and USDA security risk assessment approved for work with Tier 1 Select Agents

Fellowships:

2013-2014 Center for	Emerging Leaders in Biosecurity Fellowship awarded by the Biosecurity at the University of Pittsburgh Medical Center: Competitive fellowship with the aim of bringing together a diverse group of individuals interested in a career in biosecurity.
2011	UTMB-Fogarty Fellowship: Worked through the Naval Medical Research Unit -6 in Lima, Peru and the Peruvian Health Department in Puerto Maldonado. Research consisted of house-to-house visits, collection of samples from febrile patients, and administration of a questionnaire with the goal of tracking Influenza in the region. Additionally, assisted with the local health department with childhood and young-adult vaccination programs.

Grant Support:

2010-2011	1UL1RR029876-01 NIH/Institute of Translational Sciences UTMB, <i>Imaging of CNS invasion by Venezuelan Equine Encephalitis Virus.</i>
-----------	---

Competitive Awards and Scholarships:

2013	Edwards S. Reynolds award- Annual Pathology Trainee Day
2013	ASV 2013 Annual Conference Travel award
2013	ICAAC 2013 Annual Conference Travel award
2013	Robert Shope PhD Endowed Scholarship award
2013	Christina Fleischmann GSBS Travel award
2012	Betty Williams, PhD General Scholarship
2012	Sealy Center for Tropical Diseases Scholarship
2011	Field Epidemiology Course Fellowship-Naval Medical Research Unit-6 and UTMB
2011	Zhou Sisters Great Expectations Scholarship

2011	ASV 2011 Annual Conference Travel award
2010	James E. Beall II Memorial Best Poster Presentation in Neuroscience-NSRF
2010	Sealy Center for Vaccine Development travel award
2007	UTMB SURP Best Poster Presentation award

Committee Responsibilities:

2009-Present	Student and Post-Doctoral Organization for Committee for Career Development
2010-2012	Graduate Student Government Webmaster
2011-2012	Graduate Student Government Treasurer- Organized the annual UTMB schoolwide event
2011-2013	Public Health Organization Treasurer
2012-2013	Public Health Organization Outreach Coordinator-Organized multiple presentations with the community including elementary students focusing on the importance of vaccination and herd immunity.

Extra-Curricular

2009-Present	Founder and Organizer of UTMB Volleyball: Scheduling, organizing, and communicating tri-weekly an organization consisting of more than 30 students, professors and members of the surrounding community.
--------------	--

Society Memberships:

2012	American Public Health Association
2010	American Society for Virology
2009	American Association for the Advancement of Science
2007	Sigma Xi

Certified Training Experience:

UTMB Biosafety Level 4, 3, and 2 access
UTMB Animal Biosafety Level 3 and 2 (Murine, Guinea Pig, Ferret, Non-Human Primate)

Naval Medical Research Unit 6 Field Epidemiology training, Lima and Tumbes, Peru

Equipment and Technical Skills:

Laboratory Techniques: PCR, real-time PCR, quantitative PCR, Western blots, Southern

blots, tissue culture, virus propagation, recombinant genetics, *in vivo* imaging systems (IVIS), histology, immunohistochemistry, ELISA, high containment research, cloning

Technical Skills: GraphPad Prism, Clone Manager, Word, Powerpoint, Excel, GIS, Dreamweaver, Movie Maker

Published Abstracts, Posters, and Presentations:

Patterson, M., et al. *The Development Of A Reverse Genetics System For The Rescue Of A Recombinant Machupo Virus*. Oral presentation at: 32nd Annual American Society for Virology; 2013 July 20-24. State College, PA.

Patterson, M., et al. *The Development Of A Reverse Genetics System For The Rescue Of A Recombinant Machupo Virus*. Poster presented at: McLaughlin Colloquium; 2013 April 12. Galveston, TX.

Patterson, M., et al. *The Development Of A Reverse Genetics System For The Rescue Of A Recombinant Machupo Virus*. Poster presented at: UTMB Pathology Department Trainee Research Day; 2013 April 1. Galveston, TX.

Patterson, M., Poussard, A.*, et al. *Utilizing in vivo imaging systems in neuroinvasive alphavirus infection: rapidly identifying potential vaccines and therapeutics*. Oral presentation at: American Society for Virology annual meeting; 2011 July 15. Minneapolis, MI 2011. *Submitted by Patterson, Presented by Poussard

Patterson, M., et al. *In VIVO Imaging of Alphavirus Infection: Visualizing the Early CNS Infection Using Non-Invasive Technique*. Poster presented at: 2010 Texas-UK Symposium 'Controlling Emerging Infectious Diseases in the 21st Century'; 2010, Feb. 26-28. Galveston TX

Patterson, M., et al. *In VIVO Imaging of Alphavirus Infection: Visualizing the Early CNS Infection Using Non-Invasive Technique*. Poster presented at: National Foundation of Infectious Diseases: Vaccine; 2011 May 16-18. Boston, MA.

Patterson, M., et al. *In VIVO Imaging of Alphavirus Infection: Visualizing the Early CNS Infection Using Non-Invasive Technique*. Poster presented at: National Student Research Forum; 2010 April 22-23. Galveston, TX.

Patterson, M., et al. *Effects of Exercise and Oxandrolone Treatment on the Proteomic Biomarkers in Skeletal Muscle (PRISM) after Severe Burn Injury in Children*. Poster presented at: Whitman College Undergraduate Conference; 2008 April 14. Walla Walla, WA

Patterson, M., et al. *Effects of Exercise and Oxandrolone Treatment on the Proteomic Biomarkers in Skeletal Muscle (PRISM) after Severe Burn Injury in Children*. Poster presented at: UTMB SURP Poster Presentation; 2007 August. Galveston, TX.